Design and Test of a 1.8K Liquid Helium Refrigerator

by

Daniel W. Hoch

A thesis submitted in partial fulfillment of

the requirements for the degree of

Master of Science

(Mechanical Engineering)

at the

UNIVERSITY OF WISCONSIN-MADISON

2004

Abstract

A liquid helium refrigeration system is being developed that will be capable of testing superconducting specimens at temperatures down to 1.8 K, currents up to 15 kA, and magnetic fields from 0 to 5 Tesla. The superconducting specimens will be immersed in a bath of subcooled, superfluid helium at atmospheric pressure. Subcooled superfluid helium is an ideal coolant for superconductors as it has an exceptionally high thermal conductivity, high heat capacity, and will not readily evaporate. These characteristics allow superconducting specimens to be tested at a constant temperature and therefore allow precise measurement of the critical surface associated with the sample. Argonne National Laboratory (ANL) has requested the design and fabrication of this liquid helium refrigeration system in order to characterize Niobium-Titanium superconducting wires and coils that will be installed in the Advanced Photon Source (APS). The low temperature, high current and high magnetic field requirements make this refrigeration system unique and not readily available within ANL or its contractors.

This thesis describes the design, fabrication, and an initial test run of the refrigeration system. The proof-of-concept test demonstrated that the system was capable of producing subcooled, superfluid helium, verified the integrity of the cryostat components and instrumentation at cryogenic temperatures, and identified several system enhancements that can be made in order to improve the refrigerator's performance during future testing.

Acknowledgments

I would like to say thank you to….

Argonne National Laboratory for the financial support provided to this project.

My advisor, Professor Greg Nellis, for all of his help, guidance, encouragement, and concern throughout this project. I have thoroughly enjoyed working with him and deeply appreciate his desire to insure my success.

My other advisor, Professor John Pfotenhauer, for willingly sharing his cryogenic expertise and making himself accessible throughout this project. I was very fortunate to have one of the world's experts on this topic readily available for consultation.

Orrie Lokken, a very capable engineer who offered a great deal of advice and provided me the opportunity to discuss many design concerns.

Robert Slowinski, Michael Rothaupt, Ryan Bolin and Greg Perlock for their contributions and attention to detail during the fabrication of this project.

My mother, for her constant encouragement and making me believe I could succeed in anything I put my mind to.

My father, who initiated my interest in engineering, answered countless questions while I was growing up, and made the time to teach me about mechanical systems.

And my wife, Cynthia, who provided support, love and motivation to set a goal and work hard to achieve it. I could not have gained this experience without her encouragement and patience. I am extremely grateful for the opportunities she has given me and admire the unselfish way in which she has provided it. She has always been my inspiration.

Table of Contents

List of Figures

List of Tables

Definition of Symbols Used

Area	cross-sectional area	[m^2]
C	heat capacity	[J/K-s]
c_p	specific heat	[J/kg-K]
Cr	heat capacity ratio	[--]
D	diameter	[m]
D_h	hydraulic diameter	[m]
E	blackbody emissive power	[W/m^2]
ε	emissivity	[--]
F	force	[N]
F_T	peak heat flux	[$kW/m^{5/3}$]
h	heat transfer coefficient	[W/m^2-K]
h_{fg}	enthalpy of vaporization	[kJ/kg]
I	electrical current	[amp]
ID	inside diameter	[m]
k	integrated thermal conductivity	[W/m-K]
L	length	[m]
$\dot{m}$	mass flow rate	[kg/s]
mass	mass	[kg]
μ	viscosity	[Pa-s]
NTU	number of transfer units	[--]
Nu	Nusselt number	[--]
OD	outside diameter	[m]

P	Pressure	[Pa]
P_w	wetted perimeter	[m]
Power	electrical power	[W]
Pr	Prandtl number	[--]
$\dot{Q}$"	heat flux	[kW/m^2]
$\dot{Q}$	heat transfer rate	[W]
r	radius	[m]
R	thermal resistance	[K/W]
Re	Reynolds Number	[--]
Resistance	electrical resistance	[ohm]
ρ	density	[kg/m^3]
ρ_e	electrical resistivity	[ohm-in]
σ	Stefan-Boltzmann Constant	[W/m^2-K^4]
S_T	dimensionless temperature sensitivity	[--]
T	temperature	[K]
μ_0	permeability of free space	[N/amp^2]
UA	overall heat transfer coefficient	[W/K]
u_T	temperature uncertainty	[K]
V	voltage	[volt]
VF	volumetric flow rate	[cfm]
Volume	volume	[m^3]

Chapter 1 Introduction

1.1 Advanced Photon Source

The Advanced Photon Source (APS) is a synchrotron light source that provides X-rays of high brilliance for research. APS users include universities, major corporations, and several government departments. The APS is located at Argonne National Laboratory (ANL) in the western suburbs of Chicago, Illinois and is operated by the University of Chicago for the Department of Energy.

At the APS, positrons (the antimatter counterparts of electrons) that have been accelerated to nearly the speed of light circulate through a storage ring about a kilometer in circumference. Because the positrons follow a curved path, they emit electromagnetic radiation, called synchrotron radiation. Synchrotron X-ray sources have allowed scientists to conduct molecular-level examinations of semiconductor surfaces and organic thin films, both of which are essential to the development of designer materials for new technologies (Argonne National Laboratory, 1997).

The wavelengths of light in synchrotron radiation cover a broad segment of the spectrum, extending beyond deep-violet, invisible to the human eye. These wavelengths, which include ultraviolet and X-radiation, are small relative to the visible part of the spectrum, and match the corresponding features of atoms, molecules, crystals, and cells, just as the wavelengths of larger visible light waves in the middle of the spectrum match the sizes of the smallest things that we can observe with our eyes. With a bright, penetrating light like X-rays from synchrotron radiation, scientific instruments can “see” deep into the

atomic structure of matter. Depending on the type of experiment being carried out, the energy of photons from synchrotron radiation can be minutely adjusted, or tuned, to the wavelength that is most useful.

The exceptional capability of the APS lies in its use of special devices, known as undulators, which are placed in straight sections of the storage ring. These undulators are capable of producing the most brilliant X-ray beams in the world; these X-rays allow scientists to study smaller samples, more complex systems and faster reactions and processes than ever before. Some examples of investigations that have been carried out using the APS include interplanetary dust, biological systems such as cell membranes, as well as the magnetic and surface properties of various materials (Argonne National Laboratory, 1997).

A storage ring is actually a set of curves connected by straight sections. Linear arrays of north-south permanent magnets with alternating polarity are inserted into the straight sections, one array above the beam path, the other below. When charged particles in the storage ring pass through the alternating fields they undulate and this action greatly enhances the synchrotron radiation that is produced, as shown in Figure 1.1 (Goldman and Johnston, 2000).

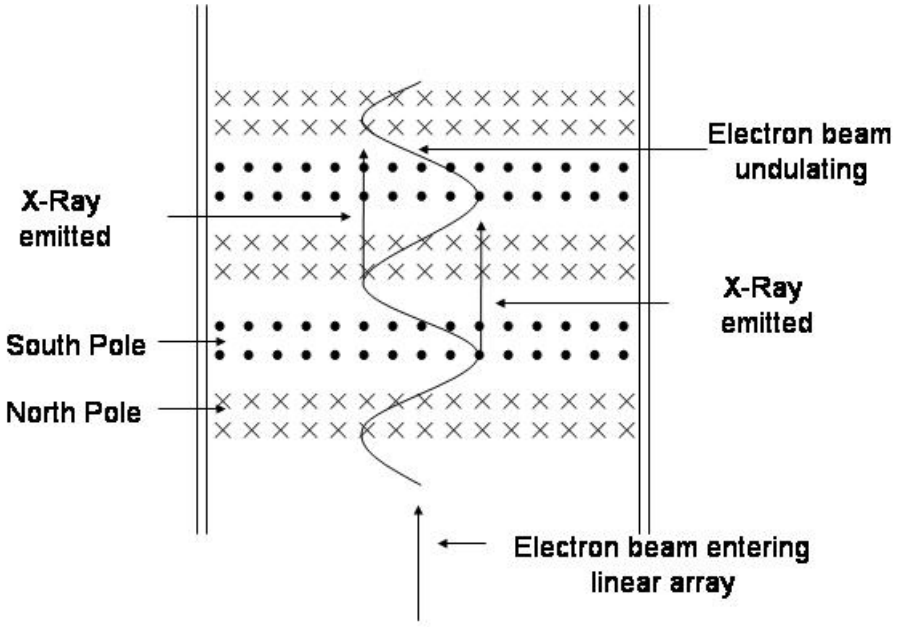

Figure 1.1. Top view of an electron beam undulating in linear arrays of north-south permanent magnets with alternating polarity.

The permanent magnets in the storage ring produce a magnetic field that allows the radiation from each pole to interfere constructively with the neighboring pole. This interference creates peak intensities at certain energies and results in high-brilliance beams at these energies. In an effort to further enhance the X-ray intensity, it has been proposed to replace the permanent magnets in the storage ring with superconducting magnets made of Niobium-Titanium. The superconducting magnets are smaller than their permanent magnet counterparts and therefore can be placed closer together. The superconducting magnets can also generate a higher magnetic field than permanent magnets. The results will be larger, higher frequency undulations and therefore even

more intense X-rays (Goldman and Johnston, 2000). One concept for the superconducting undulator design is illustrated in Figure 1.2. Notice the superconducting coils surrounding iron flux paths and placed in alternating polarity. The superconductor windings wrap around the iron yoke where the helium channel is the axis of rotation.

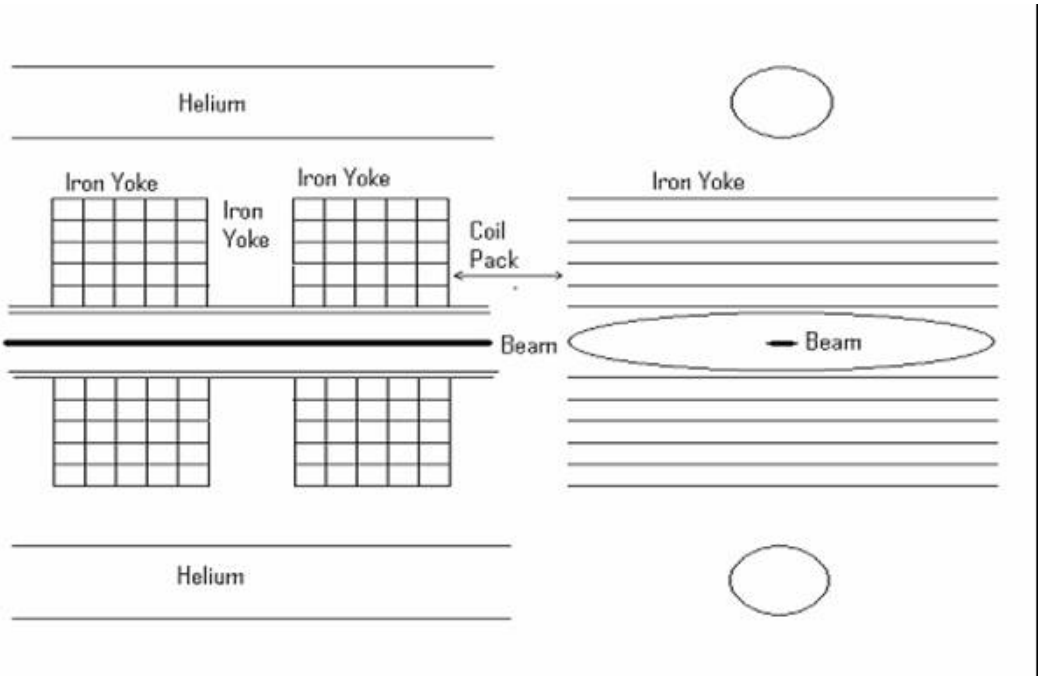

Figure 1.2. One concept for the superconducting undulator design.

The baseline design for the superconducting windings uses Niobium-Titanium conductors operating near 4.2 K. Alternate and improved performance designs will operate near 1.8 K. In order to remain superconducting in the high current, high magnetic field environment associated with the undulator, these windings must be cooled by subcooled, superfluid helium (Goldman, 1996).

With a storage ring circumference of 1 kilometer, the conversion from permanent to superconducting magnets will be a significant undertaking. In order to ensure the success

of this project, ANL will initially carry out experiments that characterize the Niobium-Titanium conductors for the superconducting windings. The conductors in their superconducting states have zero resistance to the flow of electricity. However, all types of superconductors have critical parameters including temperature, current and magnetic field. When these critical parameters are exceeded then the conductor loses its superconducting properties and becomes resistive. The process of a superconductor becoming resistive is referred to as “going normal”. Figure 1.3 illustrates the critical surface for several superconductors; the critical surface is the locus of applied field, temperature, and current density above which the superconductor "goes normal".

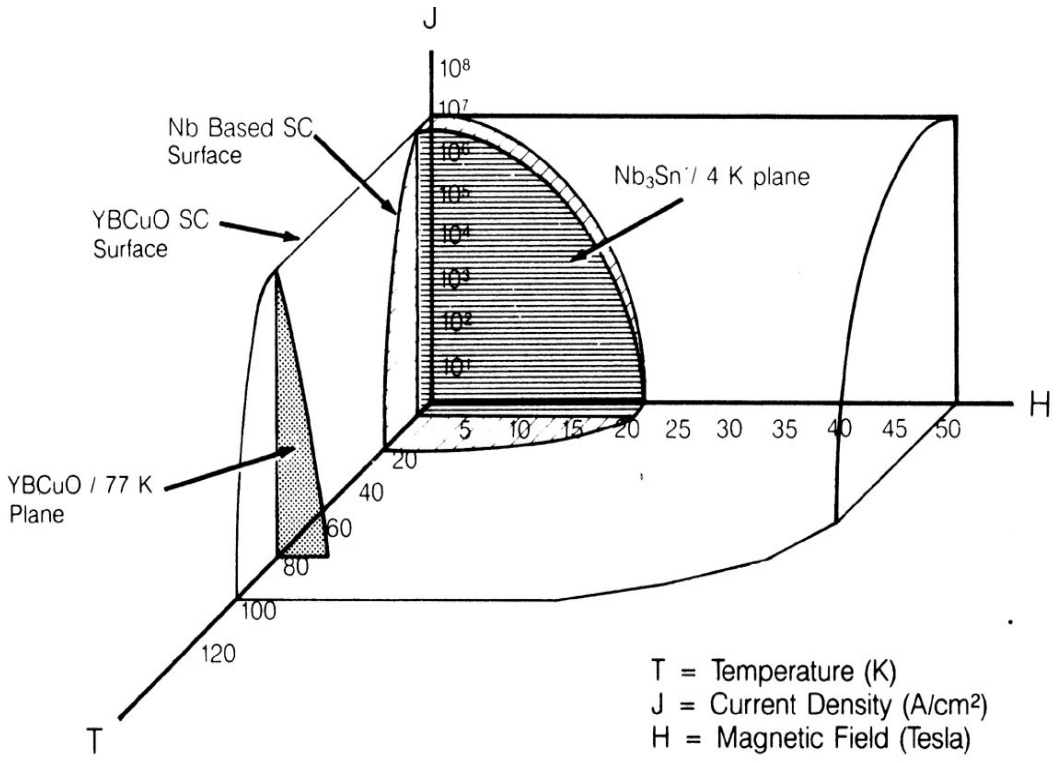

Figure 1.3. Critical surface for several superconductors.

The critical parameters of interest to ANL are maximum current carrying capacity and maximum magnet field. The critical temperature for Niobium-Titanium is 10 K; this material will become resistive at temperatures greater than this critical temperature regardless of the level of current or applied field. Notice that non-zero values of current or applied field will reduce the acceptable temperature of the conductor. For the values of applied field and current density required in the superconducting undulators, it is beneficial to operate the conductor at temperatures less than 2 K. Furthermore, subcooled superfluid helium has several properties that make it an ideal heat transfer fluid for cooling superconducting magnets and therefore operation below the so-called lambda line (the transition between normal and superfluid helium) is desirable. The lambda line for helium is nominally 2.1768 K and therefore this requirement is consistent with the properties of the superconductor itself.

The objective of this project is to design and build a 1.8 K refrigeration system that can be used to provide the required subcooled superfluid He II environment for testing ANL's Niobium-Titanium wire samples. The sample testing will establish the critical surface at levels of current and applied field and in configurations that are consistent with the eventual undulator design.

1.2 Liquid Helium

Helium was first liquefied by Kamerlingh Onnes in 1908 (Khalatnokov, 1965); its normal boiling point is 4.2 K at atmospheric pressure. Liquid helium remains in the liquid phase under its own vapor pressure and would apparently do so right down to absolute zero

temperature. Due to the small mass and extremely weak forces between the helium atoms, significant pressure is required to produce solid helium (25 atmospheres or more). Figure 1.4 illustrates the pressure-temperature diagram for helium.

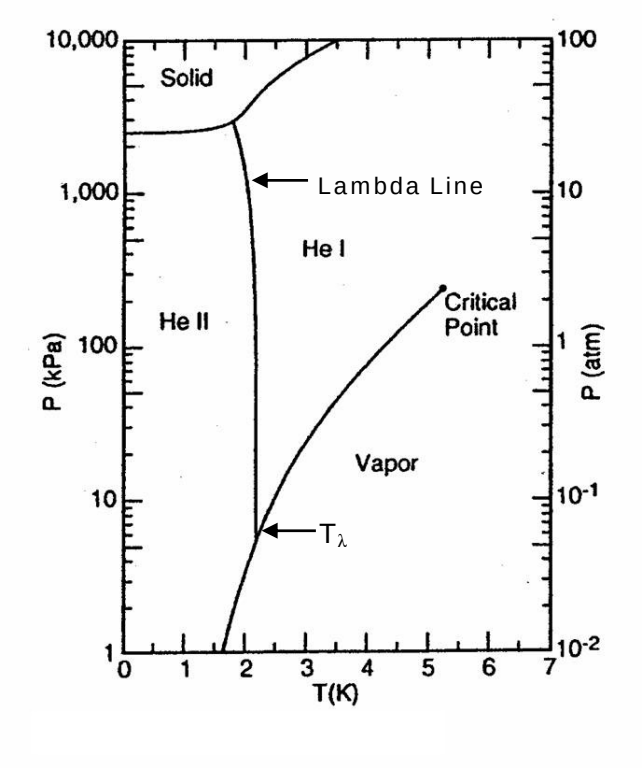

Figure 1.4. Pressure-Temperature diagram for helium.

When liquid helium is cooled to 2.1768 K, it undergoes a phase transition from normal to superfluid helium, shown by the lambda line in Figure 1.4. The phase transition between normal and superfluid helium is referred to as the lambda line because the shape of the specific heat curve, when traced through the transition, appears like the Greek letter λ. The temperature at which the superfluid transition takes place is called the lambda temperature (T_λ). There is no specific volume change or latent heat associated with the lambda transition. Keesom (1927) used the terms He I and He II to distinguish the liquid states that exist above and below T_λ, respectively. He I behaves like a Newtonian fluid.

However, He II has remarkably strange properties due to its quantum effects. In 1938, Kapitza (1941) and independently Allen and Jones (1938) reported that there is no measurable resistance to the flow of He II through small capillaries with diameter on the order of $10^{(-4)}$ cm. Kapitza therefore referred to He II as the "superfluid". On the other hand, experiments using oscillating disks by Keesom and Meyer (1940) demonstrated the existence of a viscous drag, consistent with a viscosity coefficient that was not much less than that of helium gas. It seems as He II is capable of being both viscous and inviscid at the same time. This led to the formulation of the two fluid model by Tisza and Landau (Khalatnokov, 1965).

1.3 Subcooled Superfluid He II

There are two different liquid phases of helium: liquid helium (He I), the *normal liquid*: and helium II (He II), *the superfluid*. The phase transition curve (Figure 1.4) separating the liquid phases is called the lambda line, and the point at which the lambda line intersects the vapor-pressure curve is called the lambda point. The lambda point occurs at a temperature of 2.1768 K (-455.8º F) and a pressure of 5.073 kPa (0.050 atm or 0.736 psia).

The specific heat of liquid helium varies with temperature in an unusual manner for liquids. At the lambda point, the liquid specific heat increases to a large value as the temperature is decreased through this point. The thermal conductivity of liquid helium also behaves unlike conventional fluids. The thermal conductivity of He I decreases with decreasing temperature, which is similar to the behavior of the thermal conductivity of a gas. However below the lambda point, the heat transfer characteristics of He II become

spectacular. When a container of He I is pumped on in order to reduce the pressure above the liquid, the fluid boils vigorously as the pressure of the liquid decreases. During the pumping operation, the temperature of the liquid decreases as the pressure is decreased and the liquid is boiled away. When the temperature reaches the lambda point and the helium transitions to He II, all bubbling suddenly stops. The liquid becomes clear and quiet, although it is still vaporizing quite rapidly at the surface. The thermal conductivity of the He II is so large that vapor bubbles do not have time to form within the body of the fluid before the heat is quickly conducted to the surface of the liquid. Liquid helium I has a thermal conductivity of approximately 24 mW/m-K at 3.3 K, whereas liquid helium II can have an apparent thermal conductivity as large as 85 kW/m-K, approximately 6 orders of magnitude larger. It is this characteristic that makes He II the ideal coolant for superconducting magnets (Barron, 1985).

One of the unusual properties of He II is that it exhibits superfluidity: under certain conditions, it acts as if it has zero viscosity. In order to explain this behavior, a model was developed wherein the helium is assumed to be a mixture of two different fluids: the ordinary fluid and the superfluid. The superfluid component possesses no entropy and moves past other fluids and solid boundaries without friction. Using this model to explain various experimental results requires that liquid He II have a composition of normal and superfluid that varies with temperature; at absolute zero, the liquid composition is 100 percent superfluid while at the lambda point, the liquid composition is 100 percent normal fluid.

The addition of heat to He II raises the temperature of the liquid local to the point of heat addition. According to the two-fluid model, this temperature rise will raise the concentration of normal molecules and lower the concentration of superfluid ones. The superfluid from more distant locations in the bath will move so as to equalize the superfluid concentration throughout the body of the liquid. The normal component flows away from the heat source in such a way that zero net mass flow occurs, but a significant transfer of entropy and heat occurs. The relative motions of the normal and superfluid components are often referred to as convective counterflow. Because the superfluid is frictionless, this motion can occur very rapidly. Based on this discussion, the very high apparent thermal conductivity of He II is associated with a rapid convection process as opposed to the normal, diffusive processes that typically characterize conduction (Barron, 1985).

The very large apparent thermal conductivity of He II makes it an excellent coolant for low-temperature superconductivity testing. In a properly designed cryogenic vessel, this characteristic allows the temperature of the superconductor and the surrounding He II bath to be held nearly constant despite fluctuating heat leaks from the environment and heat loads related to resistive heating at contacts. When testing a superconductor to determine its critical current carrying capacity, the superconductor can briefly go normal (become resistive) and not experience a rapid increase in temperature (that might otherwise damage the superconductor) because the large thermal conductivity of He II keeps the superconductor cool. Therefore, He II is currently being used extensively for low temperature superconductor testing and development. However, it is not sufficient to create a bath of saturated He II as can easily be done by aggressively pumping on a bath

of He I. Heat addition to a bath of saturated He II will result in the formation of normal helium vapor. The drastic decrease in thermal conductivity as liquid helium is converted from He II to vapor at the lambda line will result in large local temperature rises emanating from the point of heat addition. Instead, it is important to create a subcooled bath of liquid He II. By operating in the subcooled region, He II can absorb a large amount of heat energy before reaching the lambda line and therefore transitioning to low conductivity He I. Figure 1.5 shows a phase diagram of helium and includes the operating point associated with our liquid helium refrigeration system at 1 atm. Notice how the 1.8 K operating point at 1 atm lies in the subcooled He II region and is removed from the lambda line.

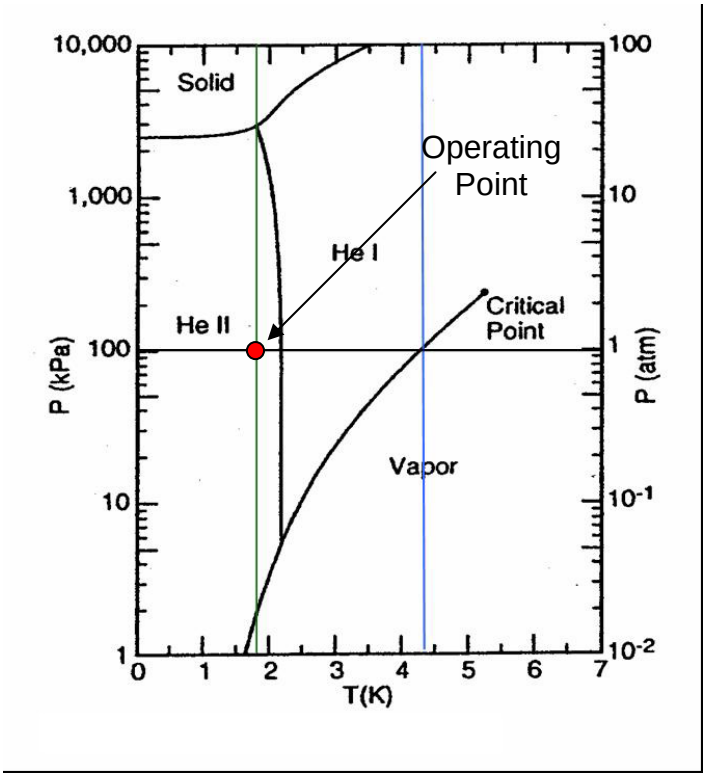

Figure 1.5. Pressure-temperature diagram for helium indicating the operating point for the liquid helium refrigeration system at 1 atm. Notice how the 1.8 K operating point at 1 atm lies in the subcooled He II region and is removed from the lambda line, representing the ideal condition for testing superconductors.

1.4 He II Refrigeration Background

The principle concern associated with the design of a cryogenic experiment or apparatus is the heat load that can be removed from the system at a given temperature. Liquid helium is the only fluid which does not suffer from a systematic decrease of its heat transfer characteristics with decreasing temperature. In fact, liquid helium exhibits outstanding transport properties with respect to heat removal when its temperature is kept below the superfluid transition near 2.18 K. Therefore, subcooled liquid He II is desired both for performing interesting experiments as well as to cool other low temperature experiments. The idea of utilizing a continuously operating refrigeration system to produce subcooled He II was first introduced by Claudet *et al.* (1974) and this type of refrigeration has been incorporated in numerous superconducting systems to date.

The typical subcooled He II refrigeration system is identical to the common, open cycle Joule-Thomson (J-T) refrigerator incorporating a recuperative heat exchanger, a Joule-Thomson valve, a saturated liquid container, and a vacuum pump that produces the pressure difference required to drive the cycle. However, in contrast to the typical J-T refrigerator in which the working fluid begins as a room temperature gas at some elevated pressure and exhausts at ambient pressure; here the working fluid begins as saturated liquid helium near ambient pressure and exhausts as cold vapor under a moderate vacuum. The system may be operated continuously as long as the supply of saturated liquid helium at ambient pressure is maintained (Pfotenhauer, 1992). Augueres (1980) reports the development of a 700 mm diameter cryostat that uses this refrigeration system to produce subcooled superfluid helium at 1.8 K and atmospheric pressure. This facility

was developed to test Niobium-Titanium coils under a magnetic field of up to 10 Tesla. Canavan *et al.* (1988) reported a similar cryostat capable of testing Niobium-Titanium coils under magnetic fields up to 13 Tesla. This facility reported unattended temperature stability of within 2 mK.

The goal of this project was to expand the open cycle helium J-T refrigerator to perform testing of Niobium-Titanium wires and coils at both moderate magnetic fields (up to 5 Tesla) as well as high current (up to 15kA). Pfotenhauer (1992) described the design steps that are required to achieve a desired cooling capacity for a helium J-T refrigerator; these steps have served as a guide during the design of this experiment. This documentation was based on the successful design and implementation of a similar experiment built as a conductor test facility for the Superconducting Magnetic Energy Storage (SMES) Engineering Test Model (ETM) as well as the Proof of Principle Experiment (POPE) (Pfotenhauer *et. al*, 1992). The SMES project was carried out at the High Current Laboratory at the University of Wisconsin-Madison and utilized a 100 kA DC power supply to power the test magnets. The experiment described in this thesis is also conducted in the High Current Laboratory and provides a smaller version of the SMES facility that is specifically tailored to ANL's test criteria. In contrast to the SMES project, this cryostat provides a similar amount of refrigeration capacity but with considerably less helium consumption due to the significant reduction in size, thermal mass and heat leaks.

1.5 Project Overview

Argonne National Labs (ANL) has requested the design and fabrication of a liquid helium refrigeration system that is capable of testing superconducting specimens at temperatures down to 1.8 K, currents up to 15 kA, and magnetic fields from 0 to 5 Tesla. The low temperature, high current and high magnetic field requirements make this refrigeration system unique and not readily available within ANL or its contractors. The Cryogenics Laboratory at the University of Wisconsin, Madison has been awarded the contract to design and build this experimental apparatus and perform tests to characterize ANL's Niobium-Titanium superconducting wires. The UW-Madison Cryogenics Lab has unique experience with the design, fabrication, and operation of this type of refrigeration system as part of the Superconducting Magnetic Energy Storage (SMES) projects during the 80's and 90's. Furthermore, the personnel at the Applied Superconductivity Center and the UW-Madison are uniquely qualified to measure the superconducting characteristics of the undulator magnet conductors. The superconducting specimens will be immersed in a bath filled with subcooled, superfluid helium at atmospheric pressure. Subcooled superfluid helium is an ideal coolant for superconductors as it has an exceptionally high thermal conductivity and high heat capacity. These characteristics allow superconducting specimens to be tested at a constant temperature.

This thesis describes the design, fabrication, and an initial test run of the refrigeration system. The shake-down test demonstrated that the system was capable of producing subcooled, superfluid helium; albeit at 2.09 K rather than the 1.80 K design target.

However, the malfunction that limited the ultimate temperature of the refrigeration system, a faulty Joule-Thomson valve, has been identified and corrected. The integrity of the cryostat components and instrumentation has been verified at cryogenic temperatures. The result of the shake-down test is a comprehensive operating procedure as well as several recommendations for system enhancements which have been noted. Preparations are currently underway to integrate the magnet and sample power supplies and begin testing superconducting samples.

1.6 Description of Refrigerator

The refrigeration system consists of a double walled, vacuum insulated stainless steel vessel (referred to as the He II liquid bath) that is placed within a larger dewar (referred to as the 4.2 K bath). Two heat exchangers, a J-T valve, and a vacuum system make up the remaining key components of the refrigeration system, as shown in Figure 1.6. The first heat exchanger is a recuperator with a shell and tube geometry. This heat exchanger is referred to as the recuperator and mounted to the top of the He II liquid bath. The hot inlet for this heat exchanger is fed by the 4.2 K bath. The hot exit is connected to an externally located vacuum pump via a pump line. A J-T valve is connected to the cold exit of the recuperator. The J-T valve feeds a second heat exchanger that is referred to as the He II heat exchanger. The He II heat exchanger is a large copper pipe that is immersed in the He II liquid bath.

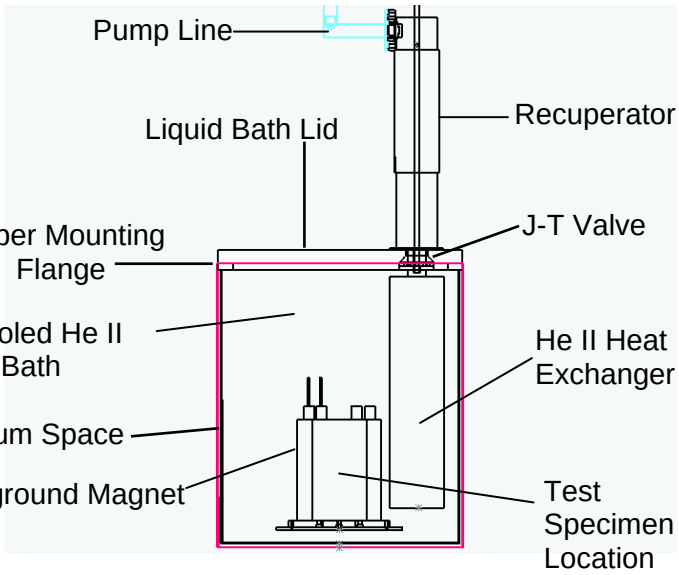

Figure 1.6. Key components that make up the refrigeration system.

The superconducting test specimen is placed in the bore of the background magnet that is immersed in the He II liquid bath. The background magnet produces a magnetic field of up to 5 Tesla in order to simulate the magnetic field that the conductors will be exposed to during operation within the APS undulator.

Figure 1.7 shows the refrigeration system and the state points for the helium refrigerant on a pressure-temperature diagram that is consistent with operating the refrigeration system at steady state.

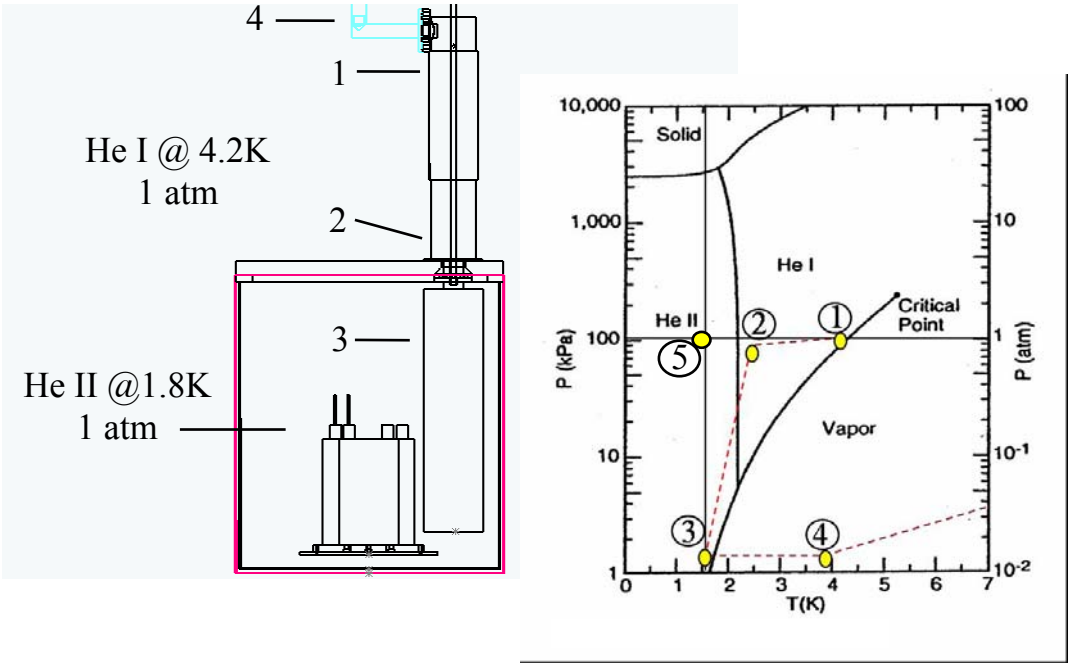

Figure 1.7. He II J-T refrigeration system schematic and the state points associated with the helium refrigerant during steady state operation.

Initially, both the large 4.2 K bath and smaller He II liquid bath are filled with liquid helium at 4.2 K and 1 atm (State 1). Once activated, the external vacuum pump will reduce the pressure within the He II heat exchanger to approximately 1.6 kPa (State 3). This pressure difference causes liquid helium to be drawn from the 4.2 K bath into the recuperator (the shell and tube heat exchanger); the helium is pre-cooled and expanded through the J-T valve where it is ultimately throttled to approximately 1.7 K (and in the process converted to superfluid helium, or He II). This cold, saturated He II enters the He II heat exchanger (State 3) and cools the helium at 1 atm located inside of the He II liquid bath. The vapor from the He II heat exchanger is drawn into the low-pressure side of the recuperator, pre-cooling the incoming helium (State 4). Finally, the helium passes through the vacuum pump and exits to the atmosphere.

Liquid He I at 4.2 K and 1 atm is located on the He I - vapor line in Figure 1.7. As the pressure is reduced, the temperature of the helium follows the contour of this vapor line. Thus, the He II inside of the He II heat exchanger at state (3) in Figure 1.7 is at 1.7 K and 1.01 kPa and is a saturated mixture. As energy is added to this saturated mixture it will rapidly boil and turn to vapor. Vaporized helium has a low thermal conductivity when compared to He II, and therefore it is undesirable as a means of keeping the superconducting specimen cool. However, the 1.7 K saturated mixture inside of the heat exchanger can be used to cool the helium that fills the He II liquid bath; this helium is initially at 4.2 K but its temperature is reduced to 1.8 K due to its thermal communication with the He II heat exchanger. The helium that fills the He II liquid bath remains at 1 atm during this process. The phase diagram shows state (5) which is the operating point of the 1.8 K refrigerator that is in the He II subcooled region. By operating at this point, energy can be added to the He II without rapidly converting it to vapor and therefore the superconducting sample is mounted in the subcooled He II liquid bath.

Figure 1.8 shows the key refrigeration system components as well as the two mechanisms that are used to control the refrigeration system. A pneumatic actuator adjusts the position of the J-T valve in order to control the mass flow rate of helium through the refrigeration system and therefore the level of saturated He II in the He II heat exchanger. A butterfly valve is located in the external vacuum line. The position of the butterfly valve adjusts the pressure in the He II heat exchanger and therefore the temperature in the system.

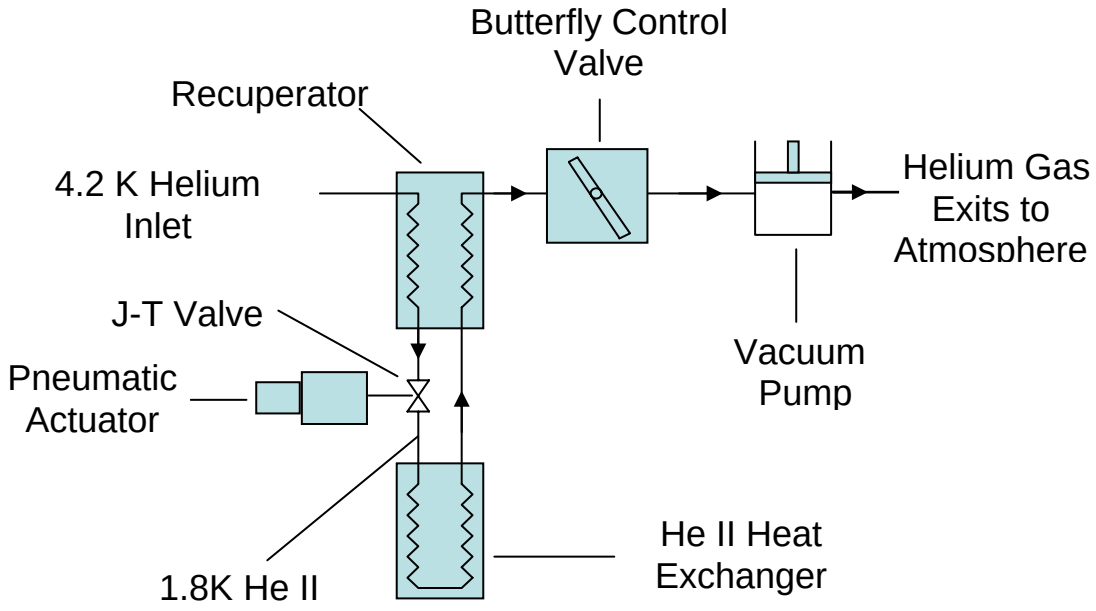

Figure 1.8. 1.8K liquid helium refrigeration cycle.

Chapter 2 Test Facility Design and Construction

Figure 2.1 illustrates the cryostat assembly and the dewar that accepts the cryostat. This section will describe the design and fabrication of the major components of the cryostat assembly as well as the dewar.

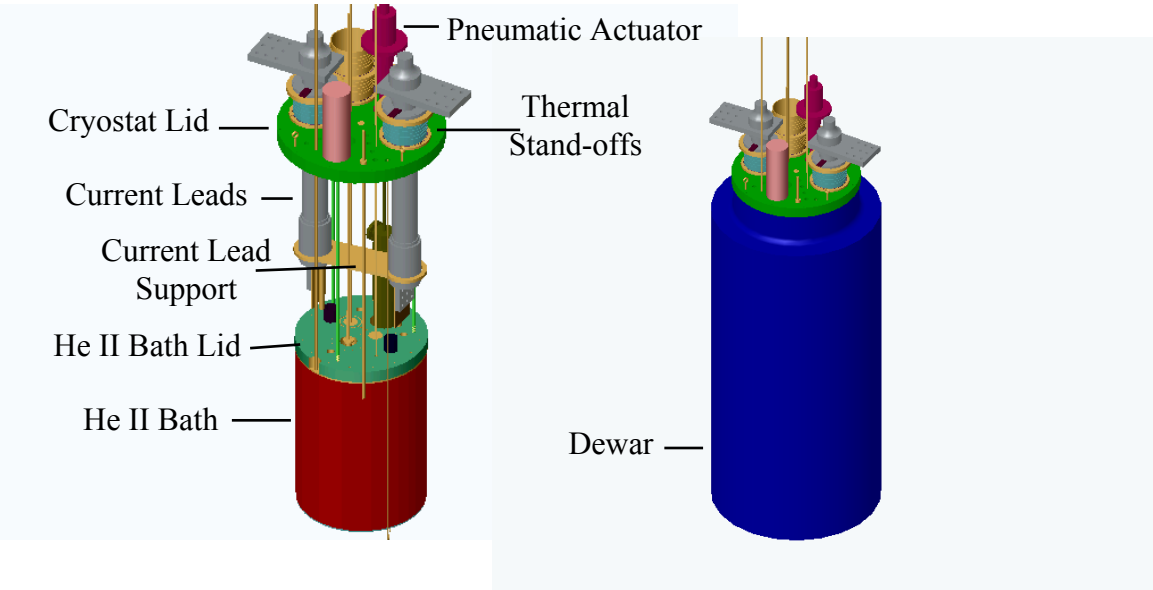

Figure 2.1. Cryostat assembly and dewar.

2.1 Dewar

The purpose of the dewar is to provide an environment that is suitable for carrying out very low temperature experiments. The space within the dewar can be maintained at liquid helium temperatures without consuming excessive amounts of liquid helium cryogen. The dewar used for this experiment was manufactured by Precision Cryogenic Systems, Inc. The inside diameter and depth are 20 inches and 65 inches, respectively. The wall of the dewar consists of several layers including an outer aluminum shell, an evacuated space with multi-layer radiation insulation, a liquid nitrogen jacket, and a G-10 inner shell. These layers taken together create an extremely effective thermal barrier that

minimizes the heat leak between the ambient surroundings and the cryogenic experiment housed by the dewar.

2.2 He II Bath

The purpose of the He II bath is to contain the subcooled, superfluid helium used to test the superconducting samples. The He II bath is a two-piece assembly including the He II bath lid and the He II bath container, as shown in Figure 2.2. The He II bath container is attached to the lid via fasteners through the upper mounting flange and can therefore be removed to expose the hardware and samples that are mounted inside the He II bath.

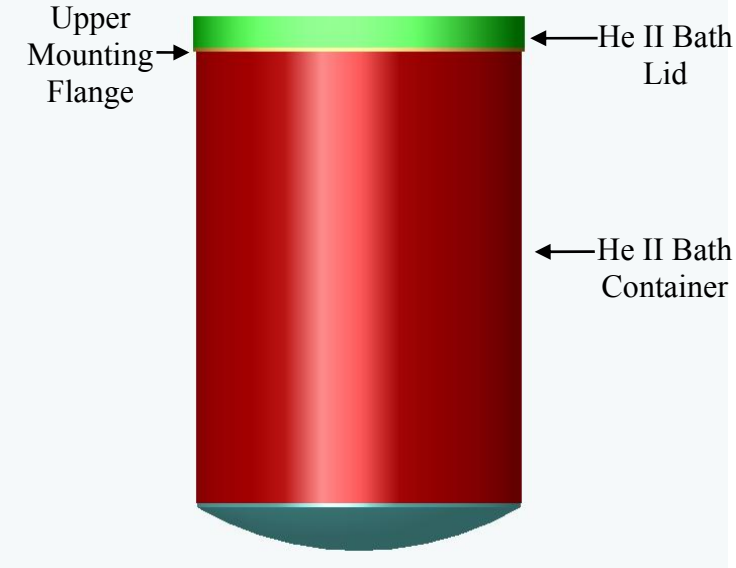

Figure 2.2. He II bath consisting of the He II bath lid and He II bath container.

The He II bath container is a double walled, vacuum insulated stainless steel container that is bucket-shaped and, when mounted to the He-II bath lid, provides an enclosed volume that contains the subcooled superfluid helium. The He II bath container was constructed from the following components, all of which are composed of 304 stainless steel:

- the upper mounting flange was fabricated from 1 inch thick plate,

- the inner cylindrical wall was rolled from 0.075 inch thick sheet metal,
- the outer cylindrical wall was rolled from 0.075 inch thick sheet metal,
- the 0.075 inch thick inner dome was manufactured at Acme Metal Spinning, Inc., and
- the 0.075 inch thick outer dome was also manufactured at Acme Metal Spinning, Inc.

These components were tungsten inert gas (TIG) welded in order to form a hermetic vacuum space. The vacuum space was leak checked using a helium leak detector.

Figure 2.3 illustrates the He II bath integrated with the other key components of the refrigeration system and experiment.

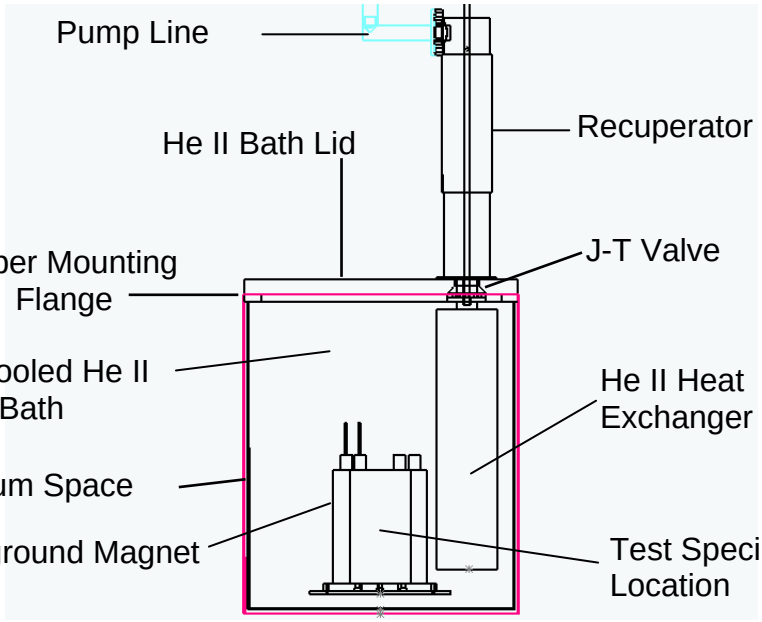

Figure 2.3. He II bath integrated with the key refrigeration system and experiment components.

Heat leaks from the 4.2 K bath into the 1.8 K He II bath constitute the majority of the refrigeration requirement that must be met by the 1.8 K refrigerator, as described in

Chapter 1. Because the refrigeration system capacity is limited by the pumping capacity that is available, these heat leaks must be kept to a minimum to ensure that the 20 W of available refrigeration capacity is not exceeded. Therefore, calculation and control of the thermal paths constituted the key design challenge for this component. The various heat leaks are carefully calculated and tabulated in the subsequent section.

2.2.1 He II Bath Heat Leaks

2.2.1.1 Vent/Fill Cones

The He II bath lid was constructed from a 2.5 inch thick plate of G-10. In order to allow liquid helium from the 4.2 K bath to fill the He II bath prior to activating the refrigeration system it is necessary to provide a controllable opening in the He II bath lid. A separate opening is included to allow vapor to escape as the internal components in the He II bath are initially cooled. These openings are also necessary from a safety standpoint as they provide pressure relief in the event of a magnet quench or other large release of heat in the He II bath.

However, these openings constitute large potential sources of heat leak from the 4.2 K bath to the 1.8 K bath. The crack that characterizes any opening in the lid, even when it is re-sealed, will eventually be occupied by superfluid liquid helium when the system is operating. As discussed in Chapter 1, superfluid helium has essentially zero viscosity and very high thermal conductivity. Therefore, even very small cracks filled with superfluid helium represent a low impedance thermal path and a significant heat leak. In order to maximize the length and resistance of this thermal path, cone shaped openings were used in the He II bath lid. This geometry had the additional benefit of being self-

sealing; that is, if a force is provided downward against the cone then the opening will close to within the tolerance associated with the machined parts.

Figure 2.4 illustrates the two cone shaped holes that were installed in the lid. The cones have a starting diameter of 2 inches on the 4.2 K side of the He II bath lid and an ending diameter of 1 inch on the 1.8 K side of the lid.

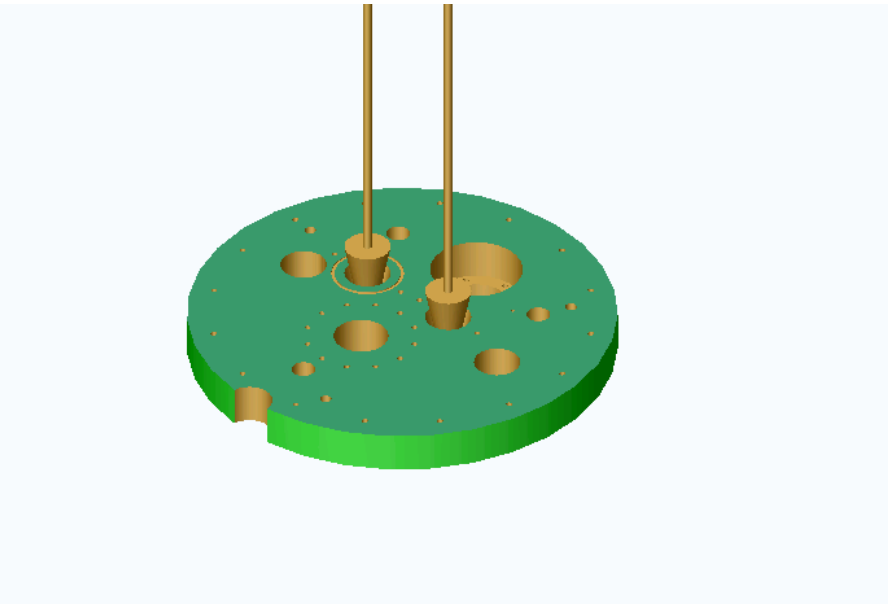

Figure 2.4. He II bath lid made of G-10. Note the conical pressure relief and fill valves made of Teflon.

The Teflon cones are held into the conical holes in the He II bath lid with springs that are captured between the top of the Teflon cones and support brackets. Two 0.375 inch diameter G-10 rods are threaded into the Teflon cones and extend through the cryostat cover in order to allow actuation of these pieces.

The Teflon cones serve two purposes: 1) provide a means to initially fill the He II bath with 4.2 K liquid helium when the cones are pulled up and away from the He II bath lid,

and 2) act as a pressure relief valve by moving up against the springs and away from the lid if the pressure within the He II bath exceeds 2 psig. The springs apply a force on the cones that tend to seat them into the G-10 cover and provide a good seal; however, this is not a hermetic seal and the superfluid He II is difficult to contain. Therefore, the heat leak between the He II and He I around the mating surfaces of the cones and the G-10 lid must be accounted for. This heat leak ($\dot{Q}_{cone}$) was calculated using the Steady State Peak Heat Flux Method:

$$\dot{Q}_{cone} = Number_{Cones}\, \dot{Q}''_{cone}\, Area_{cone\_gap} \tag{2.1}$$

$$\dot{Q}''_{cone}\, L_{cone}^{(1/3)} = F_T \tag{2.2}$$

$$F_T = 14.6835 \left[\frac{kW}{m^{5/3}} \right] \tag{2.3}$$

$$Area_{Cone\_Gap} = \pi \left[\left(\frac{D_{cone} + Gap_{cone}}{2} \right)^2 - \left(\frac{D_{cone}}{2} \right)^2 \right] \tag{2.4}$$

$$D_{cone} = \frac{D_{top\_cone} + D_{bottom\_cone}}{2} \tag{2.5}$$

where F_T is the steady state peak heat flux of He II at 1.8 K (Weisend 1998), L_{cone} is the length of the gap that the heat must travel through, $Area_{cone}$ is the average cross-sectional area of the gap, $Diameter_{cone}$ is the average diameter of the cone, $Diameter_{top\_cone}$ is the diameter of the top of the cone, $Diameter_{bottom\_cone}$ is the diameter of the bottom of the cone, $Number_{Cones}$ is the number of cones in the He II bath lid, and Gap_{cone} is the estimated gap between the G-10 and Teflon cones. Table 2.1 summarizes the parameters used in the heat leak calculations for the Vent/Fill cones.

Table 2.1. Parameters and results of mass transfer around Vent/Fill cones.

Parameter	Symbol	Value
heat flux through gap	$\dot{Q}"_{cone}$	36.8 [kW/m^2]
cross-sectional area of gap	$Area_{Cone\_Gap}$	7.61 10$^{(-6)}$ [m^2]
length of gap between cone and G-10	L_{cone}	0.0635 [m]
peak heat flux (Weisend 1998)	F_T	14.68 [kW/m$^{5/3}$]
Number of cones in He II bath lid	$Number_{cones}$	2
Average diameter of Teflon cones	$Diameter_{cone}$	0.038 [m]
Diameter of the top of cone	D_{top_cone}	0.051 [m]
Diameter of the bottom of cone	D_{bottom_cone}	0.025 [m]
Estimated gap between cone lid	Gap_{cone}	0.000127 [m]
Mass transfer heat leak around 2 cones	$\dot{Q}_{cone}$	**0.56 [W]**

Pressure relief is an important aspect of designing any cryogenic vessel. If a superconducting specimen goes normal then there is the potential to transfer a large amount of energy in the form of heat to the liquid helium due to the high current that is instantaneously being passed into the cryostat. Figure 2.5(a) illustrates the specific volume of helium as a function of temperature at a fixed pressure of 1 atm. Figure 2.5(b) illustrates the pressure as a function of temperature for a fixed specific volume that is consistent with the specific volume of the 1.8 K helium contained in the He II bath. Notice the large increase in specific volume that occurs as the temperature is increased from 4.2 K to 5 K at 1 atm, shown in Fig. 2.5(a). The vaporization of 1 cm^3 of liquid at 1.8 K yields 7.5 cm^3 of vapor at 4.2 K and 1 atm. Figure 2.5(b) illustrates that in order to prevent this natural increase in specific volume the pressure of the helium contained in the He II bath must climb to an extremely high value (over 1000 psia) if the bath was full of He II and a large heat source raised the temperature of the vapor to 20 K without proper venting. The He II container is not designed to withstand such high pressures and therefore would fail, probably catastrophically resulting in damage to both the equipment and possibly the operator.

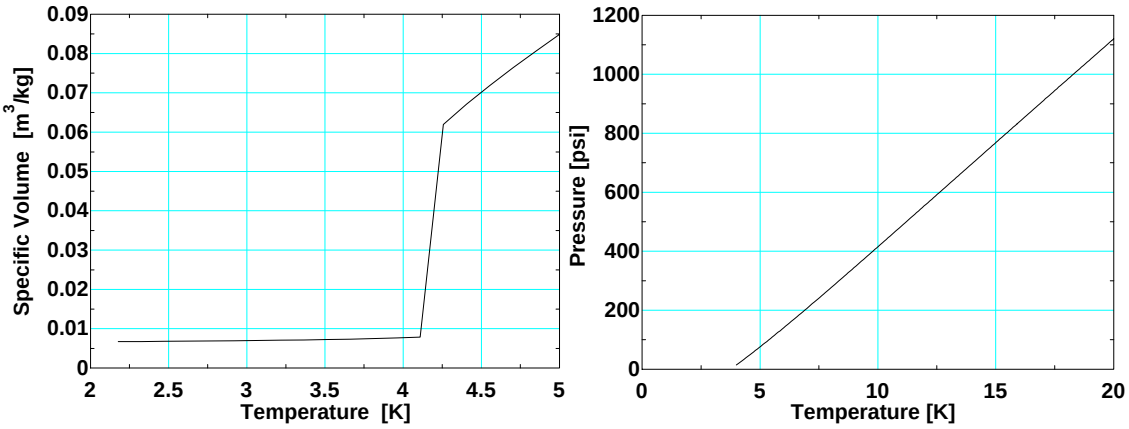

Figure 2.5. (a) Specific volume at a fixed pressure of 1 atm and (b) pressure as a function of temperature for a fixed specific volume for the helium contained in the He II bath.

The Teflon cones in the He II bath lid are designed to open against their springs when the internal bath pressure reaches 2 psig after which the contained helium will be vented to the 4.2 K bath. The 4.2 K bath has a 4 psig pressure relief valve that is installed in the cryostat cover so that this helium will ultimately vent to atmosphere (see Figure 2.6).

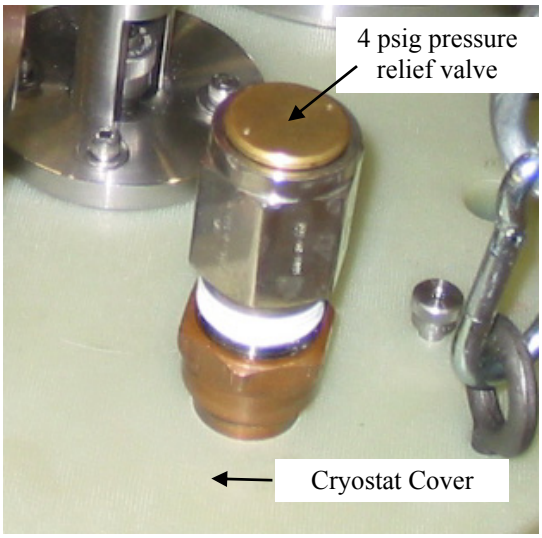

Figure 2.6. 4 psig pressure relief valve in cryostat cover.

2.2.1.2 Epoxy Seal

The superconducting test sample is installed inside of the He II bath. In order to allow access to the bath for installation and removal of the sample, it is necessary that the He II bath container can be separated from the lid and removed. The joint required for this is illustrated in Figure 2.7.

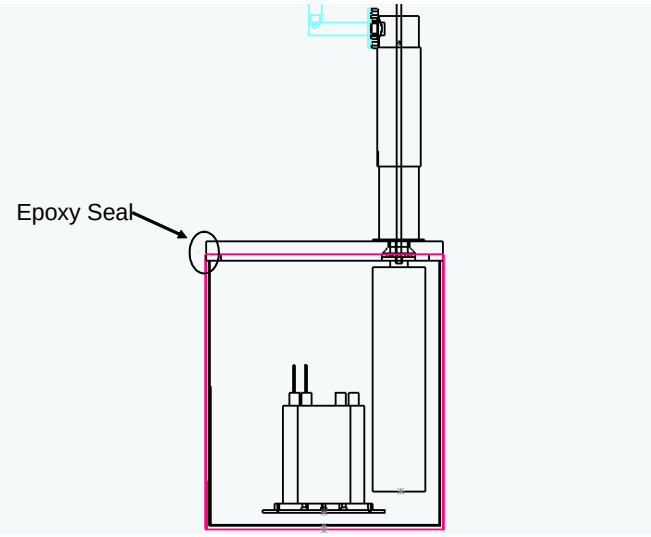

Figure 2.7. He II bath lid epoxy seal.

When the temperatures inside and outside of the He II bath are above T_λ (i.e., above the superfluid transition temperature) then standard cryogenic seals (e.g., indium wire) would be sufficient for this demountable joint. The relatively poor thermal conductivity of liquid helium above T_λ provides a sufficient degree of thermal insulation and isolates the He II bath from the 4.2 K bath. However, when the temperature within the He II bath is below T_λ, then the extremely low viscosity and high thermal conductivity of the superfluid results in a significant heat flow through the very small channel associated with this demountable seal and the design of the seal becomes critical to achieving the required performance (Pfotenhauer 1996). Conventional cryogenic, reusable seals are no longer a viable option because of the high thermal conductivity of the sealing material.

Table 2.2 summarizes the heat leak through various seal configurations calculated using a simple, geometry based conduction resistance under the condition where 4.2 K is applied to one side of the seal and 1.8 K to the other side. The four different materials considered include a copper conflat gasket, an indium wire o-ring, a Teflon wire o-ring, and McMaster Carr Cataolog#123 hand-workable epoxy putty. The seal diameter is assumed to be 16 inch for each case.

Table 2.2. Calculated heat leak through the He II bath lid seal for different materials.

Material	**Cross-sectional area [m^2]**	**Width [m]**	**Conductivity [W/m-K]**	**Heat leak**
copper conflat gasket RRR=50	$2.51\ 10^{(-3)}$	0.013	233	111 [W]
indium wire	$1.52\ 10^{(-4)}$	$1.27\ 10^{(-4)}$	633	9.1 [W]
Teflon wire	$1.52\ 10^{(-4)}$	$1.27\ 10^{(-4)}$	0.028	0.4 [mW]
epoxy	$1.52\ 10^{(-4)}$	$1.27\ 10^{(-4)}$	0.043	0.6 [mW]

Table 2.2 clearly shows that the heat leak through a copper conflat gasket or the indium o-ring is quite large and therefore unacceptable for this application. Notice that the thermal conductivity of indium is much higher than the copper conflat gasket, yet the conflat has a higher heat leak. The reason for this is the indium wire can be mechanically squeezed into a much smaller cross-sectional area compared to the copper conflat gasket. In contrast, the Teflon o-ring and the epoxy bead both exhibit a thermal resistance that is orders of magnitude less than the metal-based seals and therefore consistent with the refrigeration requirements. However, the seals created using these configurations are not hermetic and therefore the heat leak related to the superfluid through the seals to the 4.2 K bath must also be considered. An analytical model of this situation is not possible given the uncertainties associated with the geometry, in particular the size of the gap that is formed. However, Pfotenhauer (1996) measured the heat leak through an epoxy bead

and a Teflon o-ring in a similar configuration and at similar temperatures to those proposed for this project. It was determined that the overall heat leak through the epoxy bead was slightly less than the Teflon o-ring. When making the epoxy seal, Pfotenhauer coated both sealing surfaces several times with furniture wax in order to prevent the epoxy from adhering to and permanently bonding with the mating parts. These results have been used together with a geometric-based scaling factor in order to estimate the combined effect of the superfluid heat transfer and radial conduction heat leak through the epoxy seal that was used in this experiment. The scaling factor is the ratio of the average seal radius for the He II bath lid to the average seal radius used in Pfotenhauer's experiment:

$$Scaling_{lid} = \frac{r_{avg\_lid}}{r_{Pfot}} \tag{2.6}$$

$$r_{avg\_lid} = \frac{r_{2\_epoxy\_lid} + r_{1\_epoxy\_lid}}{2} \tag{2.7}$$

The heat leak through an epoxy seal is then calculated as follows:

$$\dot{Q}_{epoxy\_lid\_He\_leak} = Scaling_{lid}\ He_{leak\_Pfot} \tag{2.8}$$

$$He_{leak\_Pfot} = 3.4\ \ 10^{(-2)}\ [W] \tag{2.9}$$

$$\dot{Q}_{epoxy\_lid\_He\_leak} = 0.20[W] \tag{2.10}$$

where $Scaling_{lid}$ is the scaling factor, and He_{leak_Pfot} is the heat leak that was experimentally observed by Pfotenhauer. Table 2.3 summarizes the parameters and results used for this calculation.

Table 2.3. Parameters and results used in He II bath lid epoxy seal heat leak calculation.

Parameter	Symbol	Value
Geometry- based scaling factor	$Scaling_{lid}$	5.68
Average radius of seal	$r_{avg,lid}$	0.20 [m]
Average radius of seal used in Pfotenhauer's experiment	r_{Pfot}	0.035 [m]
Outside radius of epoxy seal	$r_{2\_epoxy\_lid}$	0.21 [m]
Inside radius of epoxy seal	$r_{1\_epoxy\_lid}$	0.19 [m]
Heat leak experimentally observed by Pfotenhauer	He_{leak_Pfot}	0.034 [W]
Calculated heat leak through epoxy seal	$\dot{Q}_{epoxy\_lid\_He\_leak}$	**0.20 [W]**

The He II bath lid is sealed to the stainless steel upper flange with a 0.25 inch diameter epoxy bead of McMaster Carr Catalog #123 hand-workable putty (Part Number 7531A11). Both sealing surfaces were coated several times with epoxy releasing agent in order to prevent the epoxy from permanently bonding the He II bath lid to the He II bath container. Four, 5 mm thick flat washers were placed on the edge of the upper flange 90 degrees apart. The flat washers act as a mechanical stop and maintain a consistent epoxy seal thickness when the two flanges are drawn together. Bellville washers were used under the heads of the He II bath lid bolts in order to maintain tension on the bolts even as the G-10, epoxy and stainless steel contract at different rates during cool-down.

2.2.1.3 Recuperator Mounting Flange

Figure 2.8 illustrates how the recuperator is bolted to the He II bath lid via a mounting flange. The flange was sealed to the G-10 lid with epoxy and epoxy release agent using a design consistent with the bath lid to bath container joint discussed in the previous section.

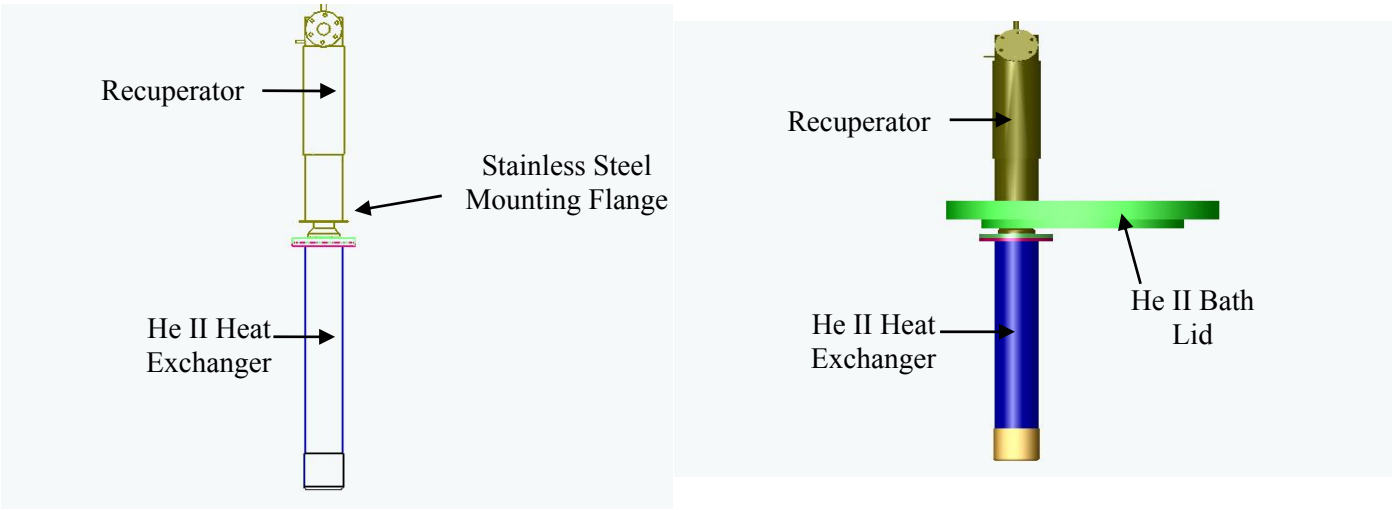

Figure 2.8. Recuperator is mounted to He II bath lid with a stainless steel mounting flange.

Conduction through the flange is therefore:

$$\dot{Q}_{cond\_HXCH\_flange} = k_{ss}\ Area_{HXCH\_flange}\left[\frac{T_{s2} - T_{s1}}{L_{HXCH\_flange}}\right] \tag{2.11}$$

$$\dot{Q}_{cond\_HXCH\_flange} = 0.20\,[W] \tag{2.12}$$

where k_{ss} is the thermal conductivity of stainless steel, $Area_{HXCH\_flange}$ is the cross-sectional area of the flange relative to conduction, L_{HXCH_flange} is the nominal conduction length, and T_{s2} and T_{s1} are the temperatures driving the heat leak through the flange. The heat leak related to the superfluid helium and radial conduction through the epoxy bead is calculated using the experimental data from Pfotenhauer as described in the previous section:

$$\dot{Q}_{HXCH\_HE\_Leak} = Scaling_{HXCH}\ He_{leak\_Pfot} \tag{2.13}$$

where the scaling factor is:

$$Scaling_{HXCH} = \frac{r_{avg\_HXCH}}{r_{Pfot}} \tag{2.14}$$

and the average radius of the heat exchanger epoxy bead is:

$$r_{avg\_HXCH} = \frac{r_{2\_epoxy\_HXCH} + r_{1\_epoxy\_HXCH}}{2} \tag{2.15}$$

$$\dot{Q}_{HXCH\_HE\_Leak} = 0.036\ [W] \tag{2.16}$$

The total heat transferred through the recuperator flange is therefore:

$$\dot{Q}_{\_HXCH\_heat\_leak\_Total} = \dot{Q}_{cond\_HXCH\_flange} + \dot{Q}_{HXCH\_HE\_Leak} \tag{2.17}$$

$$\dot{Q}_{\_HXCH\_heat\_leak\_Total} = 0.23[W] \tag{2.18}$$

Table 2.4 summarizes the parameters and results used for this calculation.

Table 2.4. Parameters and results used in recuperator flange and seal heat leak calculations.

Parameter	Symbol	Value
Average thermal conductivity of 304 stainless steel	k_{ss}	0.16 [W/m-K]
Cross-sectional area of recuperator flange	$Area_{HXCH\_flange}$	0.0032 [m^2]
Temperature of He I bath	T_{s2}	4.2 [K]
Temperature of He II bath	T_{s1}	1.8 [K]
Thickness of recuperator flange	L_{HXCH_flange}	0.0064 [m]
Average radius of recuperator flange	r_{avg_HXCH}	0.037 [m]
Geometry- based scaling factor	$Scaling_{HXCH}$	1.044
Average radius of seal used in Pfotenhauer's experiment	r_{Pfot}	0.035 [m]
Outside radius of recuperator flange epoxy seal	$r_{2\_epoxy\_HXCH}$	0.041 [m]
Inside radius of recuperator flange epoxy seal	$r_{1\_epoxy\_HXCH}$	0.032 [m]
Conductive heat leak through recuperator flange	$Q_{cond\_HXCH\_flange}$	0.20 [W]
He II heat leak through recuperator flange epoxy seal	$Q_{HXCH\_HE\_Leak}$	0.036 [W]
Total heat leak through recuperator flange and epoxy seal	$\dot{Q}_{\_HXCH\_heat\_leak\_Total}$	**0.23 [W]**

2.2.1.4 Hall-Effect Access Hole Cover

A 2.375 inch access hole was placed in the He II bath lid in order to provide future access for a hall-effect probe that will allow the magnetic field produced/experienced by a superconducting sample to be accurately measured and mapped. The hall-effect access

hole cover was made of 2 inch thick G-10 and sealed with McMaster Carr Catalog #123 hand workable epoxy putty and epoxy release agent (see Figure 2.9).

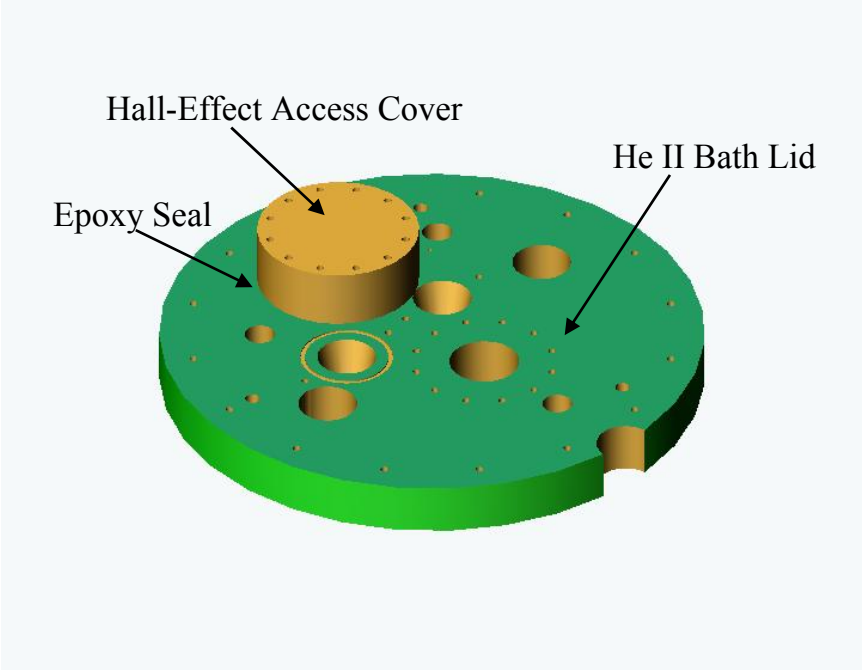

Figure 2.9. Hall-effect access cover is mounted to He II bath lid with an epoxy seal.

Axial conduction through the G-10 hall-effect access cover was calculated:

$$\dot{Q}_{cond\_Hall\_Effect} = k_{G10}\ Area_{Hall\_Effect}\left[\frac{(T_{s2}-T_{s1})}{L_{Hall\_Effect}}\right] \tag{2.19}$$

$$\dot{Q}_{cond\_Hall\_Effect} = 0.0074\ [W] \tag{2.20}$$

where L_{Hall_Effect} is the thickness of the access hole cover, k_{G10} is the thermal conductivity of G-10, and $Area_{Hall\_Effect}$ is the cross-sectional area of the access cover.

The heat leak between the He II and He I and radial conduction through the epoxy bead is:

$$\dot{Q}_{HALL\_EFFECT\_HE\_Leak} = Scaling_{Hall\_Effect}\ He_{leak\_Pfot} \tag{2.21}$$

$$Scaling_{Hall\_Effect} = \frac{r_{avg\_Hall\_Effect}}{r_{Pfot}} \tag{2.22}$$

$$r_{avg\_Hall\_Effect} = \frac{r_{2\_Hall\_Effect} + r_{1\_Hall\_Effect}}{2} \tag{2.23}$$

$$\dot{Q}_{Hall\_Effect\_HE\_Leak} = 0.039\ [W] \tag{2.24}$$

$$\dot{Q}_{\_Hall\_Effect\_heat\_leak\_Total} = \dot{Q}_{cond\_Hall\_Effect} + \dot{Q}_{Hall\_Effect\_HE\_Leak} \tag{2.25}$$

$$\dot{Q}_{\_Hall\_Effect\_Heat\_leak\_Total} = 0.046\ [W] \tag{2.26}$$

Table 2.5 summarizes the parameters and results used for this calculation.

Table 2.5. Parameters and results used in hall-effect access hole cover and seal heat leak.

Parameter	Symbol	Value
Thermal conductivity of G-10	k_{G10}	0.054 [W/m-K]
Cross-sectional area exposed to 1.8 K	$Area_{Hall\ Effect}$	0.0029 [m^2]
Temperature of the He I bath	T_{s2}	4.2 [K]
Temperature of the He II bath	T_{s1}	1.8 [K]
Thickness of cover	$L_{Hall\ Effect}$	0.051 [m]
Average radius of epoxy seal	$r_{avg\ Hall\ Effect}$	0.040 [m]
Geometry-based scaling factor	$Scaling_{Hall\ Effect}$	1.135
Average radius of epoxy seal used in Pfotenhauer's experiment	r_{Pfot}	0.035 [m]
Outside radius of seal	$r_{2\ Hall\ Effect}$	0.048 [m]
Inside radius of seal	$r_{1\ Hall\ Effect}$	0.032 [m]
Conductive heat leak through cover	$Q_{cond\ Hall\ Effect}$	0.0074 [W]
Mass transfer heat leak through epoxy seal	$Q_{Hall\_Effect\_HE\_Leak}$	0.039 [W]
Total heat leak through hall-effect access cover	$\dot{Q}_{\_Hall\_Effect\_Heat\_leak\_Total}$	**0.046 [W]**

2.2.1.5 He II Bath Upper Mounting Flange

The He II bath lid mounts to the He II bath via an upper mounting flange. The upper mounting flange was machined from 1 inch thick 304 stainless steel and is sealed to the G-10 He II bath lid with epoxy putty and releasing agent. The heat leak through the

stainless steel flange was approximated by separately calculating both the 1-D axial and radial conduction, as shown in Figure 2.10.

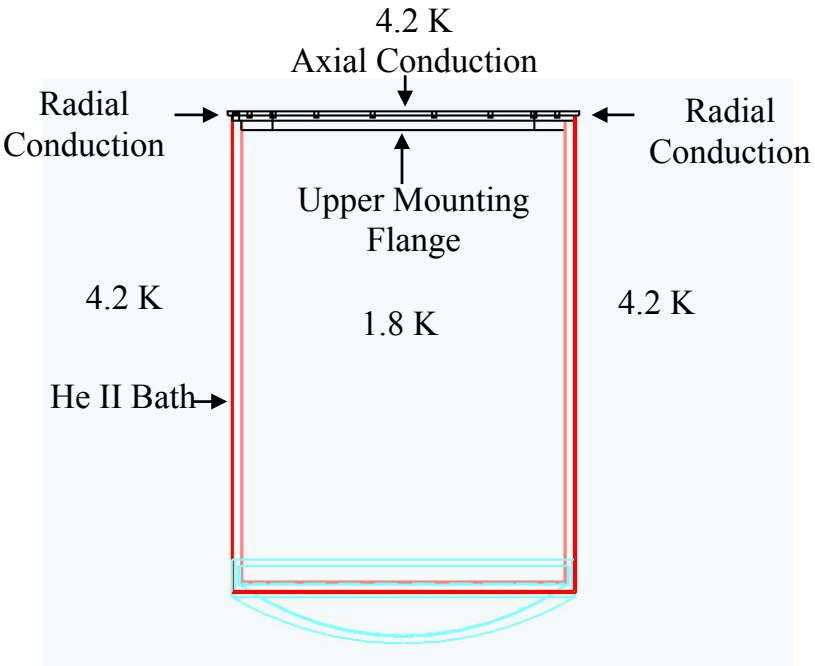

Figure 2.10. Conduction paths through the He II bath upper mounting flange.

The radial conduction through the He II bath upper mounting flange of the He II bath was calculated:

$$\dot{Q}_{ss\_flange\_radial} = 2\,\pi\, L_{ss\_flange\_radial}\;\; k_{ss} \left[\frac{(T_{s2} - T_{s1})}{\ln\left[\frac{OD_{ss\_flange}}{ID_{ss\_flange}} \right]} \right] \tag{2.27}$$

$$\dot{Q}_{ss\_flange\_radial} = 0.11\,[W] \tag{2.28}$$

where k_{ss} is the thermal conductivity of 304 stainless steel, T_{s1} is the temperature of the inside diameter, T_{s2} is the temperature of the outside diameter and $L_{ss\_flange\_radial}$ is the thickness of the upper mounting flange. Figure 2.11 illustrates that the thickness is different for the axial and radial conduction calculations. The radial conduction thickness

is smaller than the axial conduction thickness because of the steps machined in the flange to accommodate welding of the inner and outer cylinder walls. The bottom half of the flange is exposed to the evacuated space between the two walls and therefore the effective thickness for radial conduction is half of the total flange thickness.

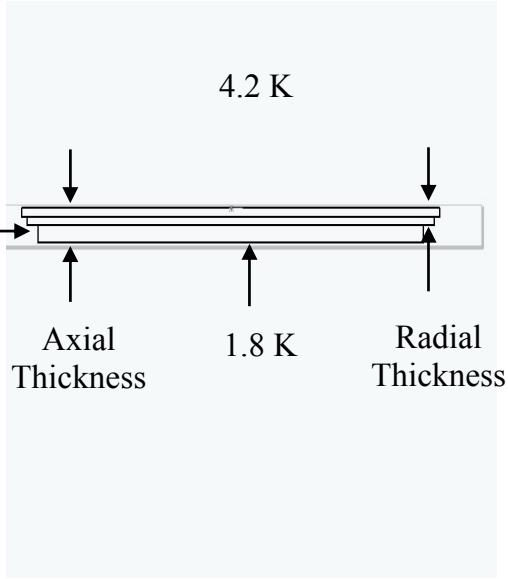

Figure 2.11. Radial and axial thickness of He II bath upper mounting flange.

The axial conduction through the flange is:

$$\dot{Q}_{ss\_flange\_axial} = k_{ss}\ Area_{ss\_flange}\left[\frac{T_{s2} - T_{s1}}{L_{ss\_flange}}\right] \tag{2.29}$$

$$\dot{Q}_{ss\_flange\_axial} = 0.92\ [W] \tag{2.30}$$

where $Area_{ss\_flange}$ is the surface area of the flange. The total heat leak associated with conduction through this flange is therefore:

$$\dot{Q}_{ss\_flange\_Heat\_Leak\_Total} = \dot{Q}_{ss\_flange\_radial} + \dot{Q}_{ss\_flange\_axial} \tag{2.31}$$

Table 2.6 summarizes the parameters and results used for this calculation.

Table 2.6. Parameters and results used in He II bath upper mounting flange radial and axial conductive heat leaks.

Parameter	Symbol	Value
Axial thickness of flange	L_{ss_flange}	0.025 [m]
Radial thickness of flange	$L_{ss\_flange\_radial}$	0.013 [m]
Average thermal conductivity of 304 stainless steel	k_{ss}	0.16 [W/m-K]
Temperature of He I bath	T_{s2}	4.2 [K]
Temperature of He II bath	T_{s1}	1.8 [K]
Outside diameter of flange	OD_{ss_flange}	0.47 [m]
Inside diameter of flange	ID_{ss_flange}	0.35 [m]
Cross-sectional area of flange	$Area_{ss\_flange}$	0.059 [m^2]
Radial conduction through flange	$Q_{ss\_flange\_radial}$	0.11 [W]
Axial conduction through flange	$Q_{ss\_flange\_axial}$	0.92 [W]
Total heat leak through flange	$\dot{Q}_{ss\_flange\_Heat\_Leak\_Total}$	**1.03 [W]**

2.2.1.6 Radiation Through He II Bath Walls

The heat leak due to radiation from the 4.2 K bath to He II bath is (Incropera *et al*. 2002):

$$\dot{Q}_{radition} = \sigma \, \pi \, D_{inside} \, L \left[\frac{T_{outside}{}^4 - T_{inside}{}^4}{\frac{1}{\varepsilon 1} + \left(\frac{1-\varepsilon 2}{\varepsilon 2} \right) \frac{D_{inside}}{D_{outside}}} \right] \tag{2.32}$$

$$\dot{Q}_{radiation} = 0.000015 \, [W] \tag{2.33}$$

where D_{inside} is the diameter of the inside surface which is at 1.8 K, $D_{outside}$ is the diameter of the outside surface which is at 4.2 K, and ε_1 and ε_2 are the emissivities of the inside and outside surfaces, respectively. Table 2.7 summarizes the parameters and results used for this calculation.

Table 2.7. Parameters and results used in calculating the radiation heat leak through the walls of the He II bath.

Parameter	Symbol	Value
Stefan-Boltzmann Constant	σ	5.67 10^{-8} [W/m^2-K^4]
Diameter of inside surface at 1.8 K	D_{inside}	0.44 [m]
Diameter of outside surface at 4.2 K	$D_{outside}$	0.46 [m]
Black-body emissivity of inside wall	ε_1	1.0
Black-body emissivity of outside wall	ε_2	1.0
Height of He II bath walls	L	0.64 [m]
Temperature of He I bath	T_{inside}	4.2 [K]
Temperature of He II bath	$T_{outside}$	1.8 [K]
Estimated radiative heat leak into He II bath	$\dot{Q}_{radiation}$	**1.51 $10^{(-5)}$ [W]**

2.2.1.7 He II Bath Lid

The heat leak through the G-10 He II bath lid was accounted for by calculating the axial conduction through the portion of the lid exposed to 1.8 K. This area is equivalent to the area encompassed by the inner diameter of the He II bath upper flange less the area of the hall-effect access hole and the recuperator mounting hole. The conduction through these holes has been separately accounted for by the individual component calculations.

$$\dot{Q}_{He\_II\_lid\_axial\_cond} = k_{ss}\ Area_{He\_II\_lid}\left[\frac{T_{s2} - T_{s1}}{L_{He\_II\_lid}}\right] \tag{2.34}$$

$$\dot{Q}_{He\_II\_Lid\_axial\_cond} = 0.19\ [W] \tag{2.35}$$

Figure 2.12 illustrates the predicted heat leak as a function of the thickness of the He II bath lid.

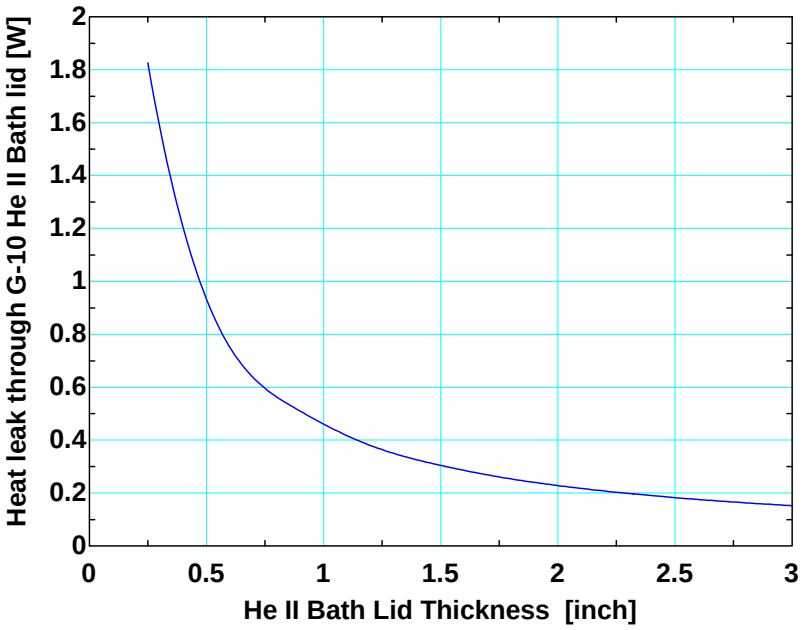

Figure 2.12. Axial conduction into the He II bath as a function of He II bath lid thickness.

Table 2.8 summarizes the parameters and results used for these calculations.

Table 2.8. Parameters and results of axial conduction and radiation heat leak calculations through the He II bath lid.

Parameter	Symbol	Value
Average thermal conductivity	k_{ss}	0.16 [W/m-K]
Cross-sectional area exposed to 1.8 K	$Area_{He\_II\_Lid}$	0.089 [m^2]
Temperature of He I bath	T_{s2}	4.2 [K]
Temperature of He II bath	T_{s1}	1.8 [K]
Thickness of He II bath lid	$L_{He\ II\ Lid}$	0.064 [m]
Axial conduction heat leak through He II bath lid	$\dot{Q}_{He\_II\_Lid\_axial\_cond}$	**0.19 [W]**

2.2.1.8 BSCCO Tubes

The test specimen must be supplied with up to 15 kA of current. The current is passed into the He II bath through BSCCO 2212 ($Bi_2Sr_2Ca_1Cu_2O_y$) superconducting tubes; this material was chosen because BSCCO is a high temperature (T_c=90-95 K) superconductor that has very low thermal conductivity (0.1 W/m-K). Therefore, the resistive loss associated with the current will be essentially zero and the heat leak will also be very

small. Figure 2.13 illustrates how the BSCCO tubes are mounted into the He II bath lid using Stycast epoxy and extend 1.75 inches from either side of the He II bath lid.

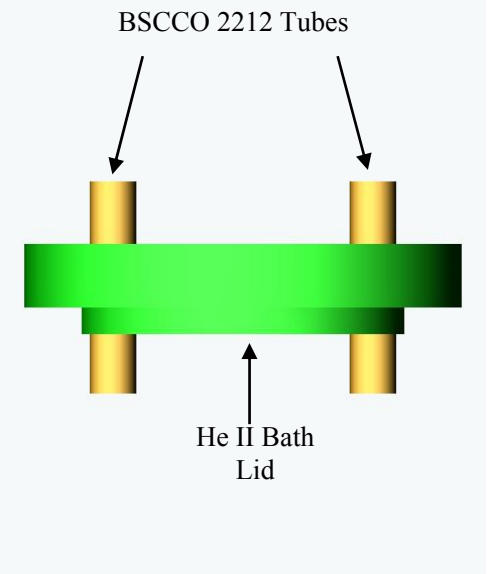

Figure 2.13. BSCCO 2212 superconducting tubes potted in He II bath lid.

The axial conduction through the tubes is:

$$\dot{Q}_{BSCCO} = Number_{tubes}\ k_{BSCCO}\ Area_{BSCCO}\left[\frac{T_{s2}-T_{s1}}{L_{BSCCO}}\right] \tag{2.36}$$

$$\dot{Q}_{BSCCO} = 0.0093\,[W] \tag{2.37}$$

The BSCCO tubes are hollow in the center and therefore must be plugged to prevent the escape of the superfluid helium. A 1.375 inch diameter G-10 rod was mounted in the center of the BSCCO tube using Stycast epoxy. The axial conduction through the G-10 rods is:

$$\dot{Q}_{G10\_Rods} = Number_{tubes}\ k_{G10}\ Area_{G10\_Rods}\left[\frac{T_{s2}-T_{s1}}{L_{G10\_Rods}}\right] \tag{2.38}$$

$$\dot{Q}_{G10\_Rods} = 0.0025\,[W] \tag{2.39}$$

The total heat leak into the He II bath through the BSCCO tube assembly is therefore:

$$\dot{Q}_{BSCCO\_Heat\_Leak\_Total} = \dot{Q}_{G10\_Rods} + \dot{Q}_{BSCCO} \tag{2.40}$$

$$\dot{Q}_{BSCCO\_Heat\_Leak\_Total} = 0.019[W] \tag{2.41}$$

Table 2.9 summarizes the parameters and results used for these calculations.

Table 2.9. Parameters and results of the axial conduction heat leak calculations through the BSCCO tube assemblies in the He II bath lid.

Parameter	Symbol	Value
Thermal conductivity of BSCCO	k_{BSCCO}	0.1 [W/m-K]
Cross-sectional area of BSCCO	$Area_{BSCCO}$	0.0020 [m^2]
Temperature of He I bath	T_{S2}	4.2 [K]
Temperature of He II bath	T_{S1}	1.8 [K]
Length of BSCCO tube exposed to temperature gradient	L_{BSCCO}	0.064 [m]
Average thermal conductivity of G-10	k_{G10}	0.054 [W/m-K]
Number of BSCCO tubes	$Number_{Tubes}$	2
Cross-sectional area of G-10 Rods	$Area_{G10\ Rods}$	0.00096 [m^2]
Length of G-10 rods exposed to temperature gradient	$L_{G10\ Rods}$	0.064 [m]
Conductive heat leak through BSCCO tubes	Q_{BSCCO}	0.015 [W]
Conductive heat leak through G-10 Rods	$Q_{G10\ Rods}$	0.0039 [W]
Total heat leak into He II bath through 2 BSCCO tube assemblies	$\dot{Q}_{BSCCO\_Heat\_Leak\_Total}$	**0.019 [W]**

2.2.1.9 Voltage-Tap Wires

One objective of the experimental apparatus is the measurement of the critical current density, temperature, and magnetic field for the superconducting samples. The measurement of these parameters is related to detecting the onset of the transition from superconducting to normal behavior. This measurement is typically related to the detection of the small voltage rise that signals the onset of the sample going normal. Therefore, thirty 0.016 inch diameter copper wires are installed in the He II bath lid using Stycast epoxy in order to allow voltage measurements along the sample. These voltage-taps pass directly through the G-10 cover rather than using intermediate, electrical

connectors in order to provide an uninterrupted signal path between the test sample and the measurement device. This is desirable for the most accurate results. The heat leak through these voltage-taps is computed:

$$\dot{Q}_{voltage\_tap} = Number_{vTaps}\ k_{cu}\ Area_{wire}\left[\frac{T_{s2} - T_{s1}}{L_{wire}}\right] \tag{2.42}$$

$$\dot{Q}_{voltage\_Tap} = 0.069\,[W] \tag{2.43}$$

Table 2.10 summarizes the parameters and results of these calculations.

Table 2.10. Axial conduction heat leak through voltage-tap wires entering the He II bath.

Parameter	Symbol	Value
Number of voltage-tap wires entering He II bath	$Number_{vTaps}$	30
Average thermal conductivity of copper	k_{cu}	471 [W/m-K]
Cross-sectional area of wires	$Area_{wire}$	1.30 $10^{(-7)}$ [m^2]
Temperature of He I bath	T_{s2}	4.2 [K]
Temperature of He II bath	T_{s1}	1.8 [K]
Length of voltage-taps exposed to temperature gradient	L_{wire}	0.063 [m]
Heat leak through voltage-taps	$\dot{Q}_{voltage\_Tap}$	**0.069 [W]**

2.2.1.10 Background Magnet Wires

A background magnet is mounted within the He II bath. The sample will be installed in the magnet bore in order to allow the application of a controlled, high magnetic field and therefore simulate the magnetic field that the test sample will be exposed to in the APS. The background magnet is powered with up to 100 amp that must be passed through the He II bath lid. The current passes through the lid via 6 Niobium-Titanium superconducting wires that are encased in copper. The copper makes up the majority of the cross-sectional area and is much more thermally conductive than the superconductor.

Therefore the heat leak through the wires can be conservatively modeled using the properties of pure copper:

$$\dot{Q}_{Background\_magnet\_wires} = Number_{wires}\ k_{cu}\ Area_{wire}\left[\frac{T_{s2} - T_{s1}}{L_{background\_magnet\_wire}}\right] \tag{2.44}$$

$$\dot{Q}_{Background\_magnet\_wires} = 0.22\,[W] \tag{2.45}$$

Table 2.11 summarizes the parameters and results of these calculations.

Table 2.11. Axial conduction heat leak through background magnet wires entering the He II bath.

Parameter	Symbol	Value
Number of current carrying wires	$Number_{wires}$	6
Average thermal conductivity of copper	k_{cu}	471 [W/m-K]
Cross-sectional area of copper wires	$Area_{wire}$	2.08 $10^{(-6)}$ [m^2]
Temperature of He I bath	T_{s2}	4.2 [K]
Temperature of He II bath	T_{s1}	1.8 [K]
Length of wires exposed to temperature gradient	$L_{background\ magnet\ wire}$	0.064 [m]
Heat leak into He II bath through magnet power wires	$\dot{Q}_{Background\_magnet\_wires}$	**0.22 [W]**

2.2.1.11 Pressure Tap Capillary Tube

The pressure within the He II heat exchanger must be monitored as it provides a direct measure of the temperature within the bath and is used to control the vacuum pump via a butterfly valve. The pressure is measured using a room temperature pressure transducer that is connected to the He II heat exchanger via a capillary tube. The capillary tube is connected to a pressure tap installed on the side of the He II heat exchanger mounting flange and within the He II bath. The 0.125 inch diameter stainless steel capillary tube with a 0.031 inch wall passes through the He II bath lid via an epoxy seal. The axial conduction into the He II bath due to this capillary tube is:

$$\dot{Q}_{cap\_tube} = k_{ss}\ Area_{cap\_tube}\left[\frac{T_{s2} - T_{s1}}{L_{cap\_tube}}\right] \tag{2.46}$$

$$\dot{Q}_{cap\_tube} = 3.96\ 10^{(-6)}\ [W] \tag{2.47}$$

Table 2.12 summarizes the results of this calculation.

Table 2.12. Axial conduction heat leak through pressure tap capillary tube entering the He II bath.

Parameter	Symbol	Value
Integrated thermal conductivity of stainless steel	k_{ss}	0.16 [W/m-K]
Cross-sectional area of capillary tube	$Area_{cap\ tube}$	6.39 $10^{(-6)}$ [m^2]
Temperature of He I bath	T_{s2}	4.2 [K]
Temperature of He II bath	T_{s1}	1.8 [K]
Length of capillary tube exposed to temperature gradient	L_{cap_tube}	0.064 [m]
Heat leak into He II bath through capillary tube	$\dot{Q}_{cap\_tube}$	**3.96 $10^{(-5)}$ [W]**

The total predicted heat leak into the He II bath during normal operation is 2.56 W, less than 12.8% of the predicted refrigeration capacity. The heat leak is made up of many parasitic loses that are summarized in Table 2.13. The dominant heat leaks are related to the presence of superfluid in the gaps between the Teflon cones and the lid and also to conduction through the stainless steel mounting flange.

$$\dot{Q}_{He\_II\_Bath\_Heat\_Leak\_Total} = 2.56[W] \tag{2.48}$$

Table 2.13. Total calculated heat leak into He II bath.

Parameter	Symbol	Value [W]	% of Total Heat Leak
Teflon Cones	$\dot{Q}_{cone}$	0.56	21.87
He II bath lid epoxy seal	$\dot{Q}_{epoxy\_lid\_He\_leak}$	0.20	7.81
Recuperator mounting flange	$\dot{Q}_{\_HXCH\_heat\_leak\_Total}$	0.23	8.98
Hall-effect cover	$\dot{Q}_{\_Hall\_Effect\_Heat\_leak\_Total}$	0.046	1.8
He II bath upper mounting flange	$\dot{Q}_{ss\_flange\_Heat\_Leak\_Total}$	1.03	40.23
Radiation through He II bath walls	$\dot{Q}_{radiation}$	$1.51\ 10^{(-5)}$	0.00059
Conduction through He II bath lid	$\dot{Q}_{He\_II\_Lid\_axial\_cond}$	0.19	7.42
BSCCO tube assembly	$\dot{Q}_{BSCCO\_Heat\_Leak\_Total}$	0.019	0.74
Voltage-tap wires	$\dot{Q}_{voltage\_Tap}$	0.069	2.7
Background magnet power wires	$\dot{Q}_{Background\_magnet\_wires}$	0.22	8.59
Pressure tap capillary tube	$\dot{Q}_{cap\_tube}$	$3.96\ 10^{(-5)}$	0.00155
Total He II bath heat leak	$\dot{Q}_{He\_II\_Bath\_Heat\_Leak\_Total}$	**2.56**	

2.2.2 He II Bath Fabrication and Assembly

This section describes the details associated with the fabrication and assembly of the He II bath, shown in Figure 2.14. The section is divided into subsections related to the individual pieces that were required to fabricate the bath. The He II bath forms a critical piece of the refrigeration system; it contains the superfluid helium and the total load on the refrigeration cycle is dominated by the details of the He II bath.

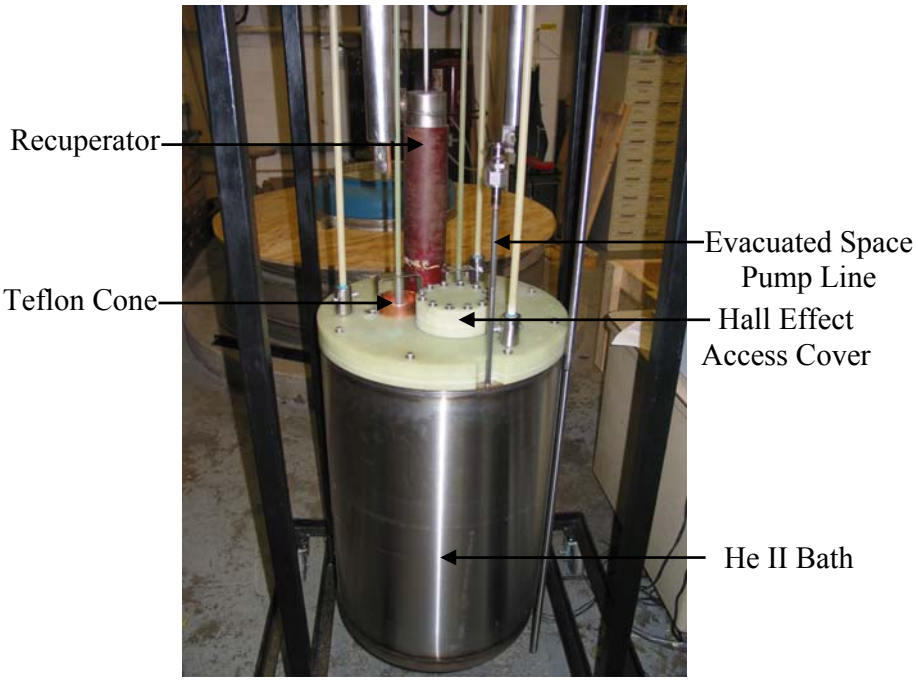

Figure 2.14. Key components bolted to He II bath lid.

2.2.2.1 Upper Mounting Flange

Figure 2.15 illustrates the upper mounting flange for the He II bath container. Notice that the upper mounting flange was machined with a step that facilitates welding both the inner and outer walls to the flange. The steps in the flange create a 0.425 inch gap between the inner and outer walls. The volume trapped between the inner and outer walls will be evacuated during the tests in order to reduce the conductive heat leak between the 4.2 K and 1.8 K baths.

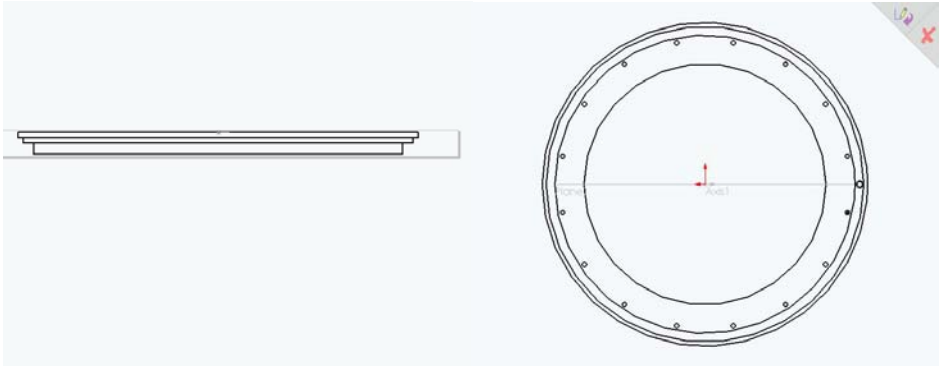

Figure 2.15. He II bath upper mounting flange. Note the steps in the flange to facilitate welding of the inner and outer walls.

2.2.2.2 Cylindrical Walls

The inner and outer walls of the He II bath were formed from stainless steel sheets that were rolled into cylinders. The inner wall was subsequently welded to the upper flange and the seam of the cylinder was welded. Finally, the smaller domed bottom was welded to the inner cylinder wall.

At this point these welds were helium leak tested; it was important to leak test these welds prior to covering them with the outer wall after which any repair operation would become problematic. A KF25 flange was welded to a 0.50 inch thick stainless steel plate in order to make a temporary leak detection flange. A layer of 0.75 inch thick closed cell foam was attached to the side of the flange opposite the KF25 fitting. The He II bath sub-assembly consisting of the inner cylinder and dome attached to the mounting flange was placed with the mounting flange facing downward and resting on the foam side of the leak detection flange. A helium leak detector was attached to the KF25 fitting. Light pressure was initially applied to the He II bath to create a seal between the mounting flange and the foam. Once a vacuum was established, the weight of the bath and the force produced by the pressure differential provided adequate pressure to maintain the seal. All welds were then leak tested and found to be helium leak tight.

Figure 2.16 illustrates six, 0.25 inch diameter G-10 rods which were taped to the outer wall of the inner cylinder in order to prevent any direct contact between the inner and outer walls which would result in a large, conductive heat leak. The outer cylinder was welded to the upper flange and the domed bottom was welded to the outer cylinder. The

space between the inner and outer cylinder was helium leak detected using the vacuum access port installed in the mounting flange, described in the subsequent section.

Figure 2.16. The He II bath inner wall with G-10 rods taped to it in order to avoid direct contact with the outer wall.

2.2.2.3 Evacuated Space

A 0.375 inch stainless steel tube was welded to the sealing surface of the upper flange concentric to a thru-hole that leads into the evacuated space. A 0.375 inch VCR gland was welded to the rod in order to provide a demountable connection with the vacuum pump and therefore allow the He II bath to be removed from the cryostat lid.

2.2.2.4 G-10 Support Rods

The He II bath is suspended from the cryostat lid with three 0.75 inch diameter hollow G-10 tubes. A thermal gradient exists through the vapor space in the 4.2 K dewar; the top of the dewar adjacent to the cryostat lid will be at approximately room temperature.

Therefore, the top of the G-10 support rods will be near 300 K. The bottom of the G-10 support rods will be submerged in 4.2 K liquid helium. The heat leak through the G-10 rods into the 4.2 K bath can be estimated according to:

$$\dot{Q}_{0.75\_G10\_tube} = NumberRods\ k_{G10\_0.75}\ Area_{G10\_0.75}\left[\frac{T_{s2}-T_{s1}}{L_{G10\_0.75}}\right] \tag{2.49}$$

$$\dot{Q}_{0.75\_G10\_tube} = 0.075[W] \tag{2.50}$$

where $k_{G10\_0.75}$ is the thermal conductivity of G-10, $Area_{G10\_0.75}$ is the cross-sectional area of the G-10 tubes, and $L_{G10\_0.75}$ is the length of the G-10 tubes. Table 2.14 summarizes the parameters and results of these calculations.

Table 2.14. Axial conduction heat leak into the 4.2 K bath through the He II bath support rods.

Parameter	Symbol	Value
Average thermal conductivity of G-10	$k_{G10\_0.75}$	0.456 [W/m-K]
Cross-sectional area of G-10 rods	$Area_{G10\ 0.75}$	1.583 $10^{(-4)}$ [m^2]
Temperature at top of He I bath	T_{s2}	300 [K]
Number of G-10 rods	$NumberRods$	3
Temperature at bottom of He I bath	T_{s1}	4.2 [K]
Length of G-10 rods exposed to thermal gradient	$L_{G10\ 0.75}$	0.8509 [m]
Heat leak into He I bath through G-10 rods	$Q_{0.75\ G10\ tube}$	**0.0251 [W]**

2.3 Current Carrying Components

This section describes the design of the components that are required to carry the high current (up to 15,000 amp) to the superconducting sample. The conductors required to carry this current from room temperature to 4.2 K are not superconducting and are therefore resistive. Careful consideration is required for these components in order to assure that there is not an excessive consumption of 4.2 K liquid helium during operation.

2.3.1 Thermal Stand-off

The current leads used to carry current from room temperature to the 4.2 K bath are vapor cooled leads manufactured by American Magnetics. These leads were not purchased as part of this project but rather had been procured for a previous experiment. The heat capacity of helium vapor is used in these counter-flow leads in order to minimize the liquid helium consumption for a specified operating current by balancing the conducted and generated heat of the lead. The helium vapor passing through the lead is produced by the heat leak into the bath from the operation of the current leads. The current lead is designed to warm the helium gas exiting the lead to 300 K when operating under the maximum rated current. This arrangement makes optimal use of the available cryogen as it uses not only the latent but also the sensible heat capacity of the liquid helium to the greatest possible extent.

However, at less than the maximum current, the gas vapor exiting the current lead can be quite cold. Therefore, the current lead must be bolted to a thermal stand-off so that the cryostat lid does not also become cold and therefore freeze the o-ring that seals the cryostat lid to the dewar as well as o-rings at other locations on the lid. Polymer o-rings have a limited temperature range and therefore must be protected from temperature extremes in either direction. The bellows design for the thermal stand-off also allows for some motion of the current carrying components within the dewar relative to the cryostat lid due to thermal contraction/expansion during cool-down and warm-up.

Figure 2.17 illustrates the helium vapor-cooled current lead and thermal stand-off assembly. The upper flange is epoxied to the outside wall of the current lead and is in good thermal communication with the exiting helium vapor. The temperature of this flange with no-current load can be as low as 20 K depending on the rate of liquid helium consumption due to other heat leaks. The upper flange is bolted to the bellows mounting flange and sealed with a 0.125 diameter indium wire. The bellows acts like a finned surface in that it has a substantial amount of surface area for a given length; this effect increases the convective heat transfer with the ambient air. The thin stainless steel wall creates a resistive path for conduction along the bellows.

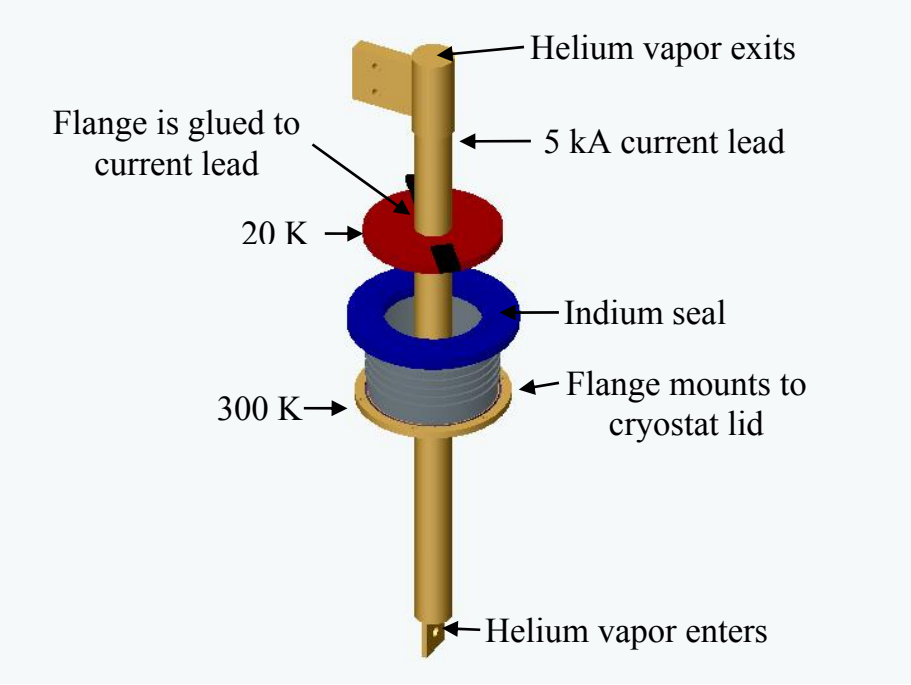

Figure 2.17. 5 kA helium vapor-cooled current lead with thermal stand-off.

A 6 inch diameter bellows was selected based on its ability to accommodate larger diameter current leads for future experiments. The length of the bellows was selected so that the flange that connects the bellows to the cryostat lid was maintained near 300 K.

The Biot number was calculated to insure the validity of using the lumped capacitance method on the upper flange:

$$Bi = \frac{h\ L_c}{k} \tag{2.51}$$

$$Bi = 0.0038 \tag{2.52}$$

where L_c is the characteristic length of the upper flange:

$$L_c = \frac{volume}{surface\_area} \tag{2.53}$$

The resistive thermal network that represents the thermal standoff included convection off of the edge of the upper flange:

$$R_{conv\_flange} = \frac{1}{h\ Area\_flange} \tag{2.54}$$

conduction through the upper flange:

$$R_{cond\_flange} = \frac{\ln\left[\frac{r_2}{r_1}\right]}{2\ \pi\ L_{flange}\ k_{ss}} \tag{2.55}$$

and finally a resistance associated with the bellows which is modeled as an extended surface:

$$R_{fin} = \frac{1}{\sqrt{h\ P_w\ k_{ss}\ Area_c}} \tag{2.56}$$

The total thermal resistance network, shown in Figure 2.18 is:

$$R_{total} = R_{cond\_flange} + \frac{R_{conv\_flange}\ R_{fin}}{R_{conv\_flange} + R_{fin}} \tag{2.57}$$

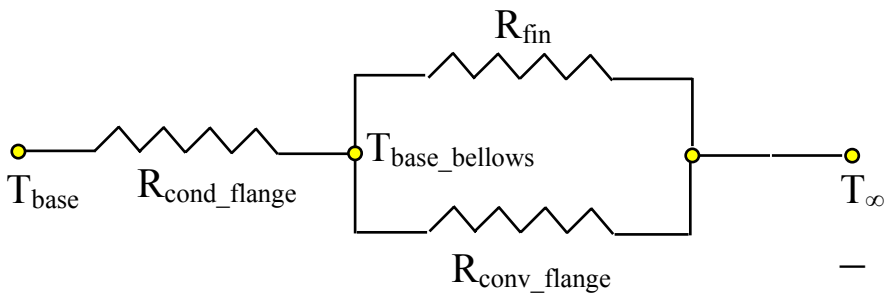

Figure 2.18. Thermal resistance network of current lead thermal stand-off.

The heat transfer from the finned surface is (Incropera *et al*. 2002):

$$\dot{Q}_{fin} = \left(T_{\infty} - T_{base\_bellows}\right)\sqrt{h\ P_w\ k_{ss}\ Area_c} \tag{2.58}$$

and the total heat transfer from the current lead is:

$$\dot{Q}_{total} = \frac{T_{\infty} - T_{base}}{R_{total}} \tag{2.59}$$

The most important parameter in the calculation is the temperature at the warm end of the bellows, adjacent to the cryostat lid. This temperature is computed assuming the temperature distribution for an infinite fin is approximately true:

$$T = T_{\infty} + (T_{base\_bellows} - T_{\infty})\,\mathrm{e}^{(-mL)} \tag{2.60}$$

$$m = \sqrt{\frac{h\ P_w}{k_{ss}\ Area_c}} \tag{2.61}$$

where h is the convective heat transfer coefficient between the bellows surface and the ambient air, A_{flange} is the surface area of the upper flange, L_{flange} is the upper flange thickness, k_{ss} is the thermal conductivity of the stainless steel bellows, A_c is the cross-sectional area of the fin, P_w is the perimeter of the bellows exposed to ambient air, and L is the length of the bellows for conduction. Table 2.15 summarizes the parameters and

results used for these calculations based on a mounting flange temperature of 20 K and a bellows diameter of 6 inches.

Table 2.15. Parameters and results of thermal stand-off calculations based on a mounting flange temperature of 20 K and a bellows diameter of 6 inches.

Parameter	Symbol	Value
Thermal resistance to convection from upper flange	R_{conv_flange}	8.97 [K/W]
Heat transfer coefficient to surrounding area	h	10 [W/m^2-K]
Surface area of upper flange	$Area_{flange}$	0.011 [m^2]
Thermal resistance to conduction through upper flange	R_{cond_flange}	0.36 [K/W]
Outside radius of upper flange	r_2	0.083 [m]
Inside radius of upper flange	r_1	0.057 [m]
Thermal resistance through bellows	R_{fin}	5.49 [K/W]
Thickness of upper flange	L_{flange}	0.013 [m]
Average thermal conductivity of stainless steel	k_{ss}	12.75 [W/m-K]
Wetted perimeter of bellows	P_w	0.48 [m]
Cross-sectional area of bellows	$Area_c$	0.00054 [m^2]
Total thermal resistance	R_{total}	3.77 [K/W]
Temperature of surrounding air	T_∞	300 [K]
Temperature of upper flange	T_{base}	20 [K]
Heat transferred from bellows	Q_{fin}	50.95 [W]
Total heat transferred through bellows assembly	Q_{total}	74.31 [W]
Temperature at the base of bellows	$T_{base\_bellows}$	77.71 [K]
Dimensionless parameter	m	26.29 [1/m]
Temperature of lower mounting flange	$\boldsymbol{T}$	**299.61 [K]**

Figure 2.19 illustrates the temperature at the warm end of the bellows as a function of bellows length for an upper mounting flange temperature of 20 K and 100 K. Figure 2.19 illustrates that for either case, a 6 inch long bellows is sufficiently large to bring the temperature at the warm end of the bellows to well above freezing and therefore effectively isolate the cryostat lid from the cold penetration.

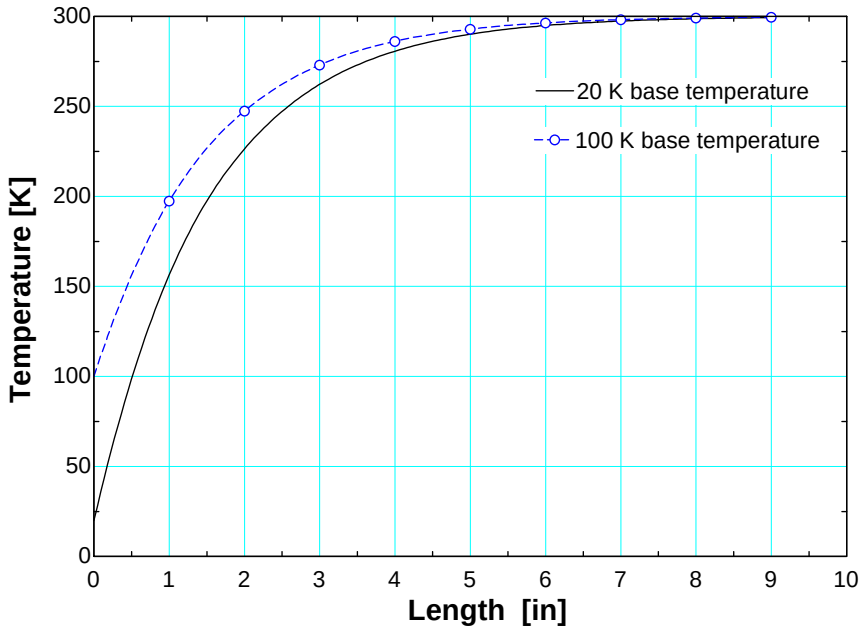

Figure 2.19. Temperature profiles of thermal stand-offs with temperatures at the cold end of 20 K and 100 K.

Figure 2.20 illustrates one of the current leads and thermal stand-off bellows during a zero current test run of the refrigeration system. Notice how the upper flange and current lead are covered with frost formed from the moisture in the lab air and therefore are obviously quite cold, far below the dew point of the air in the room. However, the amount of frost is reduced along the length of the bellows and no frost at all is evident at the lower mounting flange.

Figure 2.20. 5 kA current lead at 0 current. Note how the current lead and top flange are very cold, but the bottom mounting flange is warm.

2.3.2 Current Lead Mounting Flange

The 5 kA American Magnetics current leads used for this experiment did not originally have mounting flanges attached to them. Welding a mounting flange to the current lead was discouraged by the manufacturer due to concerns related to damaging the internal components of the current lead during the welding process. Therefore, rather than welding directly to the current lead, a two step process was employed. First, half of a stainless steel two-piece clamp-on collar was welded to the mounting flange. The half-collar was installed so that it was concentric with the hole that the current lead itself would eventually slide through (See Figure 2.21). Next, the mounting flange was glued to the current lead with Stycast epoxy. Finally, the second half of the two-piece clamp-on collar was bolted to the collar welded to the flange. The Stycast epoxy provides a hermetic seal between the flange and the current lead but cannot be subjected to any large force. The two-piece clamp-on collar provides the mechanical link and can sustain large forces.

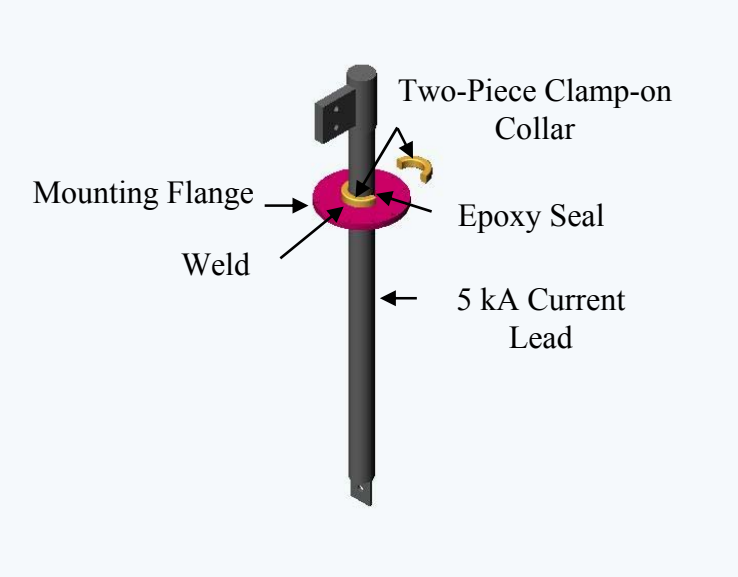

Figure 2.21. Method of mounting a flange to the 5 kA current leads without welding directly to the leads.

2.3.3 Indium Seal

A tongue-and-groove indium seal was used to seal the current lead flange to the bellows flange (see Figure 2.22).

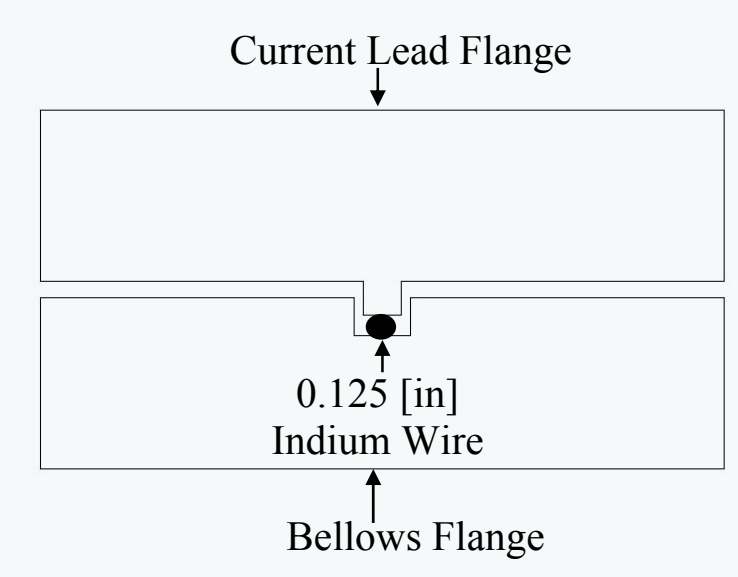

Figure 2.22. Tongue-and-Groove indium seal used on current lead flange.

The diameter of the indium wire used in the groove was approximately 25% larger than the clearance volume between the tongue and groove that would exist when the two flanges are bolted tightly together:

$$Area_{wire} = \frac{\pi}{4} diameter_{wire}^{\ 2} \tag{2.62}$$

$$Area_{wire} = 1.25\ Area_{clearance} \tag{2.63}$$

$$Area_{clearance} = Area_{groove} - Area_{tongue} \tag{2.64}$$

$$Diameter_{wire} = 0.12[in] \tag{2.65}$$

Table 2.16 summarizes the parameters and results used for these calculations.

Table 2.16. Parameters and results of calculation to determine the diameter of indium wire required to seal the current lead mounting flange.

Parameter	Symbol	Value
Cross-sectional area of wire	$Area_{wire}$	0.012 [in^2]
Cross-sectional area of groove	$Area_{groove}$	0.021 [in^2]
Cross-sectional area of tongue	$Area_{tongue}$	0.011 [in^2]
Cross-sectional area of clearance volume	$Area_{clearance}$	0.0096 [in^2]
Diameter of indium wire required	$Diameter_{wire}$	**0.12 [in]**

2.3.4 Current Lead Brace

The two current leads, when installed in the dewar, are two parallel conductors each carrying significant current in opposite directions. The opposing currents create a repulsive Lorentz force that tends to push the current carriers apart. The repulsive force is proportional to the current passed through the leads and can be calculated according to:

$$F = \frac{L\ \mu_0\ I_1\ I_2}{2\ \pi\ r} \tag{2.66}$$

$$\mu_0 = 4\ \pi\ 10^{(-7)} \tag{2.67}$$

where F is the repulsive force, L is the length of the conductor , I_1 and I_2 are the currents flowing through each lead and r is the distance between the leads.

Table 2.17 summarizes the parameters and results used for these calculations based on the maximum expected current of 15 kA.

Table 2.17. Parameters and results of calculation to determine the repulsive force generated by the 15 kA current leads operating at maximum rated current.

Parameter	Symbol	Value
Length of current leads	L	42 [in]
Permeability of free space	μ_0	$1.257\ 10^{(-6)}$ [N/amp^2]
Current flowing through current leads	I_1	15000 [amp]
Current flowing through current leads	I_2	15000 [amp]
Distance between current leads	r	13 [in]
Repulsive force generated	F	**32.68 [lbf]**

A graph of the repulsive force as a function of current is show in Figure 2.23.

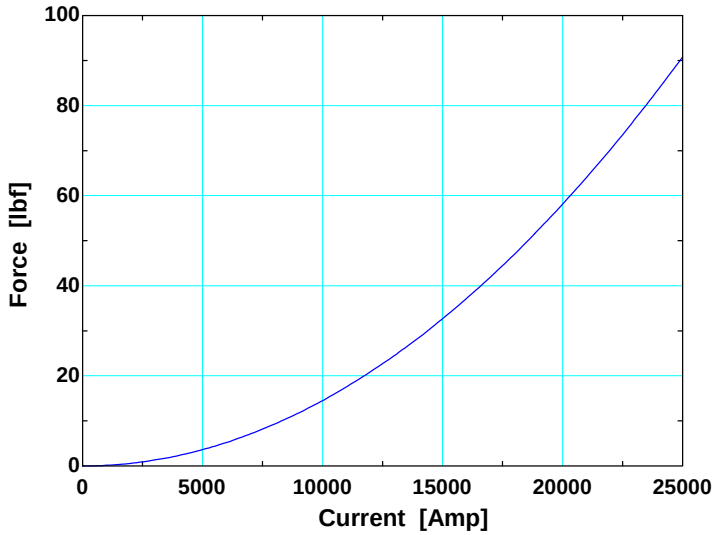

Figure 2.23. Current lead repulsive force as a function of current.

The current leads are suspended from the cryostat lid and mounted to the lid using the very compliant structure described in the previous section. The repulsive force acting on the leads can therefore generate a substantial moment that might damage the leads or the

mounting structure if their range of motion is not limited. Therefore, a rigid mechanical linkage made of G-10 was placed between the leads that was capable of carrying this force and preventing the leads from spreading apart. Figure 2.24 shows a picture of the 5 kA current lead brace.

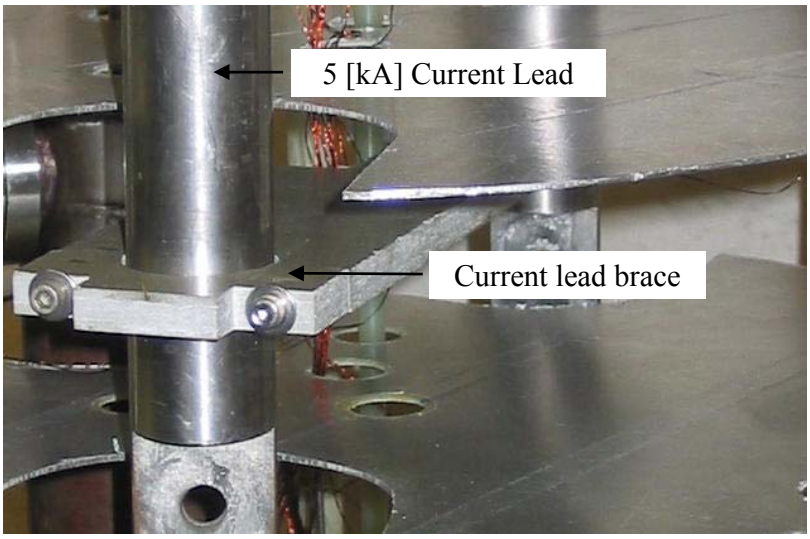

Figure 2.24. 5 kA current lead brace

2.3.5 Current Lead Electrical Connections

The current leads pass electrical current into the cryostat, but the current must also be passed from the current leads into the He II bath and finally to the test sample. A flexible connection must be made between the current lead and the He II bath to allow for thermal contraction during cool-down. To connect a flexible cable to the current lead, a 0.50 inch OFHC copper block was machined with a matching bolt pattern. The required thickness of the copper piece was determined by calculating the voltage drop and power dissipated in the copper as a function of its cross-sectional area:

$$V = I \; Resistance \tag{2.68}$$

$$Power = I^2 \; Resistance \tag{2.69}$$

$$Resistance = \rho_e \frac{L}{Area} \tag{2.70}$$

$$Area = width\ thickness \tag{2.71}$$

where V is voltage, I is the current, R is resistance, ρ_e is electrical resistivity, and $Area$ is the cross-sectional area of the copper block. Table 2.18 summarizes the parameters and results used for these calculations.

Table 2.18. Parameters and results of calculation to determine the thickness of a current carrying copper block bolted to the 5 kA current leads.

Parameter	Symbol	Value
Voltage flowing through current lead	V	1.47 $10^{(-4)}$ [Volt]
Current flowing through current lead	I	5000 [amp]
Resistance through current lead	*Resistance*	2.93 $10^{(-8)}$ [ohm]
Power	*Power*	0.73 [W]
Electrical resistivity of copper	ρe	6.42 $10^{(-9)}$ [ohm-in]
Length of copper block	L	4 [in]
Cross-sectional area of copper block	*Area*	0.87 [in^2]
Width of copper block	*width*	1.75 [in]
Thickness of copper block	*thickness*	**0.50 [in]**

Figure 2.25 illustrates the predicted voltage drop and power dissipated in a 4 inch long by 1.75 inch wide piece of OFHC copper as a function of plate thickness carrying 5kA.

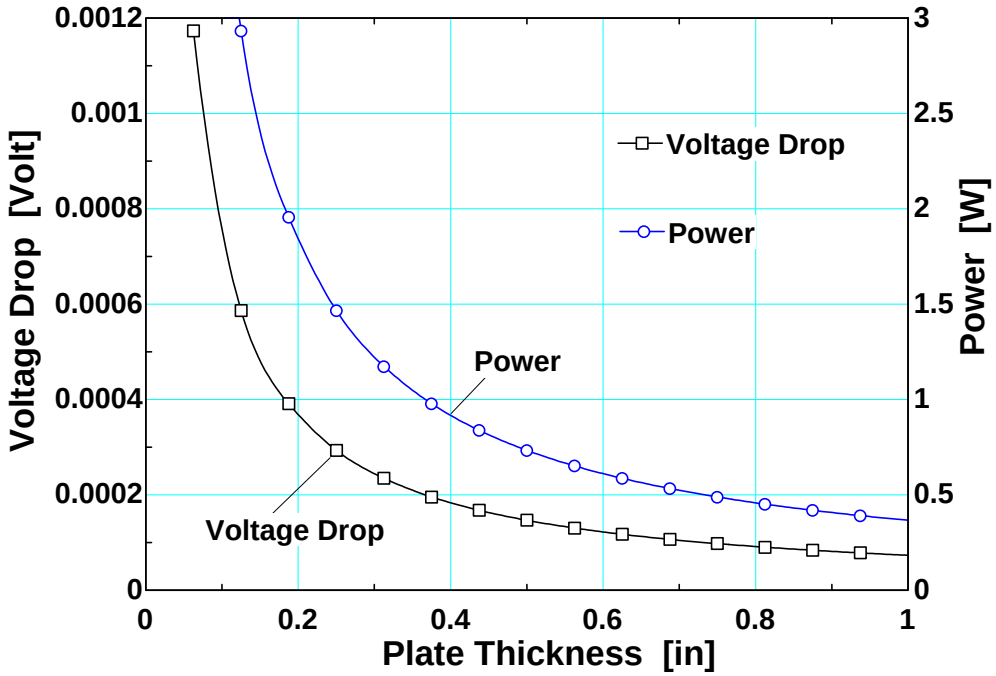

Figure 2.25. Voltage drop and power dissipated as a function of plate thickness for a 4 inch long by 1.75 inch wide piece of OFHC copper carrying 5kA.

Stranded Niobium-Titanium cable was used to make the flexible connection between the current leads and the BSCCO tubes that were installed in the He II bath lid (see Figure 2.26). Several 0.25 inch deep slots were machined in the copper blocks in order to allow the Niobium-Titanium cable to sit flush with the copper's surface and minimize the contact resistance. Tix indium solder [Allied Mfg. Corp] was used to solder the Niobium-Titanium cable to the copper block. Tix solder has a low melting temperature (275° F) compared to standard lead-tin solders (400° F). The lower melting temperature reduces the risk of damaging the superconducting cable during the soldering process. A piece of indium foil was placed between the current lead and the copper block in order to reduce the contact resistance. The two pieces were then bolted tightly together.

The connection of the Niobium-Titanium cable to the BSCCO tube was accomplished by spreading the strands of the cable around the circumference of the tube and holding them

in place with stainless steel safety wire. Tix solder was used to join the two pieces with care being taken not to overheat the superconductors during the joining operation. Niobium-Titanium cable was soldered to the He II bath side of the BSCCO tube using the same process.

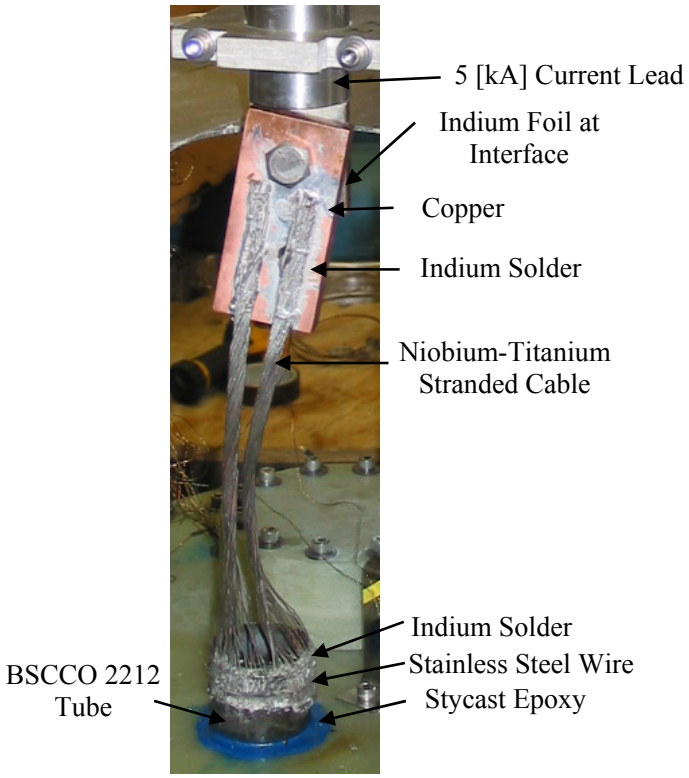

Figure 2.26. Flexible electrical connection between 5 kA current lead and BSCCO tube using Niobium-Titanium cable and Tix indium solder.

The background magnet in the He II bath must be supplied with up to 100 amp. This current was passed through the cryostat lid and to the 4.2 K bath using two, 250 kA American Magnetics helium vapor-cooled current leads. Three Niobium-Titanium wires were twisted with three 0.60 inch diameter copper wires and potted into the He II bath lid in order to pass the magnet current into the 1.8 K bath. Both ends of the twisted wire bundles were soldered to a copper block following the same procedure described for the 5

kA leads. Indium foil was placed between the copper block-to-current lead interface as well as the copper block-to-background magnet terminal interface.

2.4 Recovery Lines

The helium vapor that exits the current leads is routed to a recovery bag where it is purified and re-liquefied. Helium is a limited resource and therefore it is important to conserve it whenever practical. The recovery lines were made with copper and stainless steel pipe, and rubber vacuum hose. The rubber hose provides a mechanical and electrical isolation between the two leads and the recovery line plumbing. Four band heaters were wrapped around the recovery lines in order to heat the cold helium leaving the cryostat to above 0° C and therefore avoid freezing the recovery bag.

The current carrying capacity of the leads is a function of the temperature of the copper conductors inside of the leads. However, due to manufacturing variability the cross-sectional area for flow within each lead is not exactly the same and therefore one lead will have less resistance to flow than the other. Unequal mass flow rates through the two leads will result in one lead operating at a higher temperature. As the temperature of the lead is increased, the current carrying capacity is decreased. Therefore it is desirable to keep the temperature of the current leads equal. A butterfly valve was placed in each recovery line in order to regulate the mass flow rate of helium vapor through each current lead. Figure 2.27 illustrates the recovery lines during operation.

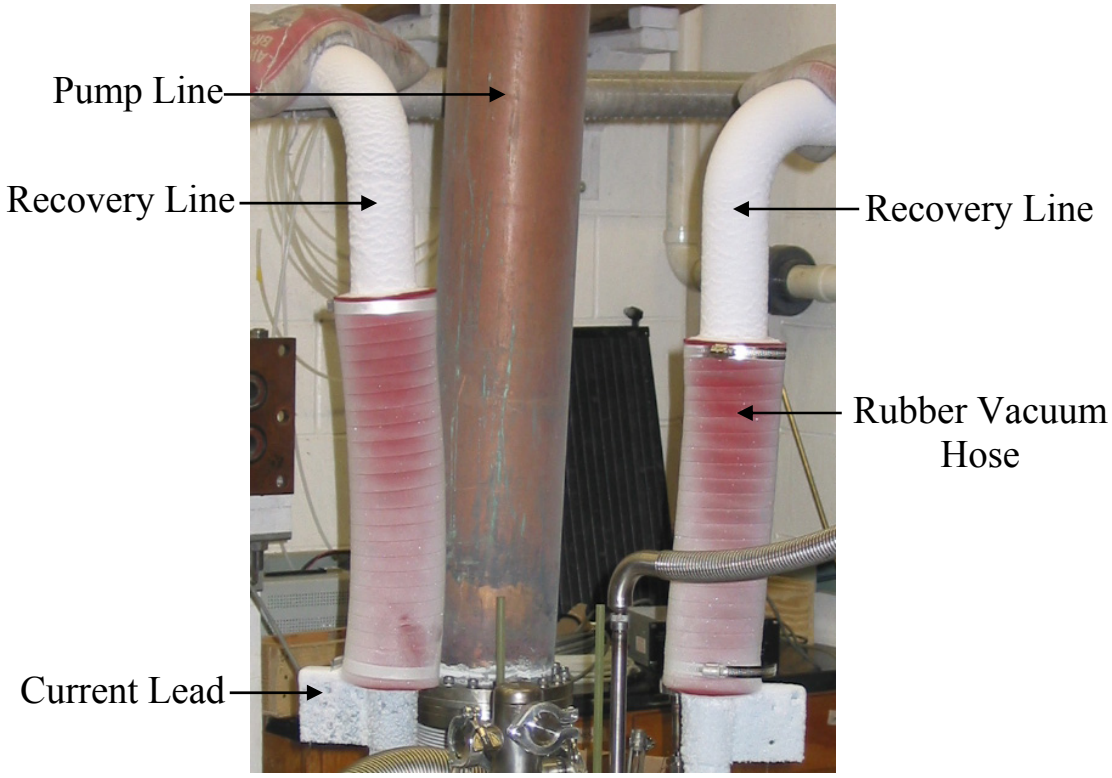

Figure 2.27. Recovery lines and current lead assembly during operation of the refrigeration system.

2.5 Radiation Shields

The dewar that accepts the cryostat is very well insulated from both conductive and radiative heat leaks. However, the G-10 cryostat lid is not as effective at suppressing heat transfer and therefore the internal surface of the cryostat lid will likely be at or near room temperature. In order to minimize the boil-off of liquid helium in the 4.2 K bath, five radiation shields were uniformly spaced between the 4.2 K liquid helium level and the bottom of the cryostat lid. The radiation shields were made of 0.125 inch thick G-10 sheets and covered on both sides with 3M aluminized tape.

The heat leak through five radiation shields is calculated using a resistance network analog for radiation. The resistance to radiation through the first four radiation shields is:

$$R = \frac{1-\varepsilon}{\varepsilon \ Area} \tag{2.72}$$

where ε is the emissivity of the 3M aluminized tape (Incropera 2002):

$$\varepsilon = 0.06 \tag{2.73}$$

The fifth radiation shield radiates to the surface of the liquid He I:

$$R_5 = \frac{1-\varepsilon_5}{e_5 \ Area} \tag{2.74}$$

where ε_5 is the emissivity of the surface of liquid He I (Van Sciver 1986):

$$\varepsilon_5 = 0.5 \tag{2.75}$$

The total resistance of the thermal network is:

$$R_{total} = R_1 + R_2 + R_3 + R_4 + R_5 \tag{2.76}$$

T_{bottom} is the temperature of the 4.2 K helium. The blackbody emissive power of this surface (E_{bottom}) is:

$$E_{bottom} = \sigma \, T^4_{\ bottom} \tag{2.77}$$

T_{top} is the temperature at the top of the cryostat and therefore its blackbody emissive power is:

$$E_{top} = \sigma \, T^4_{\ top} \tag{2.78}$$

The total radiation heat transfer to the 4.2 K liquid helium ($\dot{Q}_5$) is therefore:

$$\dot{Q}_5 = \frac{E_{top} - E_{bottom}}{R_{total}} \tag{2.79}$$

$$\dot{Q}_5 = 1.32 \, [W] \tag{2.80}$$

Table 2.19 summarizes the parameters and results of these calculations based on five radiation shields.

Table 2.19. Parameters and results of the calculations to determine the heat leak into the 4.2 K liquid helium due to radiation through five radiation shields.

Parameter	Symbol	Value
Thermal resistance through the first 4 radiation shields	R	342.6 [1/m^2]
Emissivity of 3M aluminized tape (Incropera 2002)	ε	0.06
Cross-sectional area of radiation shield	$Area$	0.18 [m^2]
Thermal resistance through 5th radiation shield	R_5	5.47 [1/m^2]
Emissivity of liquid He I (Van Sciver 1986)	ε_5	0.5
Total thermal resistance through 5 shields	R_{total}	348.1 [1/m^2]
Blackbody emissive power of bottom shield	E_{bottom}	1.76 10$^{(-5)}$ [W/m^2]
Stefan-Boltzmann Constant	σ	5.67 10$^{(-8)}$ [W/m^2-K^4]
Temperature at liquid helium level in dewar	T_{bottom}	4.2 K
Blackbody emissive power of top shield	E_{top}	459.3 [W/m^2]
Temperature at top of dewar	T_{top}	300 K
Radiative heat leak through 5 shields	$\dot{Q}_5$	**1.32 [W]**

Figure 2.28 shows the radiation heat leak as a function of the number of radiation shields. The graph clearly shows the benefits of having even one radiation shield and also the limited benefit associated with more than five shields.

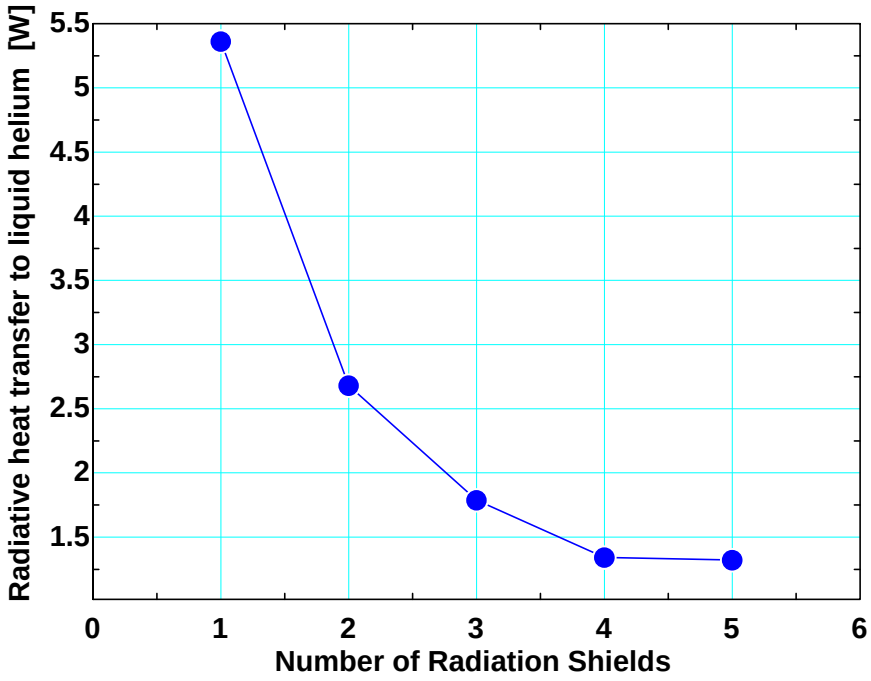

Figure 2.28. Radiation heat leak as a function of the number of radiation shields.

Figure 2.29 is a CAD drawing showing the placement of the radiation shields in the cryostat.

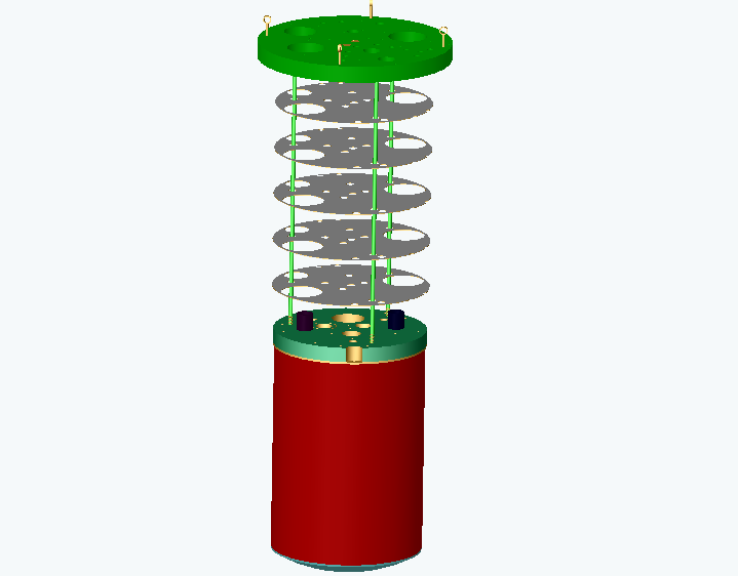

Figure 2.29. Radiation shields located between the cryostat cover and the He II bath lid.

Figures 2.30 illustrates the radiation shields mounted on the cryostat.

Figure 2.30. Radiation shields installed on the cryostat.

2.6 Refrigeration System

2.6.1 Theoretical Model of Key Components

The key refrigeration components include the He I recuperator, the He II heat exchanger, the J-T valve, and the vacuum pump. The recuperator was not designed and built as part of this project but instead was removed from a previous experiment and interfaced with this one. The recuperator is a shell and tube heat exchanger, the He II heat exchanger is a thin walled copper tube made of oxygen-free high conductivity copper (OFHC). Figure 2.31 shows the key refrigeration components and the thermodynamic states of the helium refrigerant throughout the cycle.

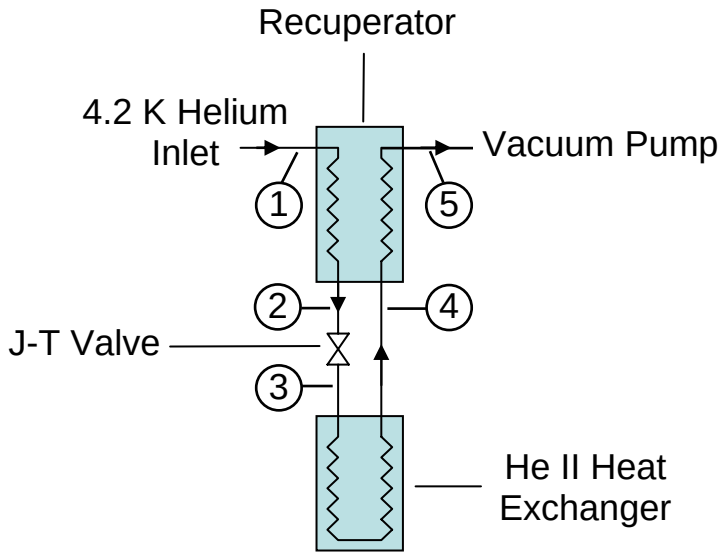

Figure 2.31. Refrigeration system components and thermodynamic states of the refrigerant.

The refrigeration system was designed to operate under the conditions summarized in Table 2.20.

Table 2.20. Refrigeration system operating conditions.

Parameter	Symbol	Value
Refrigeration capacity	$\dot{Q}_{load}$	20 [W]
Pressure of helium in 4.2 K bath	P_1	1 [atm]
Temperature of sub-cooled superfluid helium in He II Bath	T_{load}	1.80 [K]
Temperature difference across Liquid Bath Heat Exchanger	$T_{bath,HX}$	0.05 [K]
Pressure drop on high pressure side of recuperator	$P_{rec,H}$	10 [kPa]
Pressure drop on low pressure side of recuperator	$P_{rec,L}$	0.1 [kPa]

A thermodynamic analysis of the refrigeration system follows and illustrates how these specifications relate to the vacuum pump system. The results also provide inputs necessary for the design of the He II heat exchanger and other system components.

Saturated liquid helium at 4.2 K and 1 atm enters the He I heat exchanger at state (1). The quality (x) and pressure (P) at state (1) are therefore:

$$x_1 = 0.0 \tag{2.81}$$

$$P_1 = 1 \text{ atm} \tag{2.82}$$

The remaining properties of the helium at state (1) (e.g., enthalpy, temperature) are set by Equations (2.81) and (2.82). The HEPAKv3.4 Property Routine [Horizon Technologies, *HEPAK v3.4*, Cryodata, Inc., S/N 4348, October 2002] has been linked to the Engineering Equation Solver (EES) software [S. A. Klein, and F. L. Alvarado, 2002, *EES – Engineering Equation Solver,* F-Chart Inc.] and used to provide all of the thermodynamic and transport properties of normal and superfluid helium for this and all subsequent calculations.

Saturated vapor at state (4) exits the He II heat exchanger and enters the recuperator:

$$x_4 = 1.0 \tag{2.83}$$

The temperature (T) of this vapor is equal to the temperature of the sub-cooled superfluid helium in the He II bath (T_{load}) less the temperature difference required to drive the refrigeration load into the He II heat exchanger ($\delta T_{bath,HX}$):

$$T_4 = T_{load} - \delta T_{bath,HX} \tag{2.84}$$

The remaining properties at state (4) are specified by Equations (2.83) and (2.84) using the *HEPAK v3.4* program.

The helium leaves the recuperative heat exchanger and enters the J-T valve at state (2). The pressure at state (2) is equal to the pressure at state (1) less some pressure loss in the recuperator ($\delta P_{rec,H}$):

$$P_2 = P_1 - \delta P_{rec,H} \tag{2.85}$$

Practically, the lowest temperature achievable at state (2) lies on the lambda line. The transition to superfluid helium within the recuperative heat exchanger results in exceptionally high axial conduction that precludes further temperature drop. Therefore, the properties at state (2) are specified by Equation (2.85) together with the constraint that the state lie on the lambda line. This assumption implies a certain heat exchanger effectiveness; the validity of this assumption in the context of the particular geometry associated with the recuperator will be assessed in a subsequent section.

Assuming that the heat exchanger is adiabatic and operating under steady state conditions, the enthalpy (h) rise associated with the low pressure vapor must equal the enthalpy lost by the high pressure liquid:

$$h_5 = h_4 + \left(h_1 - h_2\right) \tag{2.86}$$

The pressure at state (5) is equal to the pressure at state (4) less the pressure lost in the low pressure passages of the recuperator ($\delta P_{rec,L}$):

$$P_5 = P_4 - \delta P_{rec,L} \tag{2.87}$$

The remaining properties at state (5) are constrained by Equations (2.86) and (2.87). The refrigerant at state (2) expands through the J-T valve and fills the He II heat exchanger with saturated He II at a low pressure. The saturated He II in the He II heat exchanger cools the He II inside the He II bath surrounding the sample. The J-T valve is assumed to be isenthalpic:

$$h_3 = h_2 \tag{2.88}$$

where h is the enthalpy of the fluid. The pressure at state (3) is equal to the pressure at state (4) assuming equilibrium between the liquid and vapor in the He II heat exchanger:

$$P_3 = P_4 \tag{2.89}$$

Equations (2.88) and (2.89) constrain all of the properties of the two-phase mixture in the He II heat exchanger. The mass flow rate through the recuperative heat exchanger ($\dot{m}$) is dictated by the refrigeration load ($\dot{Q}_{load}$) through an energy balance on the He II heat exchanger:

$$\dot{m} = \frac{\dot{Q}_{load}}{\left(h_4 - h_3\right)} \tag{2.90}$$

The volumetric flow rate that must be processed by the pump ($\dot{V}_{pump}$) is related to the mass flow rate and the density (ρ) of helium entering the pump:

$$\dot{V}_{pump} = \frac{\dot{m}}{\rho\left(T = 300\,K, P = P_5 - \delta P_{line}\right)} \tag{2.91}$$

where δP_{line} is the pressure lost in the pump line. The EES program used to carry out these calculations is listed in Appendix B. Table 2.21 summarizes the key results from these calculations.

Table 2.21. Predicted values of the key parameters in refrigeration system.

Parameter	Symbol	Value
Pressure of saturated helium entering recuperator	P_1	101.325 [kPa]
Pressure of subcooled helium entering J-T valve	P_2	91.335 [kPa]
Pressure of superfluid exiting J-T valve	P_3	1.37 [kPa]
Pressure of helium vapor entering recuperator	P_4	1.37 [kPa]
Pressure of helium vapor exiting recuperator	P_5	1.27 [kPa]
Volumetric flow rate through refrigeration system at vacuum pump inlet	VF	1026 [cfm]
Temperature of saturated helium entering recuperator	T_1	4.22 [K]
Assumed temperature of subcooled helium entering J-T valve	T_2	2.17 [K]
Temperature of superfluid exiting J-T valve	T_3	1.75[K]
Temperature of helium vapor entering recuperator	T_4	1.75 [K]
Temperature of helium vapor exiting recuperator	T_5	2.95 [K]
Pinch point temperature of recuperator	$\delta T_{pinch\_point\_recuperator}$	0.42 [K]

Figure 2.32 illustrates the refrigeration load as a function of the pumping capacity for various values of the temperature difference across the He II heat exchanger. The design point is also illustrated on Figure 2.32 showing that the target refrigeration capacity of 20 W is consistent with 1000 cfm pumping speed and 0.05 K temperature difference.

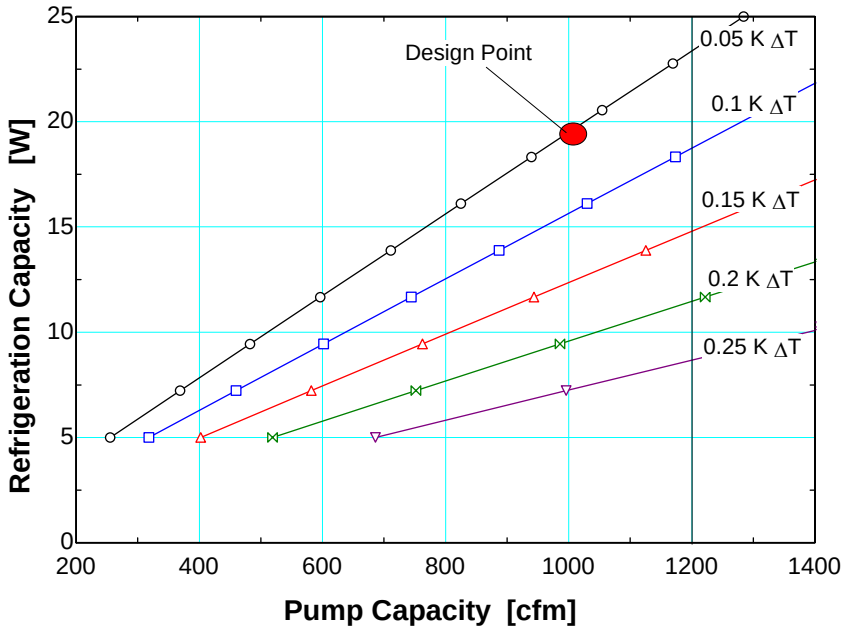

Figure 2.32. Refrigeration capacity as a function of the pump capacity for various values of the He II heat exchanger temperature difference.

2.6.2 Recuperator Model

2.6.2.1 Ideal Model

The ideal thermodynamic model in Section 2.6.1 assumed that the liquid entering the JT valve lies on the lambda line. This implies a certain heat exchanger effectiveness and therefore a certain level of thermal communication between the two streams. This assumption is examined here and used here to quantify the recuperator effectiveness that would be required in order to achieve the refrigeration capacity shown in Figure 2.32. Specifically, this section will calculate the recuperator effectiveness and overall heat transfer coefficient required for the temperature of the helium entering the J-T valve at state (2) to reach T_λ.

The pinch point temperature is the minimum temperature difference between the two recuperator streams:

$$T_{pinch} = T_2 - T_4 \tag{2.92}$$

The desired He II heat exchanger heat transfer rate was set and the thermodynamic states calculated in Section 2.6.2:

$$\dot{Q}_{load} = 20[W] \tag{2.93}$$

Knowledge of these parameters and an energy balance allow the calculation of the mass flow rate through the system:

$$\dot{m} = \frac{\dot{Q}_{load}}{(h_4 - h_3)} \tag{2.94}$$

An energy balance on the cold side of the recuperator yields the heat transferred between the two streams assuming that the external surface of the recuperator is adiabatic:

$$\dot{Q}_{recup} = \dot{m}\,(h_5 - h_4) \tag{2.95}$$

Knowledge of the heat transferred inside of the recuperator allows the average specific heat of each stream to be calculated (note that some variation in the specific heat capacity of helium vapor and liquid occur within the heat exchanger):

$$c_{p\_h} = \frac{\dot{Q}_{recup}}{\dot{m}\,(T_1 - T_2)} \tag{2.96}$$

$$c_{p\_c} = \frac{\dot{Q}_{recup}}{\dot{m}\,(T_5 - T_4)} \tag{2.97}$$

The heat capacitance rate for each stream can be determined:

$$\dot{C}_h = \dot{m}\, c_{p\_h} \tag{2.98}$$

$$\dot{C}_c = \dot{m}\, c_{p\_c} \tag{2.99}$$

The ideal recuperator effectiveness can be calculated:

$$\varepsilon = \frac{\dot{C}_h\,(T_1 - T_2)}{\dot{C}_{min}\,(T_1 - T_4)} \tag{2.100}$$

$$\varepsilon = 83\% \tag{2.101}$$

The number of transfer units (*NTU*) required by the recuperator can be determined:

$$NTU = \frac{1}{C_r - 1}\ln\left(\frac{\varepsilon - 1}{\varepsilon C_r - 1}\right) \tag{2.102}$$

where *Cr* is the capacity ratio, defined as:

$$C_r = \frac{\dot{C}_{min}}{\dot{C}_{max}} \tag{2.103}$$

Finally, the total conductance (*UA*) required can be calculated:

$$NTU = \frac{UA}{\dot{C}_{min}} \tag{2.104}$$

$$UA = 8.29\left[\frac{W}{K}\right] \tag{2.105}$$

If the actual *UA* is equal or larger than the ideal *UA* the recuperator should be capable of transferring the required amount of heat between the two streams and the refrigeration capacity predicted by Fig. 2.32 should be possible. Larger values of *UA* do not translate into higher levels of refrigeration capacity due to the inability of the heat exchanger to operate effectively with superfluid helium. However, if the actual *UA* is smaller than the ideal *UA* calculated by Eq. (2.105) then the recuperator will be unable to cool the incoming stream to T_λ which will raise the temperature of fluid entering the J-T valve and ultimately reduce the refrigeration capacity. The actual *UA* is estimated in the subsequent section.

Table 2.22 summarizes the ideal calculated results:

Table 2.22. Calculated results of ideal recuperator effectiveness and overall heat transfer coefficient.

Parameter	Symbol	Value
Pinch point temperature of recuperator	T_{pinch}	0.42 [K]
Temperature of saturated helium entering recuperator	T_1	4.22 [K]
Temperature of subcooled helium entering J-T valve	T_2	2.17 [K]
Temperature of superfluid exiting J-T valve	T_3	1.75 [K]
Temperature of helium vapor entering recuperator	T_4	1.75 [K]
Temperature of helium vapor exiting recuperator	T_5	2.95 [K]
Enthalpy of saturated helium entering recuperator	h_1	10018 [J/kg]
Enthalpy of subcooled helium entering J-T valve	h_2	3506 [J/kg]
Enthalpy of superfluid exiting J-T valve	h_3	3506 [J/kg]
Enthalpy of helium vapor entering recuperator	h_4	23985 [J/kg]
Enthalpy of helium vapor exiting recuperator	h_5	30497 [J/kg]
Mass flow rate of helium	m_{dot}	$9.766\ 10^{(-4)}$ [kg/s]
Heat exchanged between two streams in recuperator	$\dot{Q}_{recup}$	6.36 [W]
Heat load on He II heat exchanger	$\dot{Q}_{load}$	20 [W]
Specific heat of hot stream	$c_{p\ h}$	3172 [J/kg-K]
Specific heat of cold stream	$c_{p\ c}$	5417 [J/kg-K]
Heat capacity of hot stream	C_h	3.098 [J/K-s]
Heat capacity of cold stream	C_c	5.29 [J/K-s]
Minimum heat capacity between the two streams	C_{min}	3.098 [J/K-s]
Recuperator Effectiveness	$\boldsymbol{\varepsilon}$	**83%**
Maximum heat capacity between the two streams	C_{max}	5.29 [J/K-s]
Ratio of C_{min} to C_{max}	Cr	0.585
Number of transfer units	NTU	2.676
Overall recuperator heat transfer coefficient	$\boldsymbol{UA}$	**8.29 [W/K]**

2.6.2.2 Geometry Based Recuperator Model

The recuperator is a shell-and-tube heat exchanger that was originally designed and fabricated for use in another liquid helium refrigeration system that was previously developed at the University of Wisconsin, Madison. The recuperator consists of fifty-five, 15 inch long parallel stainless steel tubes each with an outside diameter of 0.1875

inches and a wall thickness of 0.010 inches. The shell-and-tube configuration is single pass on both the shell and tube sides. The internal geometry of the recuperator is used here to estimate the actual overall heat transfer coefficient and therefore effectiveness. The geometry based recuperator parameters are compared with those described in Section 2.6.2.1 and the impact on the refrigeration capacity is compared with the ideal model developed in Section 2.6.1.

The Reynolds number of the fluid flowing through the tubes is calculated:

$$Re_{tube\_ID} = \frac{4\,\dot{m}_{tube}}{\pi\, ID_{tube}\, \mu_{tube\_ID}} \tag{2.106}$$

$$Re_{tube\_ID} = 9463 \tag{2.107}$$

where $\dot{m}_{tube}$ is the mass flow rate of helium through one tube, ID_{tube} is the inside diameter of one tube, and μ_{tube_ID} is the average viscosity of helium flowing through the inside of the tubes. The Reynolds number indicates the flow through the tubes is turbulent. The Dittus-Boelter equation (Incropera 2002) is used to calculate the Nusselt number:

$$Nu_{tube\_ID} = 0.023 Re_{tube\_ID}^{\;4/5} Pr_{tube}^{\;n} \tag{2.108}$$

where $n = 0.4$ for heating, and Pr_{tube} is the average Prandtl number of the helium flowing through the tubes. Knowledge of the Nusselt number allows the calculation of the heat transfer coefficient inside of the tubes:

$$h_i = \frac{Nu_{tube\_ID}\, k_{tube\_ID}}{ID_{tube}} \tag{2.109}$$

$$h_i = 31.77\left[\frac{W}{m^2 - K}\right] \tag{2.110}$$

where k_{tube_ID} is the average thermal conductivity of the helium flowing through the tubes. The thermal resistance between the helium and the inside of the tube wall is:

$$R_{tube\_ID} = \frac{1}{h_i\ A_i} \tag{2.111}$$

$$R_{tube\_ID} = 0.112\left[\frac{K}{W}\right] \tag{2.112}$$

where A_i is the total wetted area of the inside of the tubes:

$$A_i = Number_{tubes}\ \pi\ ID_{tube}\ L_{tube} \tag{2.113}$$

$$A_i = 0.28\,[m^2] \tag{2.114}$$

where $Number_{tubes}$ is the number of tubes inside of the recuperator, and L_{tube} is the length of each tube. The thermal resistance through the stainless steel wall of the tubes can be determined:

$$R_{tube\_wall} = \frac{\ln\dfrac{OD_{tube}}{ID_{tube}}}{2\ \pi\ k_{ss}\ L_{tube}\ Number_{tubes}} \tag{2.115}$$

$$R_{tube\_wall} = 0.0071\left[\frac{K}{W}\right] \tag{2.116}$$

where OD_{tube} is the outside diameter of each tube, and k_{ss} is the integrated average thermal conductivity of 304 stainless steel. The Reynolds number of the fluid flowing through the recuperator shell can be estimated:

$$Re_{shell} = \frac{4\,\dot{m}_{shell}}{\pi\, D_{h\_shell}\, \mu_{shell}} \tag{2.117}$$

$$Re_{shell} = 21587 \tag{2.118}$$

where $\dot{m}_{shell}$ is the total mass flow rate of helium through the refrigeration system, μ_{shell} is the average viscosity of helium flowing through the shell and D_{h_shell} is the hydraulic diameter of the area between the shell and the tubes. The hydraulic diameter is defined as:

$$D_{h\_shell} = \frac{4\, Area_{c\_shell}}{P_{w\_shell}} \tag{2.119}$$

where $Area_{c\_shell}$ is defined as:

$$Area_{c\_shell} = \frac{\pi}{4}\left[ID_{shell}^{\,2} - Number_{tubes}\, OD_{tubes}^{\,2} \right] \tag{2.120}$$

where ID_{shell} is the inside diameter of the shell and P_{shell} is the wetted perimeter of the outside of the tubes:

$$P_{w\_shell} = Number_{tubes}\, \pi\, OD_{tube} \tag{2.121}$$

The Reynolds number indicates the flow through the shell is turbulent and the Dittus-Boelter equation (Incropera 2002) is applicable to calculate the Nusselt number:

$$Nu_{shell} = 0.023 Re_{shell}^{\,4/5} Pr_{shell}^{\,n} \tag{2.122}$$

where $n = 0.3$ for cooling and Pr_{shell} is the average Prandtl number of the helium flowing through the shell. The heat transfer coefficient between the outside of the tubes and the helium in the shell can then be calculated:

$$h_o = \frac{Nu_{shell}\, k_{shell}}{D_{h\_shell}} \tag{2.123}$$

$$h_o = 64.02\left[\frac{W}{m^2 - K}\right] \tag{2.124}$$

where k_{shell} is the average thermal conductivity of the helium flowing through the shell (assumed to He II everywhere).

The thermal resistance between the helium and the outside wall of the tubes is:

$$R_{OD\_tube} = \frac{1}{h_o\ A_o} \tag{2.125}$$

$$R_{OD\_tube} = 0.0498\left[\frac{K}{W}\right] \tag{2.126}$$

where A_o is the total surface area of the outside of the tubes:

$$A_o = Number_{tubes}\ \pi\ OD_{tube}\ L_{tube} \tag{2.127}$$

The geometry based overall heat transfer coefficient is therefore:

$$UA_{geometry} = \frac{1}{R_{ID\_tube} + R_{tube\_wall} + R_{OD\_tube}} \tag{2.128}$$

$$UA_{geometry} = 5.90\left[\frac{W}{K}\right] \tag{2.129}$$

Table 2.23 summarizes the results of these calculations:

Table 2.23. Calculated results of geometry based recuperator overall heat transfer coefficient.

Parameter	Symbol	Value
Reynolds number in one tube	Re_{tube_ID}	9463
Mass flow rate in one tube	$\dot{m}_{tube}$	0.000018 [kg/s]
Inside diameter of tube	ID_{tube}	0.0043 [m]
Average viscosity of helium in tube	μ_{tube_ID}	5.82 $10^{(-7)}$ [Pa-s]
Nusselt number of helium in tube	Nu_{tube_ID}	30.81
Prandtl number of helium in tube	Pr_{tube}	0.734
Heat transfer coefficient inside of tube	h_i	31.77 [W/m^2-K]
Thermal conductivity of helium in tube	k_{tube_ID}	0.0044 [W/m-K]
Thermal resistance inside of tube	R_{tube_ID}	0.112 [K/W]
Total wetted perimeter inside of tubes	A_i	0.28 [m^2]
Thermal resistance through tube wall	R_{tube_wall}	0.0071 [K/W]
Outside diameter of tube	OD_{tube}	0.0048 [m]
Thermal conductivity of stainless steel tube	k_{ss}	0.12 [W/m-K]
Number of tubes	$Number_{tubes}$	55
Length of tubes	L_{tube}	0.38 [m]
Reynolds number of helium in shell	Re_{shell}	21578
Hydraulic diameter of shell	D_{h_shell}	0.017 [m]
Viscosity of helium in shell	μ_{shell}	3.43 $10^{(-6)}$ [Pa-s]
Mass flow rate of helium in shell	$\dot{m}_{shell}$	0.0010 [kg/s]
Cross-sectional area of shell	$Area_{c\_shell}$	0.0036 [m^2]
Wetted perimeter of outside of tubes	P_{w_shell}	0.823 [m]
Nusselt number of helium in shell	Nu_{shell}	62.42
Prandtl number of helium in shell	Pr_{shell}	0.772
Heat transfer coefficient outside of tubes	h_o	64.02 [W/m^2-K]
Thermal conductivity of helium in shell	k_{shell}	0.018 [W/m-K]
Thermal resistance outside of tube	R_{OD_tube}	0.050 [K/W]
Total surface area of outside of tubes	A_o	0.31 [m^2]
Geometry based overall heat transfer coefficient	$UA_{geometry}$	**5.90 [W/K]**

Figure 2.33 illustrates the ideal UA and geometry based UA as a function of the temperature entering the J-T valve at state (2).

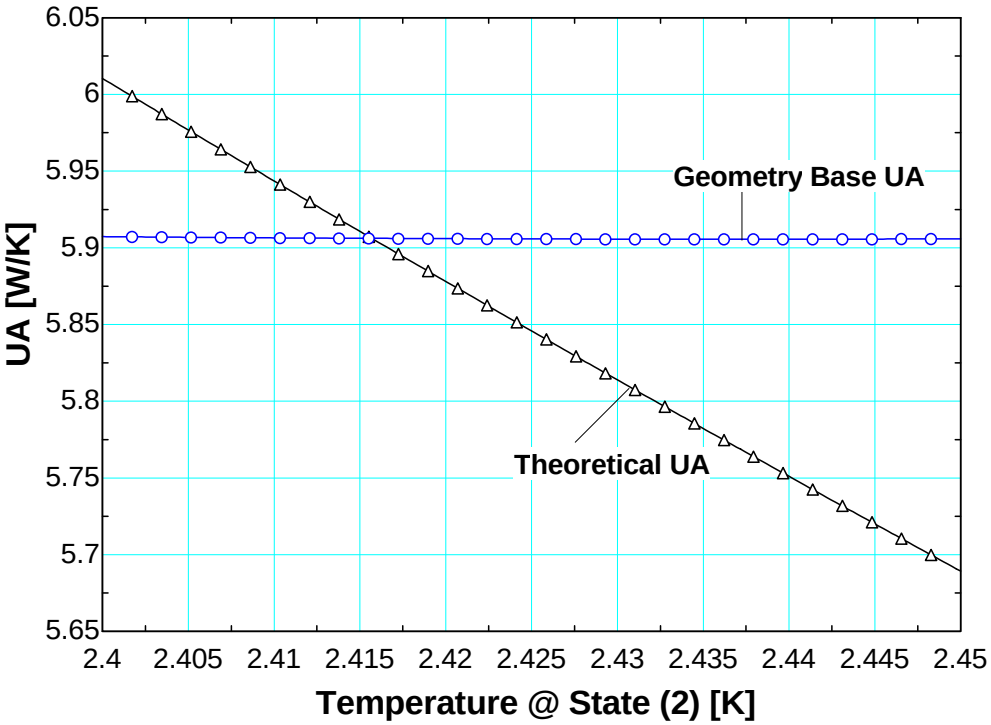

Figure 2.33. Ideal and geometry based UA as a function of temperature entering J-T valve.

The graphs in Figure 2.33 intersect at T_2= 2.416 K, indicating that the geometry based model of the recuperator will result in the temperature of the helium entering the J-T valve to be somewhat higher than T_λ. Note that the theoretical *UA* is strongly dependent on the temperature entering the J-T valve (state 2) according to equations (2.130-2.132):

$$\varepsilon = \frac{\dot{C}_h\,(T_1 - T_2)}{\dot{C}_{min}\,(T_1 - T_4)} \tag{2.130}$$

$$NTU = \frac{1}{C_r - 1}\ln\left(\frac{\varepsilon - 1}{\varepsilon C_r - 1}\right) \tag{2.131}$$

$$NTU = \frac{UA}{\dot{C}_{min}} \tag{2.132}$$

However, the geometry based *UA* calculation is only weakly dependent on the temperature of the fluid entering the J-T valve (state 2) because the property values of the

helium vapor in the tubes and liquid helium in the shell vary only slightly over the prescribed temperature ranges.

Figure 2.34 illustrates how the refrigeration capacity is affected by the temperature of the fluid entering the J-T valve at state (2). Note that raising the temperature of the fluid entering the J-T valve from T_λ (2.1768 K) to 2.416 K results in a 0.7 W reduction in refrigeration capacity.

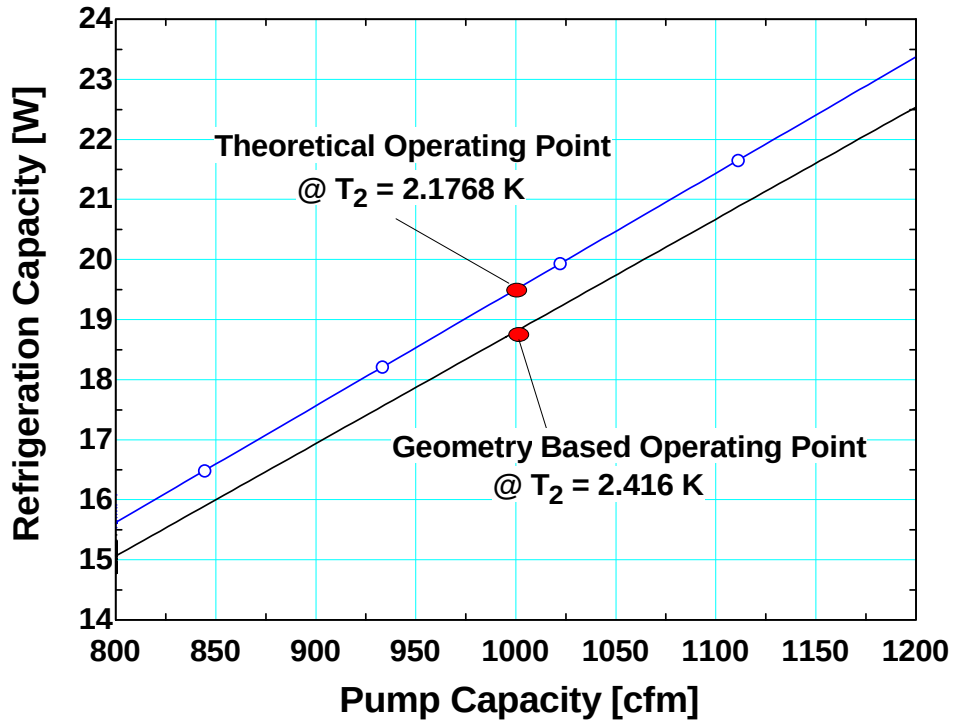

Figure 2.34. Refrigeration capacity as a function of pump capacity for two different fluid temperatures entering the J-T valve.

2.6.3 He II Heat Exchanger

In 1941 Kapitza (Wheatly 1975) discovered the presence of an interfacial resistance while studying the flow of heat around a copper block immersed in liquid He II. The temperature gradients within the liquid were seen to be negligible; however, a sizable

temperature difference was observed between the copper block and the He II. The driving force behind this phenomenon was termed the Kapitza conductance. Kapitza conductance (or its inverse, the Kapitza resistance) is of great technical interest because this resistance often results in the largest temperature difference in a He II heat transfer problem. The Kapitza resistance is the result of an interfacial effect between any two dissimilar materials. The resistance is related to a mismatch between the wavelength of the energy carriers in the two materials and manifests itself as a sharp temperature rise at the interface. At room temperature, this type of effect is important only rarely, for example in problems at the micro-scale. Kapitza conductance occurs at the interface between a metal and water at room temperature but it makes a negligible contribution to the heat transfer coefficient. At low temperatures the Kapitza resistance will become much more important (Van Sciver 1986).

There are a number of applications for He II where knowledge of the Kapitza conductance is of substantial importance. In refrigeration involving He II, its value strongly impacts the proper design of components, particularly heat exchangers. Because of its strong temperature dependence, the importance of Kapitza conductance to heat transfer problems increases with decreasing temperatures. In non-boiling He II, the heat transfer coefficient is essentially entirely related to the Kapitza conductance. Although the Kapitza conductance is an experimentally defined quantity, there has been considerable theoretical work aimed at understanding this complex phenomenon (Van Sciver 1986).

Because Kapitza conductance occurs at the metal surface to liquid He II interface, the surface preparation of the metal strongly influences the heat transfer coefficient. Based on experimental data compiled by Snyder (Princehouse 1972), Van Sciver (1986) states the approximate forms for the Kapitza conductance for a small heat flux ($\Delta T << T_{He\ II}$) are:

$$h_k \approx 0.9T^3 \text{ kW/m}^2\text{-K} \qquad \text{for clean surface} \qquad (2.133)$$

$$h_k \approx 0.4T^3 \text{ kW/m}^2\text{-K} \qquad \text{for dirty surface} \qquad (2.134)$$

but the experimental results may vary for given conditions by as much as a factor of two. The heat transfer from the He II bath to the He II inside of the He II heat exchanger is estimated using the correlation for the Kapitza conductance on a clean surface. Figure 2.35 shows a schematic of the thermal resistance network used to model the He II heat exchanger.

Figure 2.35. Thermal resistance network of the He II heat exchanger.

The desired temperature within the He II bath (the refrigeration load temperature) is 1.8 K. The resistance labeled $R_{Kapitza\ 2}$ is the Kapitza resistance associated with the outside of the He II heat exchanger, T_{OD} is the temperature on the outside surface of the He II heat exchanger, R_{copper} is the radial conduction resistance through the copper wall, T_{ID} is the temperature on the inside surface of the He II heat exchanger, $R_{Kapitza\ 1}$ is the Kapitza resistance on the inside of the He II heat exchanger, and 1.75 K is the estimated

temperature of the saturated He II inside of the He II heat exchanger used to carry out the refrigeration load calculations.

The thermal resistance through the copper wall is:

$$R_{cu} = \frac{\ln\left[\frac{r_2}{r_1}\right]}{2\,\pi\,k_{cu}\,L} \tag{2.135}$$

where *Length* is the length of the heat exchanger, k_{Cu} is the thermal conductivity of OFHC copper (RRR = 100), and *r2* and *r1* are the outside and inside radii, respectively. The Kapitza resistance on the inside of the He II heat exchanger is:

$$R_{Kapitza\_1} = \frac{1}{h_{k1}\;Area_{ID}} \tag{2.136}$$

where $Area_{ID}$ is the surface area of the inside of the He II heat exchanger:

$$h_{k1} = 0.9\,T_1^{3} \tag{2.137}$$

$$Area_{ID} = \pi\;ID\;L \tag{2.138}$$

The Kapitza resistance on the outside of the He II heat exchanger is:

$$R_{Kapitza\_2} = \frac{1}{h_{K2}\;Area_{OD}} \tag{2.139}$$

$$h_{k2} = 0.9\,T_2^{3} \tag{2.140}$$

$$Area_{OD} = \pi\;OD\;L \tag{2.141}$$

The total resistance in the thermal network is:

$$R_{total} = R_{Kapitza\_1} + R_{Kapitza\_2} + R_{cu} \tag{2.142}$$

The heat transfer from the outside to the inside of the He II heat exchanger is:

$$\dot{Q}_{He\_II\_Hxcher} = \frac{T_2 - T_1}{R_{total}} \tag{2.143}$$

The temperatures of the outside and inside wall are:

$$T_{OD} = T_2 - \dot{Q}_{He\_II\_Hxcher}\ R_{Kapitza\_2} \tag{2.144}$$

$$T_{ID} = \dot{Q}_{He\_II\_Hxcher}\ R_{Kapitza\_1} + T_1 \tag{2.145}$$

The EES code used to carry out these calculations is contained in the appendix. Table 2.24 summarizes the calculated results.

Table 2.24. Calculated results of He II heat exchanger thermal network and heat transfer.

Parameter	Symbol	Value
Thermal resistance through copper wall	R_{cu}	9.74 $10^{(-5)}$ [K/W]
Inside radius of He II heat exchanger	r_1	0.035 [m]
Outside radius of He II heat exchanger	r_2	0.038 [m]
Integrated thermal conductivity of copper RRR=100	k_{cu}	280 [W/m-K]
Length of He II heat exchanger	L	0.51 [m]
Kapitza resistance inside of He II heat exchanger	$R_{kapitza\_1}$	0.0014 [K/W]
Heat transfer coefficient on inside of He II heat exchanger	h_{k1}	6431 [W/m^2-K]
Inside surface area of He II heat exchanger	$Area_{ID}$	0.11 [m^2]
Inside diameter of He II heat exchanger	ID	0.070 [m]
Temperature inside of He II heat exchanger	T_1	1.75 [K]
Kapitza resistance outside of He II heat exchanger	$R_{Kapitza\_2}$	0.0012 [K/W]
Heat transfer coefficient outside of He II heat exchanger	h_{k2}	6998 [W/m^2-K]
Outside surface area He II heat exchanger	$Area_{OD}$	0.12 [m^2]
Outside diameter of He II heat exchanger	OD	0.076 [m]
Total thermal resistance through He II heat exchanger	R_{total}	0.0027 [K/W]
Temperature outside of He II heat exchanger	T_2	1.8 [K]
Temperature on outside surface of He II heat exchanger	T_{OD}	1.778 [K]
Temperature on inside surface of He II heat exchanger	T_{ID}	1.776 [K]
Total calculated heat transferred through He II heat exchanger	$\dot{Q}_{He\_II\_Hxcher}$	**18.75 [W]**

The calculated results show the thermal resistance through the copper wall is much smaller than the Kapitza resistance at the inside and outside walls.

2.6.4 Refrigeration Component Design

2.6.4.1 Recuperator Design

Figure 2.36 illustrates the key refrigeration components and the background magnet located in the He II bath.

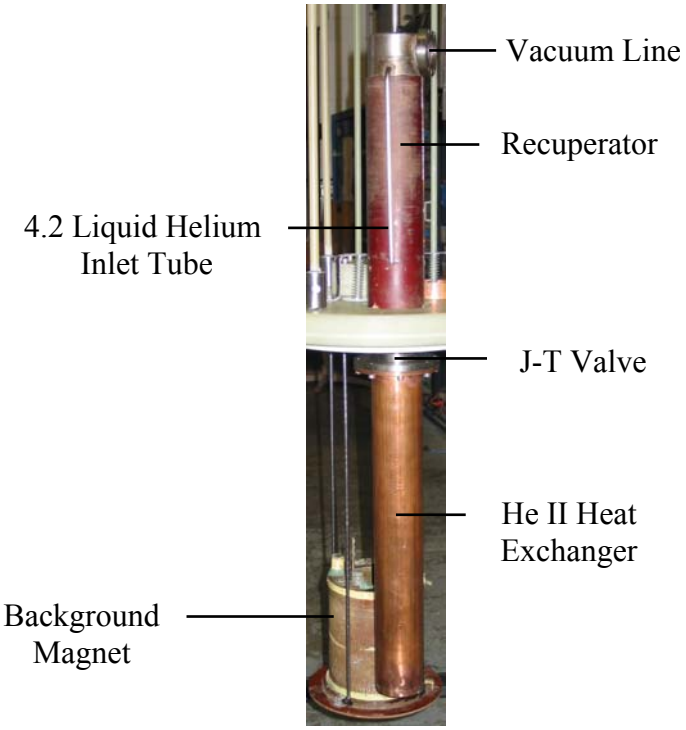

Figure 2.36. Key refrigeration components and background magnet.

Figure 2.37 shows a CAD drawing of the key refrigeration components. The recuperator is a shell and tube heat exchanger with a J-T valve located on the low pressure side of the tube. The high pressure side of the tube extends outside of the recuperator and is submerged in 4.2 K liquid helium. A vacuum line port is located on the low pressure side

of the shell. The inlet to the high pressure side of the shell sits flush with the top of the He II heat exchanger. The outside of the recuperator is insulated with micarta.

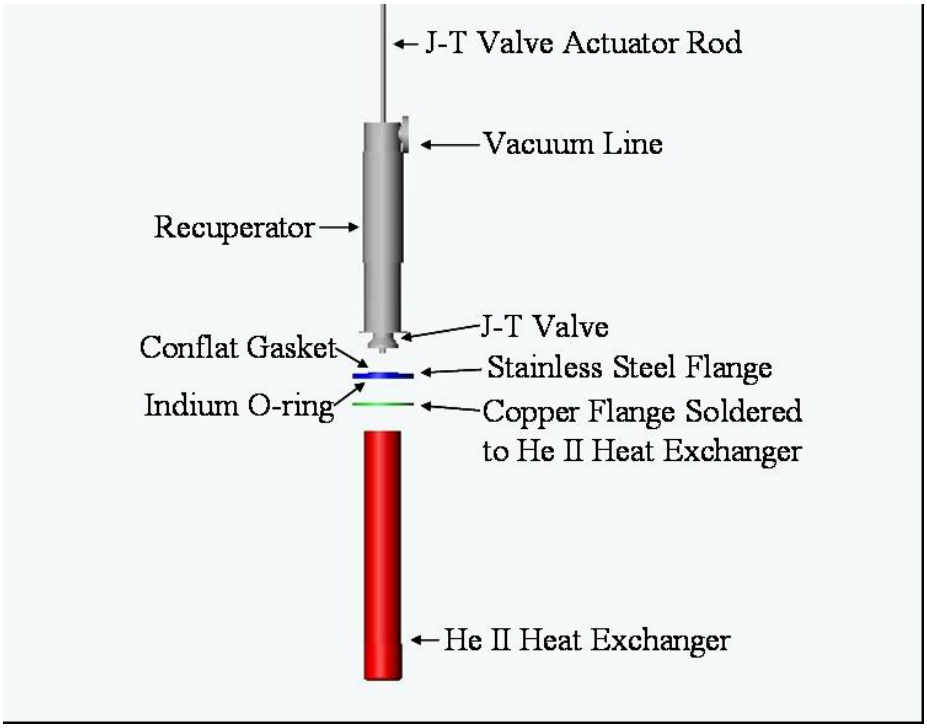

Figure 2.37. Key components of refrigeration system.

The low pressure side of the J-T valve extends 3 inches into the He II bath so that the incoming He II fills the He II heat exchanger and is not drawn into the shell. A 0.100 inch diameter rod, referred to as the J-T valve actuator rod, is attached to the needle of the J-T valve. The rod extends through the cryostat lid and is located inside of a thin walled stainless steel tube that is welded to the top of the recuperator. The rod is made of G-10 with the J-T valve needle glued to one end and a stainless steel rod glued to the other end. The glue joints were made with Stycast epoxy. Two o-ring grooves were installed in the top of the stainless steel rod. The o-rings seal against the inside of the J-T valve actuator rod tube near the top of the tube. The top of the tube extends outside of

the cryostat and therefore is at room temperature so that the o-rings do not freeze. The outside diameter of the J-T valve actuator rod tube is sealed with a Cajon fitting.

2.6.4.2 He II Heat Exchanger Design

A stainless steel flange bolts to the bottom of the recuperator at the low pressure side of the J-T valve (Figure 2.37). The flange is sealed to the recuperator with a 2.5 inch conflat gasket. A copper flange bolts to the other side of the stainless steel flange and is sealed with an indium o-ring. The copper flange is soft soldered the He II heat exchanger. The He II heat exchanger was made of an OFHC copper tube that has a 3 inch outside diameter and a 0.125 inch wall. The length of the He II heat exchanger is 20 inches. A Deteronics 18 pin electrical plug was soldered into the side of the He II heat exchanger in order to make the electrical connections with the instrumentation mounted in the heat exchanger. The bottom of the 3 inch diameter OFHC tube was sealed with a solid flange that was soft soldered in place.

2.6.4.3 Pump Line Design

Figure 2.38 illustrates a portion of the vacuum pump line located inside of the cryostat. A 1.5 inch diameter stainless steel tube was welded to a 2.5 inch conflat to connect to the low pressure side of the shell in the recuperator. The stainless steel tube was adapted to 2.5 inches inside of the cryostat to reduce pumping losses. The 2.5 inch stainless steel tube is passed through the cryostat lid and welded to a thermal stand-off that is mounted to the outside surface of the cryostat lid.

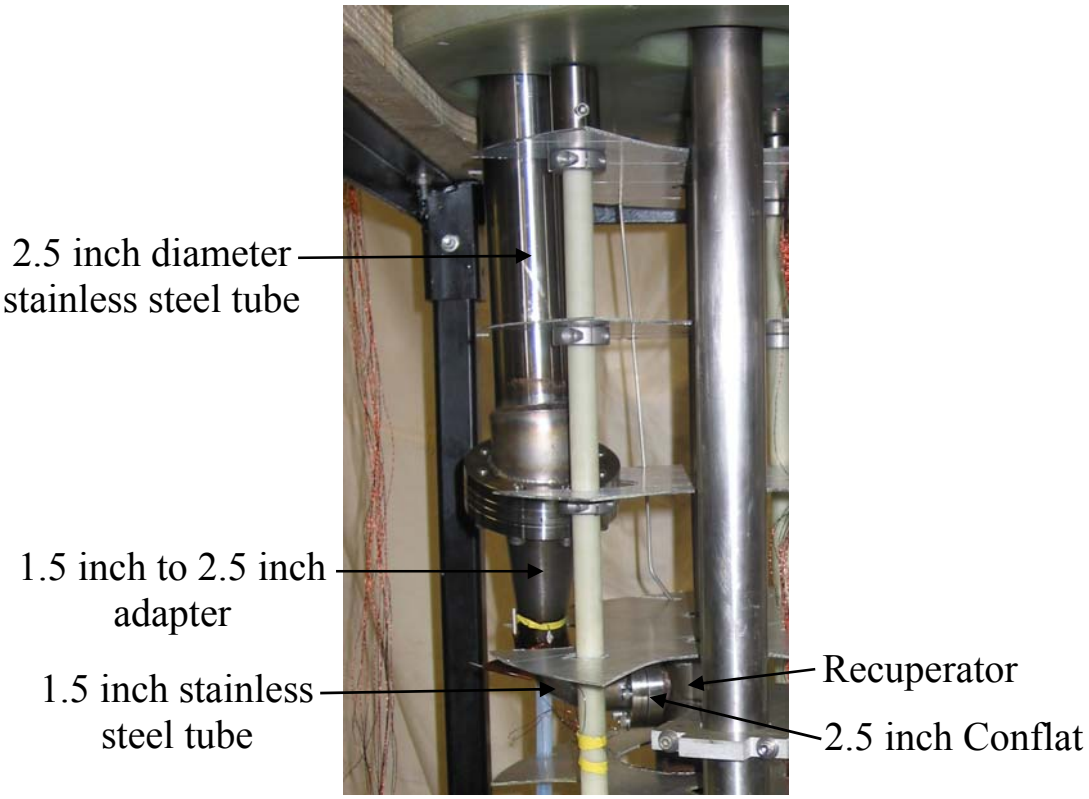

Figure 2.38. Portion of vacuum pump line located inside of cryostat.

The diameter of the internal pump line is limited by the space constraints within the cryostat. However, the pressure drop through the line must be calculated to ensure the vacuum pumps are capable of achieving the desired pressure inside of the He II heat exchanger. The ideal refrigeration model in Section 2.6.1 was used to specify the pressure of the helium leaving the recuperator (P_5). Because the helium vapor inside of the cryostat is stratified, the temperatures at the top of the cryostat and at the 1.5 to 2.5 inch pipe adapter are assumed to be 100 K and 20 K, respectively. Therefore, the pressure at the 1.5 to 2.5 inch pipe adapter was calculated using the average temperature of the adapter and the helium exiting the recuperator at state (5) (White 1999):

$$P_{adapter}{}^2 = P_5^2 - \frac{128\, R_g\, \dot{m}\, \mu_c\, T_c\, L_c}{\pi\, D_c{}^4} \tag{2.146}$$

where R_g is the helium gas constant, $\dot{m}$ is the mass flow rate, μ_c is the viscosity, T_c is the average temperature, L_c is the pipe length and D_c is the pipe diameter. The pressure at the outlet of the pipe that extends from the 1.5 to 2.5 inch adapter to the thermal stand-off mounted on the outside of the cryostat lid was calculated using the average temperature of the adapter and the top of the cryostat:

$$P_{2.5\_pipe}{}^2 = P_{adapter}{}^2 - \frac{128\, R_g\, \dot{m}\, \mu_h\, T_h\, L_h}{\pi\, D_h{}^4} \tag{2.147}$$

Therefore, the pressure drop through the internal pump line is:

$$P_{drop} = P_5 - P_{2.5\_pipe} \tag{2.148}$$

The section of pipe outside of the cryostat that connects the vacuum pumps to the internal pump line is constructed of 6 and 8 inch diameter pipe. Therefore, the pressure drop through these lines is assumed to be negligible. Table 2.25 summarizes the results of these calculations.

Table 2.25. Calculated results of pressure drop through internal pipe line.

Parameter	Symbol	Value
Pressure at 1.5 to 2.5 inch adapter	$P_{adapter}$	1261 [Pa]
Pressure of helium exiting recuperator	P_5	1266 [Pa]
Pressure of helium exiting 2.5 inch pipe	$P_{2.5\_pipe}$	1257 [Pa]
Helium gas constant	R_g	2077 [J/kg-K]
Mass flow rate through refrigeration system	$\dot{m}$	0.0010 [kg/s]
Viscosity of helium through 1.5 inch diameter pipe	μ_c	$9.22\ 10^{(-6)}$ [Pa-s]
Average temperature of helium in 1.5 inch diameter pipe	T_c	101.4 [K]
Length of 1.5 inch diameter pipe	L_c	0.305 [m]
Diameter of 1.5 inch pipe	D_c	0.0381 [m]
Viscosity of helium through 2.5 inch diameter pipe.	μ_h	$1.78\ 10^{(-5)}$ [Pa-s]
Average temperature of helium in 2.5 inch diameter pipe	T_h	250 [K]
Length of 2.5 inch diameter pipe	L_h	0.914 [m]
Diameter of 2.5 inch pipe	D_h	0.0762 [m]
Reynolds number of 1.5 inch diameter pipe	$Re_{adapter}$	949
Reynolds number of 2.5 inch diameter pipe	$Re_{2.5\ pipe}$	3673
Pressure drop through internal pump line	P_{drop}	4 [Pa]

Figure 2.39 illustrates the pump line thermal stand-off made of two 6 inch diameter by 6 inch high stainless steel bellows welded in series. The bottom flange of the thermal stand-off is bolted and glued to the cryostat lid with Stycast epoxy. The 2.5 inch diameter internal pump line is welded to the intermediate flange. An 8 inch conflat is welded to the top of the thermal stand-off and used to seal against the 6 inch copper pump line. The two bellows are placed in series to allow for both thermal contraction of the internal pump line as well as contraction of the external pump line. When the experiment is initially cooled to 4.2 K the internal pump line will contract. This contraction will pull the bellows down towards the cryostat lid. Once the internal pump line has contracted, the lower bellows is locked in place with three threaded rods that connect the bottom flange to the intermediate flange. Therefore when the vacuum pump

is turned on, the contraction due to the pressure difference on both sides of the pump line can be absorbed by the upper bellows.

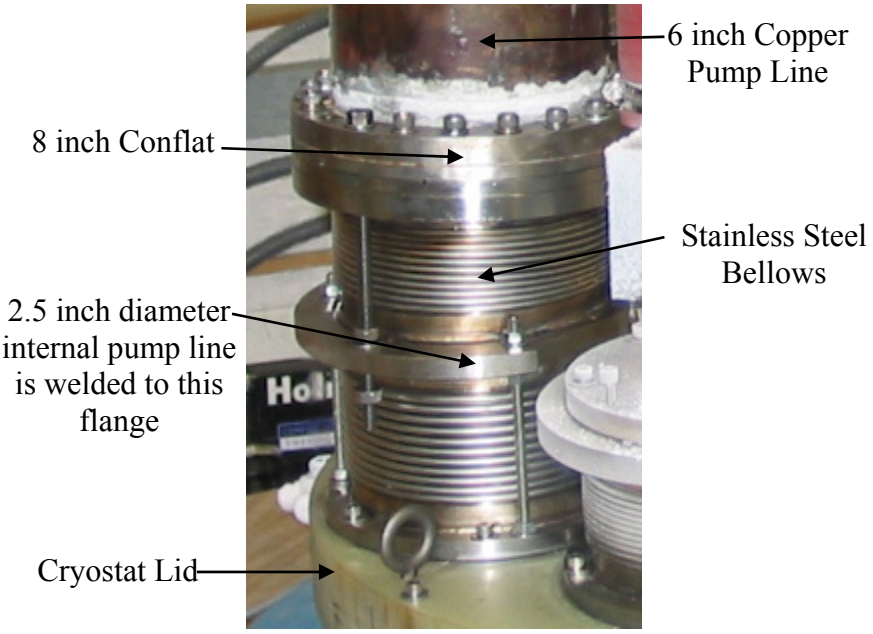

Figure 2.39. Pump line thermal stand-off.

A 6 inch copper pipe is connected to the pump line thermal stand-off and connects to an 8 inch copper pipe. The 8 inch copper pipe connects to the vacuum pumps (Figure 2.40).

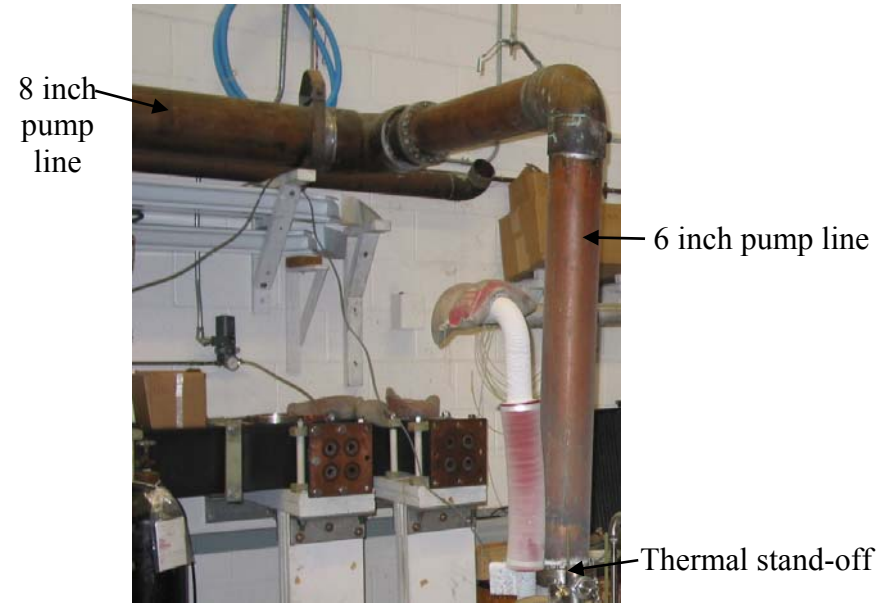

Figure 2.40. 6 inch pump line to 8 inch pump line.

2.7 Controlling Refrigeration System

The mass flow rate of helium through the refrigeration system can be controlled by changing the position of the J-T valve; closing the J-T valve reduces the mass flow rate of helium. The position of the J-T valve is controlled with a Research Control Valve pneumatic actuator (Badger Meter, Inc. Model #1017) located outside of the cryostat. The J-T valve actuator rod is connected to the pneumatic actuator with a threaded coupling. The pneumatic actuator is controlled with an Omega CN76000 Microprocessor Based Temperature/Process Controller that sends a current to a Fisher Controls Type 646 current-to-pressure converter. The current-to-pressure converter is an electronically controlled compressed air regulator that adjusts the air line pressure applied to the actuator. The air pressure pushes against a diaphragm in the pneumatic actuator. The J-T valve actuator rod is connected to the diaphragm and therefore moves up and down as the diaphragm is displaced. The correct mass flow rate is related to maintaining a constant (nearly full) level in the He II heat exchanger. The level in the heat exchanger is monitored using a level sensor. Increasing the mass flow rate (opening the JT valve) will increase the He II heat exchanger liquid level. For optimal performance, the He II heat exchanger should be approximately 95% full. However, overfilling the He II heat exchanger will result in He II filling the shell portion of the recuperator. This reduces the area of liquid helium that is pumped on in the He II heat exchanger and therefore reduces the amount of vapor produced and the refrigeration capacity.

The temperature of the He II inside of the He II heat exchanger is controlled by regulating the pressure inside of the refrigeration system. The pressure is measured by an

MKS Pressure Transducer (Model 127AA-01000D) attached to a pressure tap in the pump line. An MKS Power Supply Readout (Model PDR-C-1C) reads the signal from the pressure transducer and adjusts the position of a butterfly valve located between the cryostat and the vacuum pumps with an MKS Type 250 Exhaust Valve Controller. Two 600 cfm vacuum pumps (Stokes Vacuum Model 412-11) were used to reduce the pressure inside of the refrigeration system to 30 torr. The vacuum pumps are connected in parallel and provide 1200 cfm of pumping capacity.

2.8 Instrumentation

Three types of thermometers were used to measure the temperatures throughout the cryostat: PT-100 platinum resistance thermometers (PRT) with a range of 300 K to 50 K, Lakeshore calibrated Cernox CX-1030-SC resistance temperature sensors with a range of 120K-0.3 K, and Cernox CX-1030-SC resistance temperature sensors calibrated at the University of Wisconsin, Madison with a range of 5 K to 1.85 K. Figure 2.41 shows the position of each thermometer. Table 2.26 lists the position, type, model number, serial number, and the location where the thermometers were calibrated.

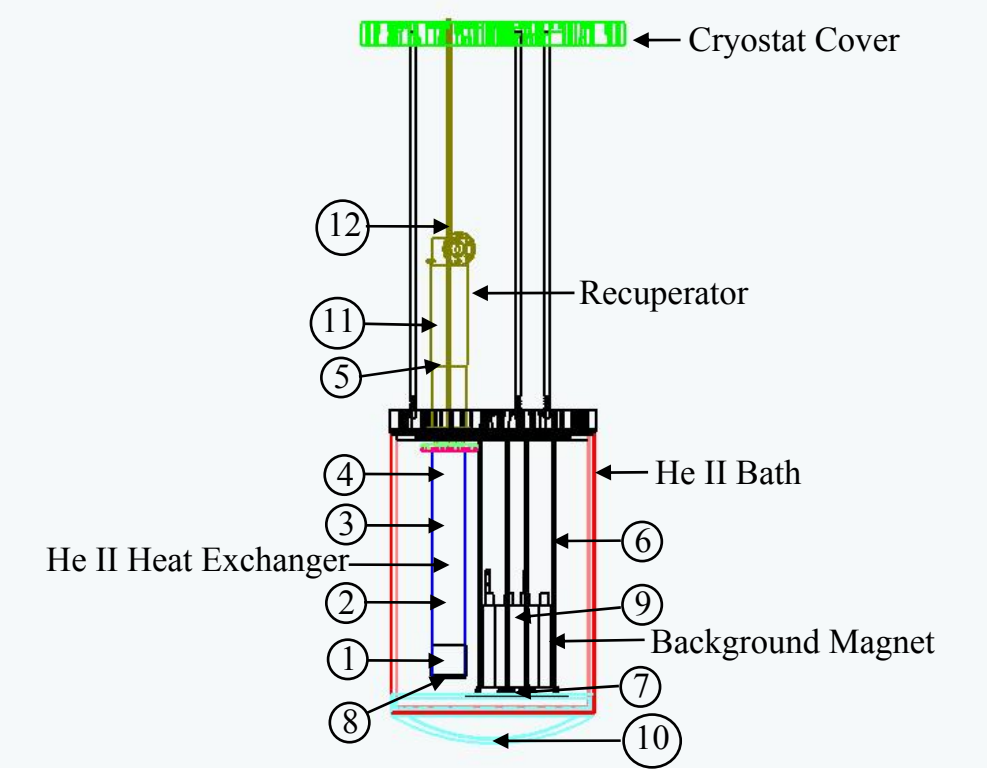

Figure 2.41. Position of thermometers in cryostat.

Table 2.26. Position and description of temperature sensors.

Position Number	Location	Sensor Description	Sensor Model or Serial Number	Calibration
1	Inside bottom of He II heat exchanger	Cernox Resistor	CX-1030-SC-1.4D X28251	UW-Madison
2	Inside middle of He II heat exchanger	Cernox Resistor	CX-1030-SC-1.4D X28253	UW-Madison
3	Inside top of He II heat exchanger	Cernox Resistor	CX-1030-SC-1.4D X27902	UW-Madison
4	Outside top of He II heat exchanger	Cernox Resistor	CX-1030-SC-1.4D X27423	UW-Madison
5	4.2 K bath on recuperator above inlet	Cernox Resistor	CX-1030-SC-1.4D X27422	UW-Madison
6	He II bath on magnet support	Cernox Resistor	CX-1030-SC-1.4D X27901	UW-Madison
7	Inside bottom of magnet bore	Cernox Resistor	CX-1030-SC-1.4D X28252	UW-Madison
8	Outside bottom of He II heat exchanger	Cernox Resistor	CX-1030-SC-1.4D X28183	Lakeshore
9	Inside top of magnet bore	Cernox Resistor	CX-1030-SC-1.4D X28250	Lakeshore
10	Outside of He II bath in 4.2 K bath	PRT	PT-100	Lakeshore
11	Outside of recuperator in 4.2 K bath	PRT	PT-100	Lakeshore
12	Outside of recuperator in 4.2 K bath	PRT	PT-100	Lakeshore

Three PRTs were placed in the 4.2 K bath in order to monitor the initial cool down to liquid nitrogen temperatures. The PRTs are not calibrated or sensitive below 50 K and therefore are of no use at liquid helium temperatures. Seven UW-Madison calibrated Cernox temperature sensors were distributed between the 4.2 K bath and the He II bath. Two Lakeshore calibrated Cernox temperature sensors, which have a guaranteed accuracy of +/- 5 mK, were placed inside of the magnet bore in the He II bath. These were the most accurate temperature sensors used inside of the cryostat and provided a

means of verifying the accuracy of the UW-Madison calibrated sensors. The temperature inside of the magnet bore is the critical temperature within the system as this is the location of the superconducting test specimen. Lakeshore QT-36 Quad-Twist Cryogenic Wire was used to wire all of the temperature sensors inside the cryostat. The twisted pairs used in the Quad-Twist Cryogenic Wire provide common mode noise cancellation which is advantageous when it is desired to minimize the pickup noise to a thermometer or test sample associated with induced currents through the wire leads. CHR Industries electrical tape was used to secure the temperature sensors in place.

The temperature sensors were powered with a Lakeshore Model 120 Constant Current Source. The sensor output was recorded by an Agilent 34970A Data Acquisition/Switch Unit that interfaced with a LabView data acquisition program. The LabView program was run on a Hewlett Packard Pavilion 510W computer.

Three liquid helium level sensors (American Magnetics) were used to measure the liquid helium level in the cryostat: 1) Inside of the 4.2 K bath 2) Inside of the He II bath 3) Inside of the He II heat exchanger. Liquid helium level monitors (American Magnetics Model 110) were used to display the level sensor output.

2.9 Uncertainty Analysis

The UW-Madison calibrated Cernox sensors provided unrealistic measurements during the initial test run of the refrigeration system. Therefore only the uncertainty associated with the Lakeshore calibrated Cernox sensors will be considered here. These sensors are

the most critical to the experiment as they will be used to determine the temperature of the superconducting sample and therefore one aspect of the critical surface.

The temperature uncertainty associated with the characteristics of the Agilent 34970A Data Acquisition/Switch Unit used to measure the voltage across these sensors (u_{T_volt}) is estimated according to:

$$u_{T\_volt} = T \frac{u_v}{S_T V} \tag{2.149}$$

where u_v is the voltage uncertainty of the data acquisition system:

$$u_v = \frac{0.005}{100} V + \frac{0.004}{100} V_{fs} \tag{2.150}$$

V is the voltage measured at the temperature sensor, V_{fs} is the full scale value used, T is the temperature being measured and S_T is the dimensionless temperature sensitivity (LakeShore):

$$S_T = \left(\frac{T}{V}\right)\left(\frac{dV}{dT}\right) \tag{2.151}$$

The temperature uncertainty inherent in the temperature sensor calibration (u_{T_cal}) is reported by the manufacturer as:

$$u_T \_ cal = 0.005\ K \tag{2.152}$$

The temperature uncertainty associated with the Lakeshore 120 current source ($u_{T\_current}$) can be estimated according to:

$$u_{T\_current} = T \frac{u_I}{I S_T} \tag{2.153}$$

where u_I is 0.1% of the current applied to the sensor:

$$u_I = 0.001\ I \tag{2.154}$$

and I is the current applied.

The total temperature uncertainty from the sources considered above (U_{T_total}) is:

$$U_{T\_total} = \sqrt{u_{T\_volt}{}^2 + u_{T\_current}{}^2 + u_{T\_cal}{}^2} \tag{2.155}$$

An additional source of error must be considered related to the self heating temperature rise caused by the dissipation of the applied current. The temperature rise associated with this phenomenon (u_{T_SH}) is:

$$u_{T\_SH} = I\ V\ R_T \tag{2.156}$$

where R_T (Lakeshore 2003) is the thermal resistance separating the temperature sensor from its surroundings (or the temperature that should be sensed). The self-heating error is not unbiased; that is, it will only contribute to a higher than actual temperature reading and is therefore considered separately from the other sources of error that are included in Equation (2.155). Table 2.27 summarizes the results of these calculations.

Table 2.27. Parameters and results of uncertainty calculations.

Parameter	Symbol	Value
Temperature uncertainty of Agilent 34970A	u_{T_volt}	0.00034 [K]
Temperature being measured	T	2.09 [K]
Multimeter voltage uncertainty	u_v	0.000400 [V]
Dimensionless temperature sensitivity (LakeShore 2003)	S_T	2.0
Voltage measured at temperature sensor	V	0.0143 [V]
Temperature uncertainty of Lakeshore calibration	u_{T_cal}	0.005 [K]
Temperature uncertainty of Lakeshore 120 constant current source	$u_{T\_current}$	0.0011 [K]
Current source uncertainty	u_I	$1.00\ 10^{(-8)}$
Current applied to temperature sensor	I	0.00001 [amp]
Total temperature uncertainty at specified temperature	U_{T_total}	0.0051 [K]
Temperature uncertainty due to self heating	u_{T_SH}	0.0014 [mK]
Thermal resistance of temperature sensor (Lakeshore 2003)	R_T	10 [K/W]

2.10 4.2 K Bath Heater

In order to minimize the liquid helium consumption during the initial cool down of the cryostat, the dewar is first pre-cooled by filling with liquid nitrogen. Liquid nitrogen is quite effective at rapidly cooling the experiment from 300 K to 77 K and is approximately 6% of the cost per liter of liquid helium. Also, the specific heat capacity of most of the materials used in the cryostat decreases with temperature and therefore the cooling from 300 K to 77 K provides most of the total energy removal that is required to reach liquid helium temperature; far more than the temperature change alone would suggest.

However, before continuing the cool down to 4.2 K, the liquid nitrogen must be completely removed. Once the experiment has reached 77 K the heat leak into the very well insulated dewar is small relative to the latent heat of vaporization of nitrogen. This

means that it takes a significant amount of time in order for the liquid nitrogen remaining in the dewar to boil off under the influence of the heat leaks through the dewar. It is extremely important that all residual nitrogen be removed from the dewar prior to the introduction of liquid helium. The solidification of nitrogen and the lower temperature changes that occur to its crystalline structure release large amounts of energy, far more (per volume) than what is required to reduce the temperature of the cryostat components. Therefore, large quantities of liquid helium would be consumed by any nitrogen remaining in the dewar. Therefore, several heaters (Minco Thermofoil^{TM}) were installed in the cryostat to accelerate the process of removing the liquid nitrogen from the 4.2 K and He II baths and also to assure a complete removal of all liquid nitrogen. Each Minco heater is capable of dissipating 200 W of power from a 115 VAC power source. Figure 2.42 shows a picture of one of the heaters.

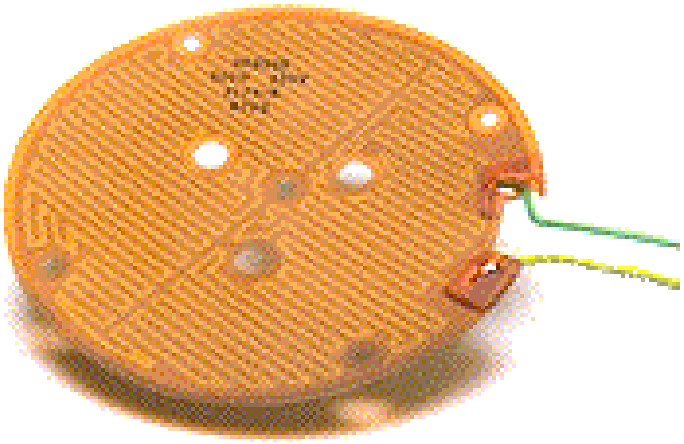

Figure 2.42. Minco Thermofoil^{TM} 200 W heater used to boil off liquid nitrogen in the 4.2 K and He II baths.

The calculations to determine the time required (*Time*) to boil off a standing puddle of liquid nitrogen that is 0.5 inch deep from the bottom of the 4.2 K bath follow:

$$Time = \frac{mass\ h_{fg}}{Power} \tag{2.157}$$

where h_{fg} is the latent heat of vaporization of liquid nitrogen at the saturation temperature and 1 atm. The power developed by the heater is:

$$Power = I^2 \; R \tag{2.158}$$

where I is the current and R is the heater resistance. The mass of the liquid nitrogen present is:

$$mass = \rho \, Volume \tag{2.159}$$

where ρ is the density and the volume is:

$$Volume = \left(\frac{\pi}{4} \right) Diameter^2 \; height \tag{2.160}$$

The time required is:

$$Time = 0.5736 [hr] \tag{2.161}$$

Table 2.28 summarizes the results of these calculations.

Table 2.28. Parameters and results of the calculated time required to boil off a 0.5 inch of liquid nitrogen from the bottom of the dewar.

Parameter	Symbol	Value
Mass of liquid nitrogen	*mass*	2.08 [kg]
Enthalpy of vaporization of nitrogen	h_{fg}	198.9 [kJ/kg]
Power supplied by heater	*Power*	200 [W]
Current supplied through heater	*I*	10 [amp]
Resistance of heater	*R*	3.2 [ohm]
Density of nitrogen	ρ	806.8 [kg/m^3]
Volume of nitrogen	*Volume*	0.0026 [m^3]
Inside diameter of dewar	*Diameter*	0.51 [m]
Height of liquid nitrogen in dewar	*height*	0.013 [m]
Time to boil off nitrogen in dewar	***Time***	**0.57 [hr]**

Chapter 3 Results and Discussion

A zero current proof-of-concept test run of the refrigeration system has been performed to verify the correct operation and integrity of the mechanical and electrical systems. This section presents the data collected during the initial proof-of-concept test run and summarizes the work that is currently being performed in order to address operational limitations and design flaws uncovered by this shake-down test. These modifications will enhance the operation of the refrigeration system during future tests, scheduled for the summer of 2004, in which superconductor samples will be installed and tested.

The zero-current shake-down test demonstrated that the refrigeration system was capable of producing subcooled, superfluid liquid helium. However, a variety of limitations were encountered that prevented the system from reaching 1.8 K; instead, the lowest steady state temperature achieved was about 2.14 K although 2.09 K was achieved in the magnet bore during a transient condition. These limitations were related to correctable issues associated with instrumentation, hardware, and possibly data acquisition software. These issues are discussed in this section and itemized at the end of the chapter.

This chapter is written in essentially chronological order relative to the operation of the experiment; a detailed test procedure is contained in Appendix A. The procedure summarizes the large number of operational details that must be accounted for in order to carrying out the test, ranging from verification of each of the vacuum spaces required by the experiment (transfer line, cryostat, etc.) to making sure that an adequate supply of

consumables is on hand for the test (e.g. helium gas, nitrogen gas, liquid helium, liquid nitrogen, etc.).

The initial step in the experiment is to bolt the cryostat into the dewar and insure that it is leak proof. Next, the dewar is evacuated and purged several times with nitrogen gas to remove the air and water vapor that may otherwise freeze during the cool down process. The pre-cooling operation involves liquid nitrogen being introduced into the cryostat in order to bring the temperature of the thermal masses involved in the hardware (e.g. the He II bath and magnet) down to near 77 K. This operation is an economic necessity given the relative expense of liquid helium and liquid nitrogen. Section 2.8 described the type and placement of thermometers used in the cryostat. Three PRTs are placed in the 4.2 K bath in order to monitor the initial cool down to liquid nitrogen temperatures. The PRTs are not calibrated or sensitive below 50 K and therefore are of no use at liquid helium temperatures. Figure 3.1 presents a graph of the temperatures recorded by the PRTs for the duration of the test. The off-scale values below 50 K were set to 4.2 K to allow continuity in the graphs.

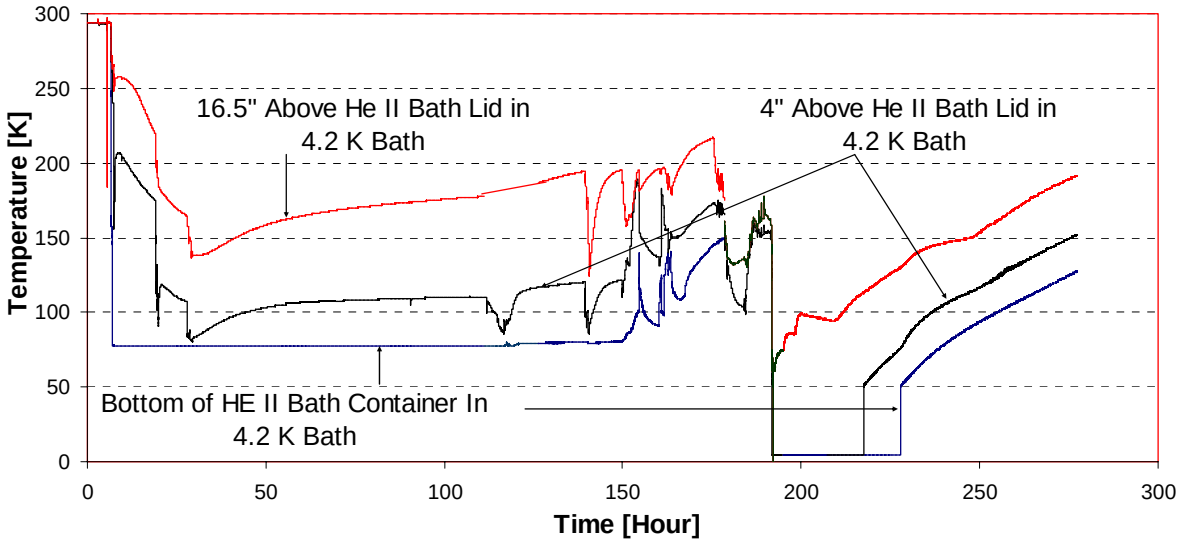

Figure 3.1. Temperatures recorded by the PRTs in the 4.2 K bath for the duration of the test. Note that the off-scale values below 50 K were set to 4.2 K to allow continuity in the graphs.

The cryostat was initially cooled with liquid nitrogen. Great care was taken to remove all of the liquid nitrogen from the 4.2 K and He II baths with the aid of an electrical heater inside of the cryostat. Figure 3.1 illustrates the initial cool-down with liquid nitrogen (from nominally 15 to 30 hours on the x-axis) and the ensuing boil-off process energized by the electric heater (from nominally 30 to 190 hr on the x-axis). The relatively long boil-off process was required to remove the liquid nitrogen that accumulated in the He II bath. There was no electric heater installed in the He II bath and therefore removal of this liquid nitrogen could occur only through the parasitic heat leaks that were present in the system. As described in Chapter 2, great care was taken to minimize these heat leaks during the design of the system and therefore this process was slow. One of the important enhancements that will be included in the facility prior to the next run is the installation of an electric heater into the He II bath in order to avoid this tedious step.

After the successful removal of all liquid nitrogen, the cryostat was purged and filled several times with helium gas then filled with 4.2 K liquid helium. This occurs at nominally 190 hr on the x-axis of Figure 3.1 and the entire low temperature run takes place in a few hours and is therefore represented by the sharp spike at 190 hr seen in Figure 3.1.

The refrigeration system's vacuum pumps were brought online and the temperature in the He II bath was allowed to reach a minimum temperature of 2.09 K. A constant supply of liquid 4.2 K liquid helium was transferred into the 4.2 K bath during the test to replenish what was being consumed by the refrigeration system.

The UW-Madison calibrated Cernox sensors were calibrated by installing them in a liquid helium cryostat (together with the Lakeshore calibrated Cernox sensors) and pumping on the liquid helium in order to achieve sub-4.2 K temperatures. The measured resistance vs. temperature (established by the Lakeshore calibrated thermometers) was used to generate a calibration curve in the form of a 6^{th} order Chebyshev polynomial. A separate curve was required for each sensor as Cernox resistance vs. temperature is extremely sample dependent. However, during operation in the refrigeration system the UW-calibrated sensors were not providing realistic temperature information. This may either be due to software errors associated with implementation of the calibration curves or systematic errors in the calibration data itself. This issue should be addressed before the next test in order to obtain a more complete set of temperature information; however, the Lakeshore calibrated Cernox sensors operated satisfactorily and provided accurate

measurements of the most important temperatures – those in the He II bath. Therefore, only the temperatures recorded by the Lakeshore calibrated Cernox censors will be considered in this Chapter. Figure 3.2 illustrates a graph of the temperature recorded at two locations inside of the He II bath taken on the day that system testing occurred (as opposed to the few days before which were dedicated to cool-down and nitrogen purge). One sensor was placed outside of the He II heat exchanger near its bottom surface whereas the second sensor was placed inside of the background magnet bore and therefore away from the He II heat exchanger. The time indicated in Figure 3.2 is relative to the initiation of testing on the day in question and the first portion of the day was spent removing the remainder of the liquid nitrogen from the 4.2 K helium bath. Notice how the warm nitrogen gas produced by the heater during the nitrogen removal process causes the temperature of the He II bath to rise as the gas expands and exits the cryostat while convectively heat exchanging with the He II bath. This process continued for about 6 hours at which point the electric heater in the liquid helium bath was deactivated.

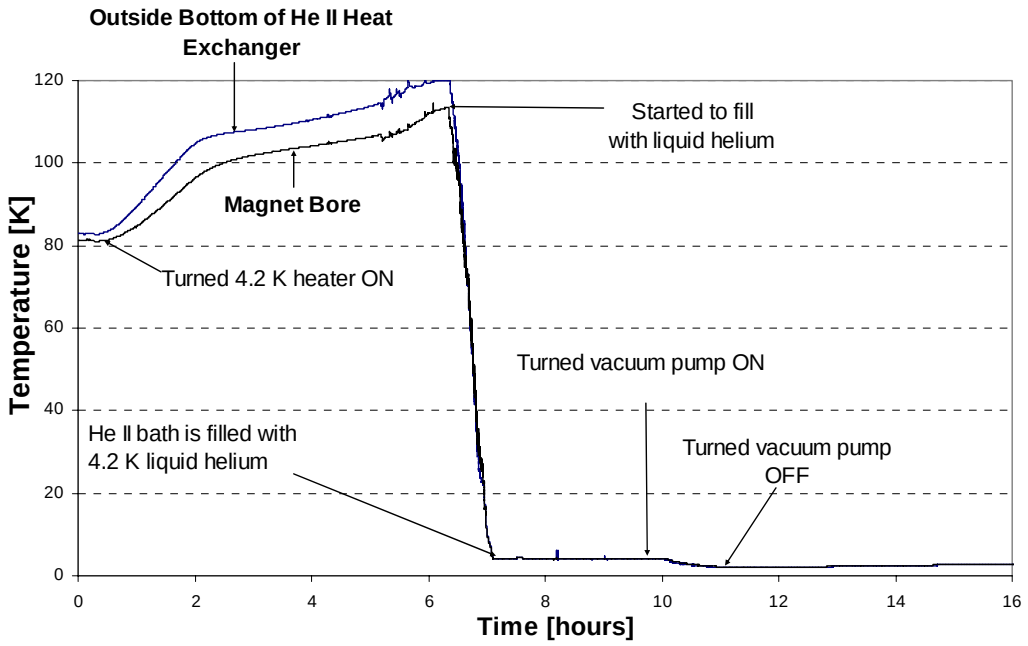

Figure 3.2. Temperature inside of He II bath during cool-down (time does not correspond to Figure 3.1).

Liquid helium was introduced into the 4.2 K helium bath via transfer lines from a portable liquid helium dewar. The liquid helium transfer line provides a highly insulated (via vacuum jacket) passage from a portable dewar to the cryostat. The rate at which liquid helium is transferred can be controlled by the back-pressure applied in the vapor space of the portable dewar which is applied from a helium gas bottle and adjusted with a regulator. The cool-down process from 77 K to 4.2 K took approximately thirty minutes. After thirty minutes the liquid helium being transferred into the cryostat was no longer immediately boiled off and started to accumulate in the 4.2 K bath and, subsequently, the He II bath. Once the 4.2 K bath liquid level rose to cover the inlet tube of the recuperator, the vacuum pumps were turned on and the refrigeration system was activated. The refrigeration system was run for approximately one hour after which a minimum temperature of 2.09 K was achieved inside of the He II bath. At the conclusion

of the test (after the vacuum pumps were turned off) the temperature within the He II bath was monitored until the heat leak from the surroundings into the dewar boiled-off all of the liquid helium.

Figure 3.3 illustrates the initial transition from saturated liquid helium at 4.2 K and 1 atm to subcooled liquid helium inside of the He II bath. Notice the steep slope of the graph down to the lambda point at 2.17 K. The lambda point identifies the conversion of subcooled He I to superfluid He II where a significant increase in energy is required to make the transition.

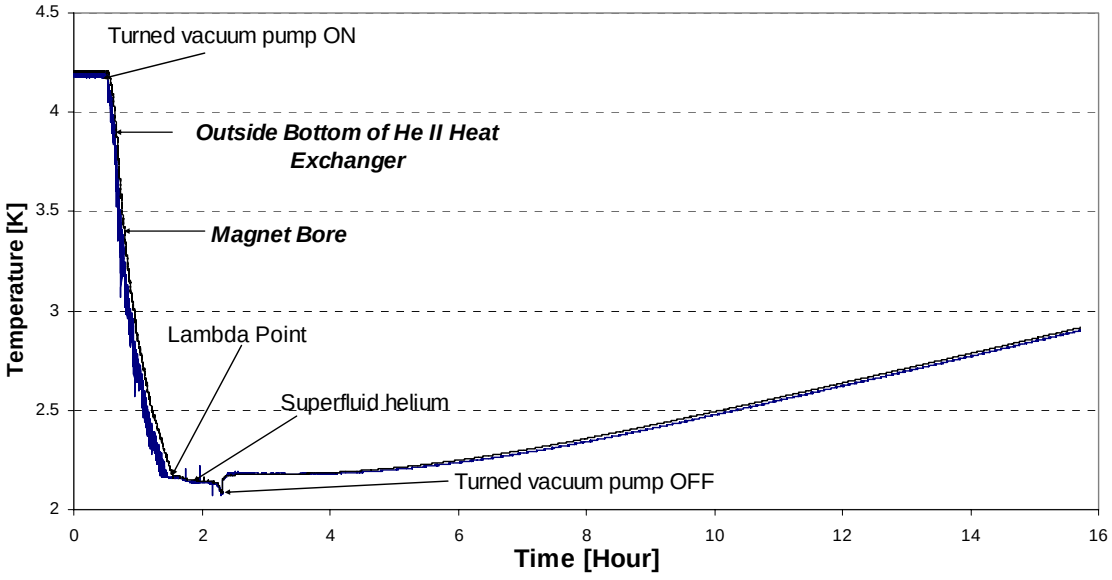

Figure 3.3. Temperature inside of He II bath during cool-down and warm-up.

The design of the refrigeration system relies on the ability to adjust the position of the J-T valve in order to regulate the level of the liquid helium with the He II heat exchanger. Unfortunately, after filling the cryostat with liquid nitrogen it was determined that the J-T valve had frozen in the "up" position (fully open) and could not be adjusted. Likely this

was related to improper venting of the J-T valve stem prior to cool down and therefore residual water caused the valve to "stick". The loss of control of the J-T valve turned out to be a more significant problem than it would initially appear. The inability to control the mass flow rate entering the He II bath resulted in a loss of performance rather than simply a loss of control of the refrigeration capacity.

The J-T valve malfunction is responsible for the inability of the system to achieve 1.8 K. By controlling the mass flow rate entering the He II heat exchanger, the liquid level in the He II heat exchanger can be maintained at a desired height. However, with the J-T valve fully open, the He II heat exchanger quickly becomes completely filled and liquid superfluid helium begins to overflow into the bottom of the recuperator. The refrigeration system operates by reducing the vapor pressure over the surface of the He II inside of the He II heat exchanger. The exposed area of the liquid in the recuperator is much less than in the heat exchanger and thus so is the refrigeration capacity. As a result of the uncontrolled mass flow rate the steady state minimum temperature obtained was only 2.14 K.

Once it had become apparent that the temperature would not decline further, the supply of 4.2 K liquid helium into the 4.2 K bath was stopped but the refrigeration system was kept operational. The vacuum pumps lowered the liquid level in the 4.2 K bath until the inlet tube of the recuperator was exposed to vapor. At this point there was no liquid mass flow into the recuperator which caused the liquid level in the He II heat exchanger to drop. The reduction of the liquid level in the He II heat exchanger increased the surface

area and therefore the refrigeration capacity. Figure 3.4 illustrates a graph of the He II bath temperature during this process.

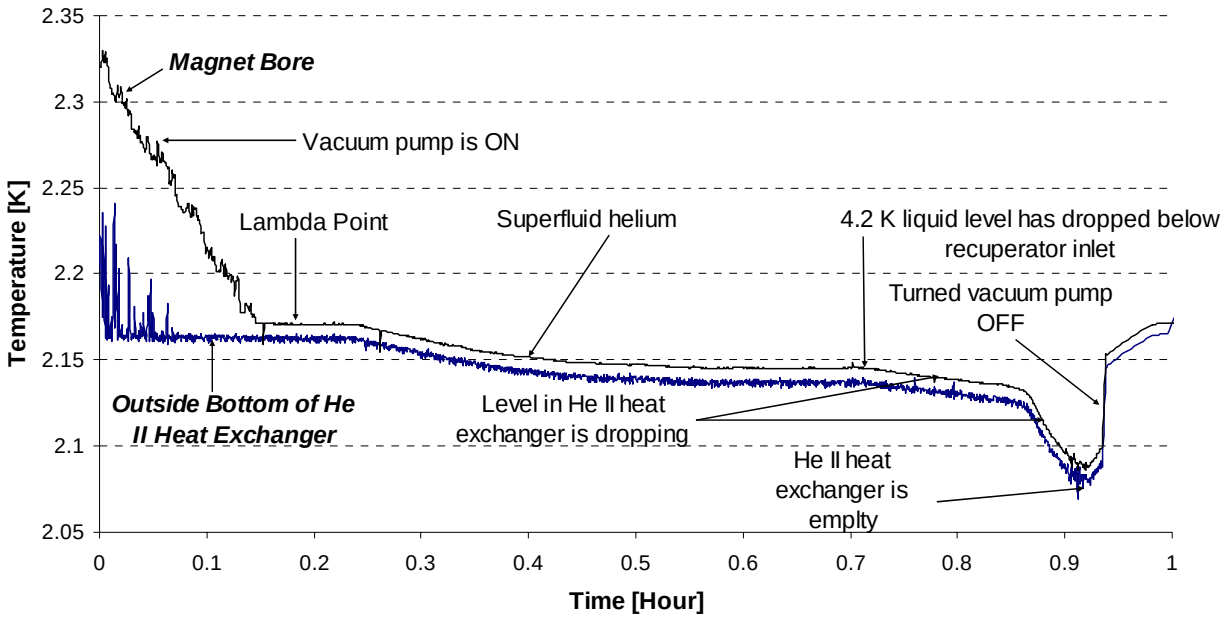

Figure 3.4. Temperature inside of He II bath during cool-down.

Note that the minimum temperature achieved during normal operation (with the He II heat exchanger overfull of liquid) was 2.14 K. However, Figure 3.4 illustrates that once the liquid level in the He II heat exchanger receded from the recuperator, the temperature in the He II bath began to decrease at a relatively fast rate; extrapolation of this rate shows that 1.8 K could likely be reached in less than 30 minutes and that the refrigeration capacity in this operating condition is more than sufficient to achieve this no-load temperature. However, without any liquid flowing into the recuperator the He II heat exchanger liquid level continued to drop and was quickly depleted; once this occurred, all refrigeration capacity was lost and temperatures began to climb under the influence of heat leak. The point were the vacuum pumps were turned off is indicated in Figure 3.4.

The graph shows a sharp increase in temperature from the He II region to the lambda point once the refrigeration capacity was depleted. The sharp increase is attributed to the warm helium vapor being drawn into the He II heat exchanger from the 4.2 K bath.

The complete cool-down operation required approximately 650 liters of liquid helium. The storage capacity of the cryostat is about 170 liters. The majority of this helium is recovered by the helium recovery system, however the test is quite expensive to carry out.

Figure 3.5 illustrates temperature recorded in the He II bath during warm up and demonstrates the functionality of the Vent/Fill cones in the He II bath lid and the 2 psig springs holding the cones in place. The cones were purposely left in the closed position during the initial warm-up period. Consequently the He II bath was not properly vented and pressure began to build inside as the liquid boiled-off. The graph in Figure 3.5 illustrates a sharp increase in temperature at 4.37 K, well above the normal boiling point of 4.2 K for liquid helium at 1 atm. The saturation pressure of liquid helium at 4.37 K is 16.82 psia or 2.1 psig. Based on the sharp increase in the slope of the graph at 4.37 K, corresponding to an increased rate of venting, it is evident that the 2 psig spring and cone assemblies were functioning as designed.

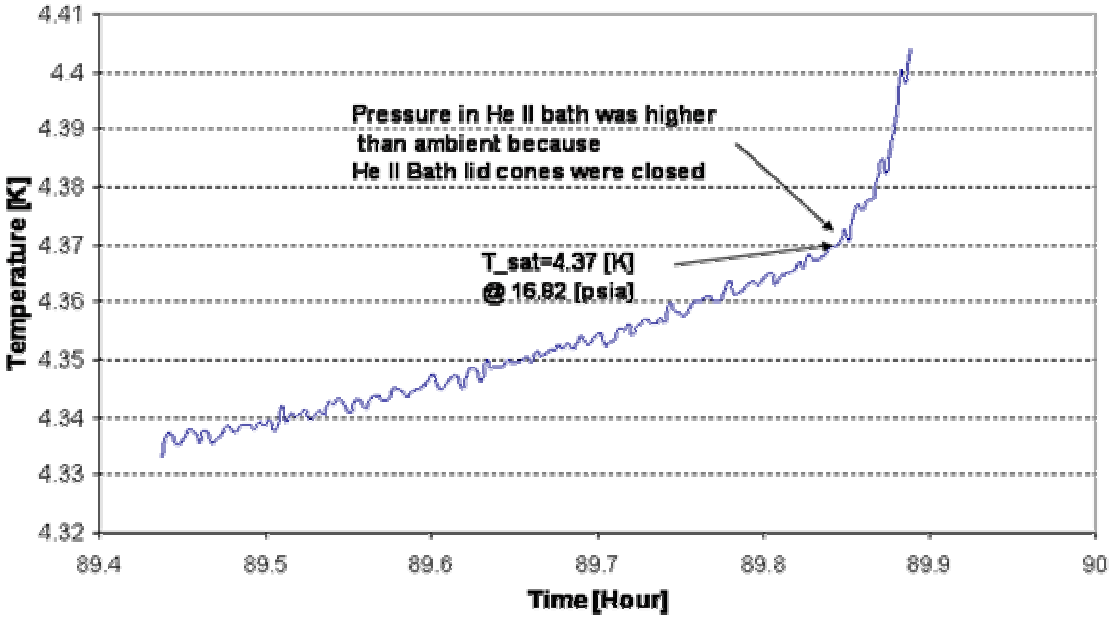

Figure 3.5. Temperature inside of He II bath during warm-up. The Fill/Vent cones were closed in the He II bath lid which allowed the pressure to build to 2.1 psig until the cones were forced off of their seats. Notice the increased slope at 4.37 K indicating the transition from saturated vapor to pure vapor.

The test described above showed that the hardware, the instrumentation, and test procedure are adequate to achieve the temperatures and loads required to test Argonne National Lab's superconducting samples. A number of issues were described during the previous sections and these all lead to required work prior to the next test run. The need to successfully address these issues prior to the next test run is amplified by the relatively expensive and labor-intensive nature of each test as well as the increased level of complexity that will be associated with subsequent runs in which a sample power supply, magnet power supply, and critical current measurements must operate at the same time that the refrigeration system is operating.

A list of the key enhancements that are being made to improve the refrigeration system's performance and make future tests more efficient are as follows:

1. To avoid the J-T valve from freezing, the pneumatic actuator should be cycled several times during the filling and purging process before liquid helium is introduced into the cryostat. Both sides of the refrigeration system should be pumped on during the purging process to ensure the complete removal of contaminants that are likely to freeze.

2. A 200 W heater is being installed in the He II bath to aid in the removal of liquid nitrogen.

3. A liquid nitrogen level sensor will be installed in the He II bath to aid in measuring the level of liquid nitrogen present during the initial cool-down process.

4. Provisions to monitor the vapor pressure inside of the He II heat exchanger will be made to provide an additional means of determining the temperature in the He II heat exchanger.

5. The accuracy of the UW-Madison calibrated Cernox sensors will be investigated to determine the discrepancy between their measurements and the measurements recorded by the Lakeshore calibrated sensors.

Bibliography

Allen, J.F. and Jones, H, *Nature* (London) **141**, 243 (1938).

Allied Manufacturing, Bozeman, Mt., (406) 586-8381

Argonne National Labs, *The Advanced Photon Source*, ANL/APS/TB-25-Rev., October (1997).

Augueres, J.L, Aymar, R., Bon Mardion, G., Faure Brac, G., Plancoulaine, J., and Senet, L., "700 mm diameter cryostats operating at 1.8 K and atmospheric pressure", *Cryogenics* Vol. 20, pp. 529-533 (1980).

Barron, R.F. Cryogenic Systems, Oxford University Press, New York, (1985).

Canavan, E.R., Larbalestier, D.C., and Van Sciver, S.W., "A 13 T-1.8 K NbTi Laboratory Test Coil", *IEEE Transactions on Magnetics*, Vol. 24, no. 2, pp. 1082-1085, (1988).

Claudet, G., Lacaze, A., Roubeau, P., and Verdier, J., "The design and operation of a refrigerator system using superfluid helium", *Proceedings of the 5th International Cryogenic Engineering Conference*, IPC Science and Tech. Press, Guildford, England, pp. 265-267, (1974).

F-Chart, Inc, *EES-Engineering Equation Solver*, Klein, S.A. and Alvarado, F.L., 2002.

Goldman, A., *Midwest Team Receives $2.8 Million for Beamline*, http:/www.external.ameslab.gov/news/release/1996rel/96beamline.html, February (1996).

Goldman, A. and Johnston, S., *Ames Laboratory Efforts Pay Off—Beam Line is Operational*, http://www.external.ameslab.gov/news/release/2000rel/00mucat.html, June (2000).

Horizon Technologies, *HEPAK v3.4*, Cryodata Inc., S/N 4348, October 2002.

Incropera, F. P. and DeWitt, David P., Introduction to Heat Transfer, John Wiley & Sons, New York (2002).

Kapitza, P.L., *J. Phys.* USSR 4, 181 (1941)

Keesom, W.H., *Helium*, Amsterdam Press, New York, (1927).

Keesom, W.H., and Meyer, L. *Physica*, **7**, p.817 (1940).

Khalatnokov, I.M. *An Introduction to the Theory of Superfluidity* W. A. Benjamin, Inc., New York, (1965).

LakeShore Temperature Measurements and Control Catalogue (2003).

Pfotenhauer, J.M., "Design Issues for a Superfluid Helium Subcooler", *Heat Transfer and Superconducting Magnetic Energy Storage*, ASME, HTD-Vol. 211, (1992).

Pfotenhauer, J.M., Bodker, F., Jiang, Z. , Lokken, O.D, Tao, B., and Yu, D., "A 100 kA, He II Cooled Conductor Test Facility", *Advances in Cryogenic Engineering*, Vol. 37, Part A, pp. 155-162, (1992).

Pfotenhauer, J.M., "Measurements of low heat demountable seals for use in superfluid helium", *Cryogenics*, **36**, pp. 963-965, (1996).

Princehouse, D.W., High-Resolution Heat Capacity Study of He Adsorbed on Bare Copper, *J. Low Temp. Phys*. **8**, 287 (1972).

Weisend, J.G., Handbook of Cryogenic Engineering, Cambridge University Press, New York (1998).

Wheatly, J.C., Three Lectures on the Experimental Properties of Liquid He, *The Helium Liquids*, Academic Press, London, 1975.

White, F.M., *Fluid Mechanics*, McGraw-Hill, Madison, WI, 1999.

Van Sciver, S.W., *Helium Cryogenics*, Plenum Press, New York

Appendix A ANL 1.8K Helium Refrigerator Operation Procedure

**The start of this procedure assumes that the test sample has been mounted, and the data acquisition system has been checked at room temperature.*

Mounting the He II Bath

NOTE: *In order for the epoxy to properly cure, your hands and work area must be clean and free from oil, dirt, etc.*

- Insert two heaters into the bottom of the He II bath.
- Clean the stainless steel sealing surface of the He II bath and the sealing surface of the G-10 He II lid with acetone.
- Apply several coats of epoxy mold release agent to both surfaces according to the manufacture's instructions.
- Using McMaster Carr Cat. #123 Hand-Workable Epoxy Putty, cut a 1" thick piece of both parts A and B and mix together according to the manufacture's instructions.
- After the epoxy is well mixed, form it into a ¼ inch diameter bead. Place the bead on the He II bath stainless steel mounting flange, halfway between the ID of the flange and the mounting bolts.
- Set four 1 mm thick flat washers on the stainless steel mounting flange, between the OD of the flange and the mounting bolts. Index the flat washers every 90 degrees. The washers will serve as spacers to maintain a consistent thickness of the epoxy seal.

- Hoist the refrigerator off of its stand and slide the stand out of the way.
- Slide the He II bath under the refrigerator, being careful not to hit the epoxy bead.
- Connect the heater wires to the plug potted in the He II bath lid.
- Carefully lower the experiment into the He II bath, but do not allow the two mounting flanges to touch at this time. The hoist lowers the experiment too quickly and makes it very difficult to get the surfaces aligned. Leave about a 1 inch gap between the two mount surfaces.
- Prepare the ¼-20 mounting bolts by coating the treads with grease or an anti-seize compound. A Bellville washer should be placed under the head of each bolt. The cone of the Bellville washer should face towards the G-10 flange.
- Using the hydraulic jack attached to the He II cradle, slowly raise the He II bath up until the mounting bolts can be started. Use the bolts to draw the two flanges together by tightening the bolts in a star pattern. Take care to ensure the two mounting flanges stay parallel and the He II bath does not become cocked. Draw the two flanges together until they are tightly seated against the 1 mm thick flat washers.
- Using a new gasket, connect the VCR fitting on the He II bath evacuated space pump line.
- Hook a turbo pump up to the KF25 fitting on the evacuated space pump line and verify that the VCR fitting is not leaking. The evacuated space should be pumped on over night to eliminate out-gassing.
- Clean any fingerprints, grease, etc. from the He II bath sides and lid.
- Use Acetone to carefully clean the surfaces of the radiation shields.

Insert Refrigerator into Dewar

- Insert two heaters into the bottom of the blue dewar.
- Pump out the vacuum space in the dewar.
- Inspect o-ring on top of the dewar.
- Carefully lower refrigerator into dewar, stopping when the dewar cover is about 1 ft from the dewar.
- Connect the heater wires to the connectors potted in the dewar lid.
- Carefully lower the experiment until the lid contacts the dewar. Be sure to avoid any wires from being pinched between the two surfaces.
- Orient the dewar lid so the vacuum line bellows lines up with the 8 inch vacuum line port mounted to the south wall.
- Coat the ¼-20 mounting bolts with grease or and anti-seize compound, and then progressively tighten in a star pattern.

Connections to the Dewar Cover

NOTE: *The conflats on both ends of the 6 inch pump line rotate. While this feature makes installation easier, it also makes the conflat vulnerable to damage because the knife-edge sticks out the farthest and is unprotected. Care must be taken to ensure the knife-edge does not get damaged during the handling of the pump line.*

The 8 inch pump line conflat is positioned vertically and care should be taken to ensure the gasket is seated properly and does not become cocked during installation.

- Prepare the 8 inch conflats on the 6 inch pump line, 8 inch vacuum line, and bellows. Clean the knife-edges with acetone and inspect them for nicks or debris. Clean two new copper gaskets with acetone.
- Coat all of the mounting bolts with grease or an anti-seize compound.
- Strap the 2 inch x 2 inch steel lifting bar to the shorter section of the 6 inch pump line. Put a 25 lb shot bag in the carrier at one end of the lifting bar. Use another 25 lb shot bag on top of the pump line to equalize the weight, making the lifting bar parallel.
- Hoist the vacuum line into place, install the new gaskets, and tighten both conflats. A conflat should be tightened by working in a circular pattern, moving from one bolt to the next closest bolt. As the gasket is compressed, the bolt first tightened will become lose. Therefore, it will require tightening in a circular pattern several times before the gasket is firmly seated. The final recommended torque of the 5/16-24 bolts is 192 in-lbs.
- Remove the lifting hoist from the pump line and move the hoist away from the experiment.
- Install a hose attached to a bottle of compressed nitrogen to one of the ½ NPT access holes in the dewar cover.
- Attach the compressed air line from the I-P converter mounted on the south wall to the red pneumatic actuator.
- Install a stainless steel vacuum line between the 6 inch conflat on the 8 inch pump line and one of the KF25 fittings on the instrumentation tree (located on the cryostat lid).

- Remove the helium fill tube (if present) from the Cajon fitting on dewar lid labeled “Bottom” and insert a plug into the Cajon fitting.
- Remove the helium fill tube (if present) from the Cajon fitting on dewar lid labeled “Middle” and insert a plug into the Cajon fitting.
- Raise both G-10 rods attached to the cones in the He II lid and hold up with a clamp, being careful not to damage the surface of the rod where the o-ring will seal when the cones are closed.
- Install clear Tygon tubes without slits onto magnet current leads and plug the ends.
- Install two 6 inch long white vacuum hoses (with plugs on one end) onto the current leads and tighten with a stainless steel hose clamp.
- Energize the I-P converter by turning on the Omega CN76000 controller located on the south wall by the sink. Once energized, manually pull up on the J-T valve rod. The rod can be accessed through the pneumatic actuator mount.

Install the Recovery Lines

NOTE: *The recovery line that makes a 90-degree bend as soon as it leaves the 4.5 inch conflat gets mounted closest to the north wall.*

The recovery line conflats are positioned vertically and care should be taken to ensure the gasket is seated properly and does not become cocked during installation.

- Prepare the four 4.5 inch conflats of the recovery lines. Clean the knife-edges with acetone and inspect them for nicks or debris. Clean two new copper gaskets with acetone.
- Coat all of the mounting bolts with grease or an anti-seize compound.
- Install the recovery lines to the recovery pipe mounted on the west wall and tighten both conflats. A conflat should be tightened by working in a circular pattern, moving from one bolt to the next closest bolt. As the gasket is compressed, the bolt first tightened will become lose. Therefore, it will require tightening in a circular pattern several times before the gasket is firmly seated. The finally recommended torque of the 5/16-24 bolts is 192 in-lbs.
- Connect the 4 inch OD red vacuum hoses to the stainless recovery lines. Do not attach the hoses to the current leads at this time.

Fill the He II Evacuated Space with Helium

- Connect the He II bath evacuated space port to a turbo pump using a KF25 T fitting.
- Connect a bottle of compressed helium to the open KF25 port in the T.
- With the Nupro valve on the evacuated space line still closed, turn on the turbo pump and evacuate the hose. The vacuum space should still be pumped out at this time.
- After the hose is evacuated, open the Nupro valve and verify that the vacuum in the evacuated space is in the $10^{(-5)}$ torr range. Use the thermocouple pressure gauge installed in the KF25 cross to read the pressure.

- After a low vacuum is verified, close the turbo pump valve. Fill the evacuated space with compressed helium to atmospheric pressure.
- Turn off the turbo pump following the manufacture's instructions.

CAUTION: ***The dewar is not designed to be under pressure. Therefore, care must be taken to ensure that the dewar is not pressurized to more than 2 psig.***

Operating the Stokes Vacuum Pumps in the Basement

- Close the slide valve on the 8 inch vacuum line located on the south wall of the High Current Lab.
- Close the electronically controlled butterfly valve by adjusting the MKS controller on the south wall of the High-Current lab.
- Close the red manually controlled valve located close to the inlet of the vacuum pump in the basement.
- Turn the pump on with the correctly numbered switch on the north wall in the basement.
- Check that the oil level in sight glasses on both the pump and the blower is at the ½ mark.
- Slowly open the red manual controlled valve right before the vacuum pump. The flow through the butterfly valve is very non-linear, so opening it just a little at first will allow a significant amount of air to pass. Do not allow the vacuum pump to receive a large quantity of air. Wait approximately 10 minutes, and then

open the valve a little more. Continue this process until the valve is completely open (this should take about 30 minutes).

- With the electronically controlled butterfly valve still closed, open the slide valve in the High-Current lab.
- Slowly open the electronically controlled valve, following the same procedure used to open the manually controlled valve.
- Watch the compound gauge, located on the 8 inch vacuum line above the slide valve, to verify that there is a vacuum in the pipe.
- A vacuum is now being drawn on the dewar through the refrigeration system and the instrumentation tree.
- Use the thermocouple pressure sensor located in the 8 inch line above the slide valve in the High Current Lab to read the pressure in the line. The pressure should drop to approximately 30 millitorr.

NOTE: *If the dewar will not pump down to the 30 millitorr range, the source of leak must be located and repaired.*

- Close the electronically actuated butterfly valve.
- Close the slide valve on the 8 inch pump line.
- Carefully fill the dewar with nitrogen gas to a pressure of no more than 2 psig.
- Manually cycle the J-T valve several times.

- Open the slide valve on the 8 inch pump line and slowly open the electronically controlled butterfly valve following the same initial start-up procedures listed above.
- Repeat the filling and purging process several times to ensure the removal of air from the dewar.
- After the purge and fill process is complete, close both the electronically controlled butterfly valve and slide valve in the 8 inch pump line.
- Fill the dewar to 2 psig with nitrogen gas.
- While maintaining a positive pressure in the dewar:
    - Remove the 6 inch long white vacuum hoses with plugs from the current leads and install the red recovery line vacuum hoses.
    - Remove the plug from the transfer line Cajon fitting labeled “bottom” and insert the 5/8 inch OD liquid nitrogen transfer line.
    - Connect the nitrogen transfer line in the blue dewar to a liquid nitrogen dewar.
    - Remove the stainless steel vacuum line from the instrumentation tree and 8 inch pump line. Block both KF fittings.
    - Turn both recovery line butterfly valves, located in the stainless steel portion of the recovery line, to the full open position.
    - Open the recovery line ball valve and the PVC ball valve on the line exiting the room.

CAUTION: *There will be a high rate of boiling when first transferring nitrogen to a warm dewar. This boiling can lead to a rapid build-up of pressure in the dewar and must be monitored very carefully.*

- Open the fill valve on the liquid nitrogen dewar (while keeping the vent valve on the dewar closed).
- Close the valve on the compressed nitrogen bottle.
- Adjust the fill valve of the dewar to keep the pressure in the blue dewar under 2 psig.
- Stop filling when the temperature sensors in the He II bath read 77 K, indicating liquid nitrogen has entered the He II bath.
- If the temperature in the He II bath begins to rise above 77 K, continue to add more liquid until the temperature stabilizes.
- Try to avoid putting more liquid nitrogen into the He II bath than is required to keep the temperature stabile at 77 K.
- Turn off the liquid nitrogen dewar fill valve and carefully remove the liquid nitrogen fill line from the dewar. The line will be very cold and should be handled with gloves. Use a heat gun to help remove the o-rings.
- Plug the transfer line Cajon fitting.
- Allow the temperature in the dewar to stabilize over night.
- After the temperature has stabilized, insert the liquid nitrogen transfer line into the Cajon fitting labeled “bottom”. Slide the transfer line into the dewar until it hits the bottom.

- Put the open end of the transfer line fill hose into a Styrofoam cooler.
- Remove the red recovery line vacuum hoses from the current leads.
- Install the 6 inch long white vacuum hoses with plugs onto the current leads.
- The only dewar vent that should now be open is the transfer line.
- Once the transfer line cools liquid nitrogen should start to collect in the Styrofoam cooler.
- Monitor the pressure in the blue dewar. Open another vent if the pressure exceeds 2 psig. Add a small amount of compressed nitrogen gas if the pressure is below 2 psig.
- Once the liquid stops flowing, insert a wooden stick into the transfer line Cajon fitting labeled "middle". Allow the stick to touch the bottom of the dewar for several seconds, then remove the stick and wave it in the air. The frost line on the stick will indicate the current liquid level.
- If the liquid level is less than ½ inch high, open the valve on the flow meter located in the dewar lid.
- Remove the liquid nitrogen transfer line and plug the Cajon fitting.
- The only dewar vent that should be open at this time is the valve on the flow meter.
- Turn both heaters on in the 4.2 K dewar and He II bath to boil off the remaining liquid nitrogen.
- Carefully monitor the nitrogen level in the dewar with the wooden stick. Turn the dewar heater off when the nitrogen in the dewar has boiled off.

- Install a 0-5 scfm flow meter into one of the ½ inch NPT holes in the dewar cover.
- Use the flow meter to determine when all of the liquid has boiled off in the He II bath. As long as there is flow through the meter there is still liquid nitrogen boiling. When the flow has stopped, turn off the He II heater and close all vents to the dewar.
- Remove the flow meter from the dewar lid and plug the port with an ½ inch NPT plug.
- Evacuate the dewar with the vacuum pump in the basement according to the guidelines above.
- Use the thermocouple pressure sensor located in the 8 inch line above the slide valve in the High Current Lab to read the pressure in the line. Once the pressure has dropped to approximately 30 millitorr, close the electronically controlled butterfly valve and slide valve in the 8 inch pump line.
- Remove the regulator from the compressed nitrogen bottle and attach it to a compressed helium bottle.
- Manually cycle the J-T valve several times.
- Fill the dewar with compressed helium gas to a pressure of 2 psig.
- Fill and purge the dewar with helium gas several times following the guide lines above.
- Close the ball valve on the recovery line.

- While maintaining a positive pressure in the dewar, remove the 6 inch long white vacuum hoses with plugs from the current leads and attach the red recovery line vacuum hoses.
- While maintaining a positive pressure in the dewar, remove the transfer line Cajon fitting plugs. Insert the long 5/8 inch OD helium transfer line tube into the Cajon fitting labeled "Bottom".
- Insert the short 5/8 inch OD helium transfer line tube into the Cajon fitting labeled "Middle".
- Insert a plug into the 3/8 inch Cajon fittings on the ends of the helium transfer line tubes.

Fill the Nitrogen Jacket in the Dewar with Liquid Nitrogen

- Insert the 3/8 inch OD liquid nitrogen transfer line into the port on the blue dewar jacket labeled "Fill".
- Open the port on the blue dewar jacket labeled "Vent".
- Attached the 3/8 inch OD liquid nitrogen transfer line to a liquid nitrogen dewar.
- Open the liquid nitrogen fill valve.
- Fill the dewar jacket with liquid nitrogen until liquid starts to flow from the vent.
- Plug both the fill and vent caps. The nitrogen jacket will now vent through the pressure relief valve.

Pump Out the Evacuated Space in the He II Bath

- Close the valve on the compressed helium bottle connected to the He II bath evacuated space pump line.
- Turn on the turbo pump connected to the He II bath evacuated space pump line.
- Open the Nupro Valve on the He II bath evacuated space line.
- Once the He II bath evacuated space has pumped down to a pressure in the $10^{(-5)}$ torr range, close the Nupro valve.
- Turn off the turbo pump.

Transfer Helium to Dewar

CAUTION: *There will be a high rate of boiling when first transferring helium to the dewar. This boiling can lead to a rapid build-up of pressure in the dewar and must be monitored very carefully.*

The transfer line used to transfer liquid helium from the portable dewar to the experiment has a vacuum space. Hook the transfer line up to the turbo pump to verify that it has a good vacuum prior to transferring helium.

- Manually cycle the J-T valve to ensure it is not frozen in place.
- Lower the two G-10 rods connected to the cones in the He II bath lid to their fully closed position.
- Increase the data acquisition sampling rate to 1 sample/sec.

- Connect a bottle of compressed helium gas to a portable liquid helium dewar. Do not turn the gas on at this time.
- Open the transfer line valve.
- Slowly insert the transfer line into the portable liquid helium dewar.
- Allow helium gas to flow through the transfer line to purge the line of air and cool the transfer line. When liquid starts to flow a white plume of gas will be seen exiting the transfer line. At this point the transfer line is ready to be installed into the experiment.
- With the transfer line valve open, remove the Cajon fitting plug from the line labeled "Bottom" in the blue dewar lid and insert the transfer line.
- Open the large recovery line ball valve on the west wall (this is the valve in parallel with the recovery bag valve). Once this valve is open, helium gas will vent to the top of the room.
- Turn the four recovery line band heaters on to 100%. Monitor the temperature of the gas flowing through the recovery line with the thermocouple digital gauge. Adjust the band heater percentage controllers accordingly to maintain the temperature of the recovered gas between 0-50 C.
- Adjust the transfer line valve to keep the blue dewar pressure under 2 psig.
- Use the compressed helium gas connected to the portable liquid helium dewar to keep the pressure in the portable liquid helium dewar around 2 psig.
- Allow the helium gas exiting the dewar to vent to the room for approximately 1 minute to purge the line of contaminants.
- Close the vent ball valve and open the recovery line ball valve.

- Turn on the three American Magnetic Liquid Helium Level Indicators.
- Fill the dewar according to the following table:

	Low Helium Level	**High Helium Level**
% Helium	57.43%	72.23%
Inches of Liquid Helium	36.46 [inch]	45.34 [inch]

- The liquid level must be below the bottom of the current leads and above the inlet to the He I heat exchanger.
- Remove the transfer line from the transfer line tube labeled “Bottom”. Install a plug in the 3/8 inch transfer line tube Cajon fitting.
- Insert the transfer line into the transfer line tube labeled “Middle”. The liquid level will be maintained by transferring liquid helium into the middle of the dewar, avoiding bubbling warm gas into the liquid at the bottom the dewar every time the transfer line is turned off and back on.
- Verify that the electronically controlled butterfly valve is closed.
- Open the slide valve in the 8 inch vacuum line in the High Current Lab.
- Slowly open the electronically controlled butterfly valve.
- Monitor the level in the He II heat exchanger. Keep the level above 90% but below 100% by adjusting the J-T valve via the pneumatic actuator. If the liquid level reaches 100% the refrigeration capacity will be significantly reduced.
- Monitor the level in the dewar and add more helium as necessary to keep the liquid level in the proper range according to the table above.
- The temperature in the He II bath should slowly decline.

Shutting Down and Warming Up the Refrigerator Without a Heater

- Close the liquid helium transfer line valve.
- Close the slide valve in the 8 inch vacuum line. Put a note on the valve actuator to ensure the valve is not reopened. If the valve is opened, the vacuum pumps will empty the recovery bag.
- Remove the helium transfer line. Use a heat gun to help in removing the o-rings.
- Plug the helium transfer line tube Cajon fitting.
- Remove the vent and fill plugs from the nitrogen jacket in the blue dewar.
- Lock the two G-10 rods attached to the cones in the He II bath lid in the full up position.
- Turn off the American Magnetics Liquid Level Sensors in the 4.2 K dewar and the He II heat exchanger.
- Turn off the recovery line band heaters.
- The liquid helium in the He II bath will remain for several days. The He II bath liquid level indicator should be monitored periodically during this time to decide when the He II bath is empty.
- Once the He II bath is empty, close the large recovery bag ball valve and open the large vent ball valve. This will allow the expanding gas in the dewar to vent to the room without contaminating the recovery bag.
- Turn off the American Magnetics Liquid Level Sensor in the He II bath.
- The temperature inside of the He II bath should be above the dew point temperature in the lab to avoid condensing liquid on the cryostat (and inside of

passages that may retain water vapor that could be challenging to remove during the next test).

Shutting Down and Warming Up the Refrigerator with a Heater

If a heater is used to speed the warming process up, follow the same procedures listed above. However, local temperatures can quickly rise to levels that could be damaging to the cryostat. THEREFORE, THE EXPERIMENT MUST NOT BE LEFT UNATTENDED WHILE THE HEATERS ARE ON. Furthermore, additional venting may be required due to the increased boil-off rate.

Removing the Cryostat from the Blue Dewar

- Remove the two red vacuum hoses from the recovery lines and current leads.
- Unbolt the 4.5 inch conflats on the ends of the stainless steel recovery lines and remove the lines.
- Use the hoist to raise the 2 inch x 2 inch lifting bar on top of the 6 inch pump line. Strap the 2 inch x 2 inch steel lifting bar to the horizontal portion of the 6 inch pump line. Put a 25 lb shot bag in the carrier at the one end of the lifting bar. Use another 25 lb shot bag on top of the pump line to equalize the weight.

NOTE: *The conflats on both ends of the 6 inch pump line rotate. While this feature makes installation easier, it also makes the conflat vulnerable to damage because the knife-edge sticks out the farthest and is unprotected. Great care must be taken to ensure the knife-edge does not get damaged during the handling of the pump line.*

- Unbolt both 8 inch conflats on the ends of the 6 inch pump line.
- Hoist the 6 inch pump line away from the cryostat and store in a safe location.
- Remove the air hose from the J-T pneumatic actuator.
- Disconnect the turbo pump from the He II evacuated space line.
- Remove the cryostat lid bolts.
- Install the cryostat lifting bar onto the hoist and attach it to the four eyebolts in the cryostat cover.

Note: *The cables on the cryostat lifting bar can easily become tangled on wires and hardware around the cryostat lid. Care must be taken to ensure the cables do not damage anything during the hoisting process*.

- Take the slack out of the cryostat lifting bar cable by carefully raising the hoist.
- Lift the cryostat about 1 ft.
- Disconnect the two heater wire plugs. Tape the heater wire plugs (that lead to the heater) to the top of the dewar to ensure they do not fall into the dewar.
- Slide the He II bath cradle under the stand.
- Carefully hoist the cryostat from the dewar and move it overtop of the stand.
- Carefully lower the cryostat onto the stand while guiding the He II bath into the cradle.
- Disconnect the He II bath evacuated space VCR fitting.
- Raise the He II bath cradle up until it lightly touches the bottom of the He II bath. Do not push on the He II bath with excessive force.
- Remove the He II bath lid bolts.

- Lower the He II bath cradle. If the He II bath does not lower, drop the cradle so there is about a ½ inch gap between the cradle and the bottom of the bath.
- Thread four of the He II bath lid bolts into the holes in the He II bath lid labeled JS (Jacking Screws).
- Turn the four bolts uniformly until the He II bath seal breaks free.
- Lower the He II bath cradle.
- Raise the cryostat up until the He II bath can be removed from under the stand.
- Clean any remaining epoxy putty from both sealing surfaces. Be careful not to damage either sealing surfaces.

Appendix B Refrigeration System EES Code

```
"Greg Nellis, 11/6/02,
Daniel Hoch, 5/6/2004
1.8K Liquid Helium JT-Cooler Program for ANL Magnet Cooling System"

$Bookmark Inputs
P_HE1_bath=101325[Pa]                    " pressure of helium-I bath in dewar"
T_HE2_bath=1.8 [K]                       " temperature of superfluid surrounding
magnet"
Q_dot_HXbath=20 [W]                      " heat load on subcooled superfluid
helium bath"
T_room=300 [K]                           " room temperature"

$Bookmark JTCooler

"Input Specifications"
DeltaT_HE2_bathHX=0.05                   "[K], temperature difference across bath
heat exchanger"
DeltaP_recL=100                          "[Pa], pressure drop on low pressure
side of recuperator"
DeltaP_recH=10000                        "[Pa], pressure drop on high pressure
side of recuperator"

"entering recuperator from He1 bath"
P[1]=P_HE1_bath                          "[Pa], pressure of helium entering
recuperator"
x[1]=0.0                                 "quality of helium entering recuperator -
saturated liquid"
CALL HEPAK_EES(1,9,P[1],x[1],1,3,11111,0.65:PROP1[1..41])
h[1]=PROP1[10] "[J/kg]"
s[1]=PROP1[9] "[J/kg-K]"
v[1]=PROP1[5] "[m^3/kg]"
T[1]=PROP1[3] "[K]"
Cp[1]=PROP1[15]

"leaving recuperator to valve"
P[2]=P[1]-DeltaP_recH "[Pa]"
{CALL HEPAK_EES(1,15,P[2],1,1,3,11111,0.65:PROP2[1..41])}
CALL HEPAK_EES(2,1,T[2],P[2],1,3,11111,0.65:PROP2[1..41])
T[2]=2.416[K]
h[2]=PROP2[10] "[J/kg]"
s[2]=PROP2[9] "[J/kg-K]"
v[2]=PROP2[5] "[m^3/kg]"
{T[2]=PROP2[3] "[K]"}
Cp[2]=PROP2[15]

"entering bath HX"
h[3]=h[2] "[J/kg]"
P[3]=P[4] "[Pa]"
CALL HEPAK_EES(6,1,h[3],P[3],1,3,11111,0.65:PROP3[1..41])
x[3]=PROP3[1]
T[3]=PROP3[3] "[K]"
s[3]=PROP3[9] "[J/kg-K]"
```

```
v[3]=PROP3[5] "[m^3/kg]"
Cp[3]=PROP3[15]

"entering recuperator from bath HX"
T[4]=T_HE2_bath-DeltaT_HE2_bathHX                    "[K], temperature required in bath HX"
x[4]=1                                               "quality of gas leaving bath HX and
entering recuperator - all saturated vapor"
CALL HEPAK_EES(2,9,T[4],x[4],1,3,11111,0.65:PROP4[1..41])
h[4]=PROP4[10] "[J/kg]"
s[4]=PROP4[9] "[J/kg-K]"
v[4]=PROP4[5] "[m^3/kg]"
P[4]=PROP4[2] "[Pa]"
Cp[4]=PROP4[15]

"leaving recuperator on low pressure side"
h[5]=h[4]+(h[1]-h[2])                                "[J/kg]"
P[5]=P[4]-DeltaP_recL                                "[Pa]"
CALL HEPAK_EES(6,1,h[5],P[5],1,3,11111,0.65:PROP5[1..41])
T[5]=PROP5[3]                                        "[K]"
s[5]=PROP5[9]                                        "[J/kg-K]"
v[5]=PROP5[5]                                        "[m^3/kg]"
DeltaT_recH=T[1]-T[5]                                "[K], recuperator temperature difference
at hot end"
Cp[5]=PROP5[15]

"Key Outputs"
m_dot_HXbath=Q_dot_HXbath/(h[4]-h[3])                "mass flow rate through system[kg/s]"
P_plc=P[5]                                           "Pressure of 1.5 inch pipe attached to
recuperator [Pa]"
P_plc_torr=P[5]*convert(Pa,torr)                     "[torr]"
VF_HXbath=m_dot_HXbath*v[4]                          "Volumetric flow rate of vacuum
pumps[m^3/s]"

$Bookmark Vacuum System
L_plc=12[in]*convert(inch,m)                         "length of 1.5 inch vacuum line[m]"
D_plc=1.5[in]*convert(inch,m)                        "Diameter of 1.5 inch vacuum line[m]"
t_plc=0.035[in]*convert(inch,m)                      "Thickness of 1.5 vacuum line[m]"
L_plh=36[in]*convert(inch,m)                         "Length of 2.5 inch vacuum line[m]"
D_plh=2.5[in]*convert(inch,m)                        "Diameter of 2.5 vacuum line[m]"
t_plh=0.065[in]*convert(inch,m)                      "Thickness of 2.5 inch vacuum line[m]"

T_pl_int=200                                         "Average temperature of internal
pumpline[K]"
intkdT_plh=14[W/cm]*convert(W/cm,W/m)
kavg_plh=intkdT_plh/(T_room-T_pl_int)                "[W/m-K]"

intkdT_plc=16.7[W/cm]*convert(W/cm,W/m)
kavg_plc=intkdT_plc/(T_pl_int-T[5])                  "[W/m-K]"

R_plh=L_plh/(kavg_plh*pi*t_plh*D_plh)                "Thermal resistance of 2.5 inch diameter
pump line[K/W]"
R_plc=L_plc/(kavg_plc*pi*t_plc*D_plc)                "Thermal resistance of 1.5 inch diameter
pump line[K/W]"
T_pl_int_calc=T[5]+R_plc*(T_room-T[5])/(R_plc+R_plh) "[K]"

Rg=(R#*convert(kJ,J)/MolarMass(Helium))              "Gas constant[J/kg-K]"
```

```
T_avg_plc=(T[5]+T_pl_int)/2                    "Average temperature of 1.5 inch pump
line[K]"
mu_avg_plc=viscosity(Helium,T=T_avg_plc,P=P_plc)    "average viscosity of fluid in 1.5 pipe"
P_pl_int^2=P_plc^2-128*Rg*m_dot_HXbath*mu_avg_plc*T_avg_plc*L_plc/(pi*D_plc^4) "[Pa^2]
Pressure drop in 1.5 inch pump line"
Re_adapter=(4*m_dot_HXbath)/(PI*D_plc*mu_avg_plc)  "Reynolds number of fluid in 1.5 inch
pump line"
T_avg_plh=(T_pl_int+T_room)/2                   "Average temperature of 2.5 inch pump
line[K]"
mu_avg_plh=viscosity(Helium,T=T_avg_plh,P=P_plc)    "Average viscosity of fluid in 2.5 inch
pump line"
P_plh^2=P_pl_int^2-128*Rg*m_dot_HXbath*mu_avg_plh*T_avg_plh*L_plh/(pi*D_plh^4) "[Pa^2]
Pressure drop in 2.5 pump line"
Re_2.5_pipe=(4*m_dot_HXbath)/(PI*D_plh*mu_avg_plh)                                    "Rey
P_plh_torr=P_plh*convert(Pa,torr)
P_plh_mmHg=P_plh*convert(Pa,mmHg)
DeltaP_pl=P_plh-P_plc                          "Pressure drop in internal pump line
[Pa]"
VF_pump=m_dot_HXbath*volume(Helium,P=P_plh,T=300) "Volumetric flow [m^3/s]"
VF_pump_cfm=VF_pump*convert(m^3/s,ft^3/min)     "[ft^3/min]"
{VF_pump_cfm=1000[cfm]}
Q_dot_pl=(T_room-T[5])/(R_plh+R_plc)           "Heat transferred into pump line
between outlet of recuperator and room [W]"

$Bookmark Bath Heat Exchanger
alpha=0.05[W/cm2-K3.3]*convert(W/cm^2-K^3.3,W/m^2-K^3.3) "Kapitza resistance [W/m^2-
K^3.3]"
ne=3.3
qflux_bath=alpha*(T_HE2_bath^ne-Tnc^ne)/2      "Heat flux from He II bath[W/m^2]"
A_HX_bath=Q_dot_HXbath/qflux_bath              "Surface area of He II heat exchanger
[m^2]"
D_HX_bath=3[in]*convert(inch,m)                "Diameter of He II heat exchanger [m]"
L_HX_bath=20[in]*convert(inch,m)               "Length of He II heat exchanger [m]"
A_HX_bath2=pi*D_HX_bath*L_HX_bath+pi*(D_HX_bath)^2/4 "[m^2]"
k_cu_bath=93[W/m-K]                            "Thermal conductivity of copper He II
heat exchanger"
t_cu_bath=0.125[in]*convert(inch,m)            "wall thickness of He II heat exchanger"
DeltaT_cu_bath=Q_dot_HXbath*t_cu_bath/(k_cu_bath*A_HX_bath2)
T[4]=Tnc-DeltaT_cu_bath                        "Temperature of saturated He II vapor
exiting He II heat exchanger"

$Bookmark Generate Helium Curves
"generate saturation line"
CALL HEPAK_EES(12,1,1,P_i,1,3,11111,0.65:PROPi[1..41])
Tsat=PROPi[3]

"generate lambda line"
CALL HEPAK_EES(15,1,1,P_i,1,3,11111,0.65:PROPi[1..41])
Tlambda=PROPi[3]

"!Recuperator"

"!NOTE:  HEPAK does not have data below 3.5K for Pr, k, and mu.  Therefore, values have been
obtained from EES"
"Ideal UA and effectiveness calculated from ideal model above"
```

```
T_Pinch_2=T[2]-T[4]                                   "Pinch point temperature"
T_Pinch_1=T[1]-T[5]                                   "Pinch point temperature"
epsilon_recup=C_h*(T[1]-T[2])/(C_min*(T[1]-T[4]))     "Ideal effectiveness of recuperator"
C_min=min(C_c,C_h)                                    "minimum heat capacitance"
C_max=max(C_c,C_h)                                    "maximum heat capacitance"
Cr=C_min/C_max                                        "capacitance ratio"
C_h=m_dot_HXbath*cp_h                                 "heat capacitance of hot fluid"
C_c=m_dot_HXbath*cp_c                                 "heat capacitance of cold fluid"
NTU=(1/(Cr-1))*ln((epsilon_recup-1)/(epsilon_recup*Cr-1))                                  "NTU
m_dot_HXbath*h[4]+Q_dot_recup=m_dot_HXbath*h[5]
Q_dot_recup=m_dot_HXbath*cp_h*(T[1]-T[2])
Q_dot_recup=m_dot_HXbath*cp_c*(T[5]-T[4])
NTU=UA/C_min

m_dot_HXbath_act=m_dot_HXbath
Q_dot_HXbath_act=20 [W]                               "heat load on subcooled superfluid
helium bath"
DeltaP_recL_act=100                                   "[Pa],pressure drop on low pressure
side of recuperator"
DeltaP_recH_act=10000                                 "[Pa], pressure drop on high pressure
side of recuperator"

h_act[3]=h_act[2]                                     "[J/kg]"
P_act[3]=P_act[4]                                     "[Pa]"
CALL HEPAK_EES(6,1,h_act[3],P_act[3],1,3,11111,0.65:PROP3_act[1..41])
T_act[3]=PROP3_act[3]

"!Geometry based UA and effectiveness calculations to be compared with ideal model computed
above"
"Inside tubes of recuperator:  States 4-5"
"!Theoretical model predicts saturated vapor at state 4 which leads HEPAK to not compute some
properties.  To correct P[4] was reduced by 1 Pa which makes state 4 pure vapor.  T[4] is still
held at 1.75 K in both models"

CALL HEPAK_EES(2,1,T_act[4],P_act[4],1,3,11111,0.65:PROP4_act[1..41])
T_act[4]=1.75[K]
P_act[4]=1365 [Pa]
h_act[4]=PROP4_act[10] "[J/kg]"

CALL HEPAK_EES(6,1,h_act[5],P_act[5],1,3,11111,0.65:PROP5_act[1..41])
h_act[5]=h_act[4]+(h_act[1]-h_act[2]) "[J/kg]"
P_act[5]=P_act[4]-DeltaP_recL_act "[Pa]"
T_act[5]=Prop5_act[3]

dTemp_tube=T_act[5]-T_act[4]                          "Temperature drop in tubes"
Number_tubes=55                                       "number of tubes"
OD_tube=0.1875[in]*convert(in,m)                      "Outside diameter of tubes"
ID_tube=0.1675[in]*convert(in,m)                      "Inside diameter of tubes"
L_tube=15[in]*convert(in,m)                           "Length of tubes"
Re_tube=4*m_dot_tube/(PI*ID_tube*mu_tube)             "Flow is turbulent"
m_dot_tube=m_dot_HXbath_act/Number_tubes              "Mass flow rate through each tube"
Nu_tube=0.023*Re_tube^(4/5)*Pr_tube^(0.4)             "Equation 8.60 for heating"
h_i=(Nu_tube*k_tube)/ID_tube                          "Heat transfer coefficient for one tube"
k_tube=(PROP4_act[27]+PROP5_act[27])/2                "average thermal conductivity of fluid in
tubes"
```

```
Pr_tube=(PROP4_act[28]+PROP5_act[28])/2                "average Prandtl number of fluid in
tubes"
mu_tube=(PROP4_act[26]+PROP5_act[26])/2                "average viscosity of fluid in tubes"
A_i=Number_tubes*PI*ID_tube*L_tube                     "surface area of inside of tubes"
R_ID_tube=1/(h_i*A_i)                                  "Thermal Resistiance inside of tube"

"Thermal resistance thru SS tube wall"
R_tube_wall=(ln(OD_tube/ID_tube))/(2*PI*k_ss*L_tube*Number_Tubes)
k_ss=0.00125 [W/cm]/dT*convert(W/cm,W/m)               "thermal conductivity of stainless steel
tubes"
dT=((PROP1_act[3]+PROP2_act[3])/2)-(PROP4_act[3]+PROP5_act[3])/2

"Shell side of recuperator: States 1 to 2"
"!The theoretical model predicts saturated liquid at state 1 which lead HEPAK to not compute
some properties at this state.  To correct T[1] was reduced by 0.001 K which makes state 1 sub-
cooled liquid.  EES was used for property values because HEPAK does not report k, mu, and Pr
below 3 K accurately.  EES data was compared with Van Sciver's book and it has the correct
order of magnitude and follows the same pattern."

dTemp_shell=T_act[1]-T[2]
CALL HEPAK_EES(1,2,P_act[1],T_act[1],1,3,11111,0.65:PROP1_act[1..41])
P_act[1]=101325[Pa] " pressure of helium-I bath in dewar"
T_act[1]=4.222[K]
h_act[1]=PROP1_act[10] "[J/kg]"
Cp_act[1]=PROP1_act[15]
{h_EES[1]=enthalpy(helium,T=T_act[1],P=P_act[1])}
rho_act[1]=PROP1_act[4]

{CALL HEPAK_EES(1,15,P_act[2],1,1,3,11111,0.65:PROP2_act[1..41])}
CALL HEPAK_EES(1,2,P_act[2],T[2],1,3,11111,0.65:PROP2_act[1..41])
P_act[2]=P_act[1]-DeltaP_recH_act "[Pa]"
h_act[2]=PROP2_act[10] "[J/kg]"
T_act[2]=PROP2_act[3]
Cp_act[2]=PROP2_act[15]
rho_act[2]=PROP2_act[4]
ID_shell=3[in]*convert(in,m)                           "inside diameter of shell"
Area_c_shell=((PI/4)*(ID_shell^2-Number_tubes*OD_tube^2))"Cross-sectional area of shell
annulus"
P_shell=Number_tubes*PI*OD_tube                        "Wetted perimeter of outside of tubes"
D_h_shell=(4*Area_c_shell)/P_shell                     "Hydraulic diameter of shell annulus"
Re_shell=(4*m_dot_HXbath_act)/(PI*D_h_shell*mu_shell)                                    "Flo
Nu_shell=0.023*Re_shell^(4/5)*Pr_shell^(0.3)           "Eq. 8.60 for cooling"
rho_shell=(rho_act[1]+rho_act[2])/2
mu_shell=(VISCOSITY(helium,T=T_act[1],P=P_act[1])+VISCOSITY(helium,T=T[2],P=P_act[2]))/
2"Viscosity of liquid in shell"
k_shell=(conductivity(helium,T=T_act[1],P=P_act[1])+conductivity(helium,T=T[2],P=P_act[2]))/2
Pr_shell=(PRANDTL(helium,T=T_act[1],P=P_act[1])+PRANDTL(helium,T=T[2],P=P_act[2]))/2                    "Pra
Cp_shell=(Cp_act[1]+Cp_act[2])/2
h_o=(Nu_shell*k_shell)/D_h_shell                       "Heat transfer coefficient for outside
surface of tubes"
A_o=Number_tubes*PI*OD_tube*L_tube                     "Surface area of outside of tubes"
R_OD_tube=1/(h_o*A_o)                                  "thermal resistance through tubes"

UA_actual=1/(R_ID_tube+R_OD_tube+R_tube_wall)          "Actual UA"

alpha1=k_shell/(rho_shell*Cp_shell)
```

```
mu_shell=(PROP1_act[26]+PROP2_act[26])/2          "Viscosity of liquid in shell"
Pr_shell=(PROP1_act[28]+PROP2_act[28])/2          "Prandtl number for liquid in shell"
k_shell=(PROP1_act[27]+PROP2_act[27])/2           "Thermal conductivity of fluid in shell"
{k_EES=CONDUCTIVITY(Helium,T=T[2],P=P_act[2])
mu_EES=VISCOSITY(Helium,T=T[2],P=P_act[2])
Pr_EES=PRANDTL(Helium, T=T[2],P=P_act[2])}
```

Appendix C He II Bath Heat Leaks

```
"Daniel Hoch
5/7/04
Program to calculate the conductive heat leaks into HE II Liquid Bath"

T_s1=1.8                                                    "Inside wall
temperature of liquid bath"
T_s2=4.2                                                    "Outside wall
temperature of liquid bath"

"!Axial Conductivity through the Large G10 Cover"
Diameter_G10=13.75[in]*convert ('in','m')                   "Diameter of G10
exposed to 1.8K bath"
Diameter_Hall_Effect_Access=2.38[in]*convert('in','m')      "Diameter of hole cut
in G10 for Hall Effect Access"
Diameter_Heat_Exchanger_Hole=2.75[in]*convert('in','m')
                    "Diameter of hole cut in G10 to pass Heat Exchanger through"
Thickness_G10=2.5[in]                                       "Thickness of G10
exposed to 1.8K bath"
k_G10=(5.42*10^(-4))*convert('W/cm-K','W/m-K')              "Thermal
Conductivity of G10 as given by Cryocomp program"
A_G10=(Pi*(Diameter_G10/2)^2)-(Pi*(Diameter_Hall_Effect_Access/2)^2)-
(Pi*(Diameter_Heat_Exchanger_Hole/2)^2)        "Area of Liquid Bath G10 cover"
L_G10=Thickness_G10*convert('in','m')                       "Thickness of Liquid
Bath G10 cover"
Q_dot_He_II_lid=k_G10*A_G10*(T_s2-T_s1)/L_G10               "Calculate the
conductive heat loss through the G10 Cover"

"!Radial Thermal Conductivity through Steel flange at top of Liquid Bath"
L_ss_ring_radial=.50[in]*convert('in','m')                  "Thickness of
stainless steel flange"
{k_ss=.164                                                  "Thermal
Conductivity of stainless flange"}
OD_ss_ring=18.5                                             "Outside diameter of
ss ring"
ID_ss_ring=13.75                                            "Inside diameter of ss
ring"
r2_ss_ring=OD_ss_ring/2*convert('in','m')                   "Outside radius of
stainless steel flange"
r1_ss_ring=ID_ss_ring/2*convert('in','m')                   "Inside radius of
stainless steel flange"
Q_dot_flange_radial=2*Pi*L_ss_ring_radial*k_ss*(T_s2-
T_s1)/ln(r2_ss_ring/r1_ss_ring)"Calculate the conductive heat loss through the stainless flange"

"!Axial conduction through thickness of Steel Ring at top of Liquid Bath"
{k_ss=1.64*10^(-3)*convert('W/cm-K','W/m-K')                "Thermal
Conductivity of SS as given by Cryocomp program"}
OD_ss_ring_effective=17.5 [in]                              "OD  of SS ring
exposed to 4.2K and 1.8K Bath"
r2_ss_ring_effective=(OD_ss_ring_effective/2)*convert('in','m')   "Radius of ss ring
exposed to 4.2K and 1.8K bath"
A_ss_ring=(Pi*(r2_ss_ring_effective)^2)-(Pi*(r1_ss_ring)^2)
                          "Area of SS ring exposed to 4.2 K and 1.8K Bath"
```

```
L_ss_ring=1.00[in]*convert('in','m')                    "Thickness of SS
ring"
Q_dot_flange_axial=k_ss*A_ss_ring*(T_s2-T_s1)/L_ss_ring    "Calculate the
conductive heat loss through the G10 Cover"


"!Axial conduction through the Hall Effect Access G10 Cover"
{Diameter_Hall_Effect_Access=2.38*convert('in','m')      "Diameter of hole cut
in G10 for Hall Effect Access"}
Thickness_H_Effect_Access_G10=2                          "Thickness of G10
exposed to 1.8K bath"
{k_G10=(5.42*10^(-4))*convert('W/cm-K','W/m-K')          "Thermal
Conductivity of G10 as given by Cryocomp program"}
A_Hall_Effect_Access_G10=(Pi*(Diameter_Hall_Effect_Access/2)^2)   "Area of Hall Effect
Access Cover Exposed to 1.8K"
L_H_Effect_Access_G10=Thickness_H_Effect_Access_G10*convert('in','m')"Thickness of
Access cover lid exposed to 1.8 K bath"
Q_dot_Hall_Effect_Access_G10=k_G10*A_Hall_Effect_Access_G10*(T_s2-
T_s1)/L_H_Effect_Access_G10 "Calculate the conductive heat loss through the G10 Cover"

"!Radial conduction through Liquid Bath Cover Epoxy Bead"
L_ep_Lid=.5[mm]*convert('mm','m')                        "Thickness of epoxy
bead"
k_ep=(4.29*10^(-4))*convert('W/cm-K','W/m-K')            "Thermal
Conductivity of epoxy as given by Cryocomp program"
ID_ep_lid=15                                             "Inside Diameter of
epoxy bead"
OD_ep_lid=16.25                                          "Outside radius of
compressed epoxy bead"
r2_ep_lid=(OD_ep_lid/2)*convert('in','m')                "Outside radius of
compressed epoxy bead"
r1_ep_lid=(ID_ep_lid/2)*convert('in','m')                "Inside radius of
compressed epoxy bead"
avg_radius_lid=(r2_ep_lid+r1_ep_lid)/2                   "average radius"
avg_exp_radius=3.496*10^(-2)                             "average radius of
Pfotenhauer's epoxy seal test"
scaling_lid=avg_radius_lid/(avg_exp_radius)              "linear scaling of
calculated radius from experimental radius"
He_leak_lid=3.4*10^(-2)                                  "Estimated helium
leak for a particular experimental radius"
Q_dot_epoxy_lid_radial=2*Pi*L_ep_lid*k_ep*(T_s2-T_s1)/ln(OD_ep_lid/ID_ep_lid)"Calculate the
conductive heat loss through the compressed epoxy bead"
Q_dot_epoxy_lid_He_leak=Q_dot_epoxy_lid_radial+(scaling_lid*He_leak_lid)"Conductive heat
loss through epoxy and from estimated helium leak"

"!Heat Leak through SS Heat Exchanger Flange"
Diameter_HXCH_Opening=2.5[in]*convert ('in','m')          "Diameter of Hole
Cut in G10 for Heat Exchanger"
k_ss=1.64*10^(-3)*convert('W/cm-K','W/m-K')              "Thermal
Conductivity of SS as given by Cryocomp program"
A_HXCH_Flange=(Pi*(Diameter_HXCH_Opening/2)^2)           "Area of Heat
Exchanger Flange exposed to 1.8K Bath"
L_HXCH_Flange=.25[in]*convert('in','m')                  "Thickness of Heat
Exchanger Flange"
Q_dot_HXCH_Flange=k_ss*A_HXCH_Flange*(T_s2-T_s1)/L_HXCH_Flange
                                  "Calculate the conductive heat loss through the G10 Cover"
```

```
"!Heat Leak  through BSSCO Superconductor Tubes"
Diameter_Bscco_Rods=50[mm]*convert ('mm','m')                    "Diameter of BSSCO
rods exposed to 1.8K bath"
k_Bscco=.1 [W/m-K]                                               "Thermal
Conductivity of BSSCO as given by NEXANS"
A_Bscco=(Pi*(Diameter_Bscco_Rods/2)^2)                           "Cross-sectional area
of BSSCO Rods"
L_Bscco=4[in]*convert('in','m')                                  "Thickness of Liquid
Bath G10 cover separating HE II and HE I baths"
Number_Rods=2                                                    "Number of
superconductor rods required"
Q_dot_Bscco=Number_Rods*k_Bscco*A_Bscco*(T_s2-T_s1)/L_Bscco      "Calculate the
conductive heat loss through the BSSCO Rods"

"!Heat leak through G-10 rod in center of BSCCO tubes"
Diameter_G10_Rod=35[mm]*convert ('mm','m')                       "Diameter of BSCCO
rods exposed to 1.8K bath"
A_G10_rod=(Pi*(Diameter_G10_Rod/2)^2)                            "Cross-sectional area
of BSCCO Rods"
L_G10_rod=4[in]*convert('in','m')                                "Thickness of Liquid
Bath G10 cover separating HE II and HE I baths"
Q_dot_G10_rods=Number_Rods*k_G10*A_G10_rod*(T_s2-T_s1)/L_G10_rod
                                "Calculate the conductive heat loss through the BSCCO Rods"

"!Heat Leak through 30 Voltage Tap pass throughs"
Diameter_Vtap=.016[in]*convert ('in','m')                        "Diameter of 28
gauge copper wire exposed to 1.8K bath"
k_copper=471 [W/m-K]                                             "Thermal
Conductivity of Copper RRR=100 as given by Cryocomp"
A_Vtap=(Pi*(Diameter_Vtap/2)^2)                                  "Cross-sectional area
of 28 gauge copper wire"
L_Vtap=4[in]*convert('in','m')
                                "Thickness of Liquid Bath G10 cover seperating HE II and HE I
baths"
Number_Vtaps=30                                                  "Number of voltage
taps"
Q_dot_voltage_tap=Number_Vtaps*k_copper*A_Vtap*(T_s2-T_s1)/L_Vtap "Calculate the
conductive heat loss from the voltage taps"

"!Heat Leak through 16 gauge wires that power the background magnet"
Diameter_Wire=.064[in]*convert ('in','m')                        "Diameter of 16
gauge copper wire exposed to 1.8K bath"
{k_copper=471 [W/m-K]}                                           "Thermal
Conductivity of Copper RRR=100 as given by Cryocomp"
A_wire=(Pi*(Diameter_Wire/2)^2)                                  "Cross-sectional area
of 16 gauge copper wire"
L_wire=4[in]*convert('in','m')                                   "Thickness of Liquid
Bath G10 cover separating HE II and HE I baths"
Number_wire=6                                                    "Number of leads"
Q_dot_copper_wire=Number_wire*k_copper*A_wire*(T_s2-T_s1)/L_wire "Calculate the
conductive heat loss from the quench detection leads"

"!Heat Leak through capillary tube passing between He I and He II baths in G10 cover"
k_ss316=.164*10^(-2)*convert(W/cm-k,W/m-K)                       "Integrated thermal
conductivity of stainless steel given by Cryocomp"
```

```
tube_ID=(.125-.035-.035)*convert(in,m)                    "Tube inside
diameter"
tube_OD=.125[in]*convert(in,m)                            "Tube outside
diameter"
tube_wall_thickness=(tube_OD-tube_ID)/2*convert(m,in)     "Tube wall thickness"
A_cap_tube=(PI/4)*(tube_OD^2)-(PI/4)*(tube_ID^2)          "Cross-sectional area
of tube"
L_cap_tube=2.5[in]*convert(in,m)                          "Length of tube
passing through thermal gradient"
Q_dot_cap_tube=(k_ss316*A_cap_tube)/L_cap_tube*(T_s2-T_s1)  "Heat leak from He I
to He II bath"

"!Total Heat leak into He II bath"
Total_Heat_Leak=Q_dot_He_II_lid+Q_dot_flange_radial+Q_dot_flange_axial+Q_dot_Hall_Effect
_Access_G10+Q_dot_epoxy_lid_He_leak+Q_dot_HXCH_Flange+Q_dot_Bscco+Q_dot_G10_rod
s+Q_dot_voltage_tap+Q_dot_copper_wire+Q_dot_cap_tube+Q_dot_cone+Q_dot_Hxcher_G10+
Q_dot_ep_H_effec_plus_He_leak

"!Heat leak from He II to He I "
{at delta T= 2.4K, Experimental Q=6*10^-3 [W]
Calculated Q at k=4x10^-2 W/m-K, Q=4.247*10^-4 [W]
Calculated He Leak = 3.4*10^-2 [W]
Bead Width=.0254 [m]
average experimental radius=3.496*10^-2 [m]}

"!Heat leak from He II to He I from the gap between the cone fill hole and the G10 Liquid Bath
Lid"
q_prime_cone*L_cone^(1/3)=F_T                             {Steady State Peak
Heat Flux Taken from the Handbook of Cryogenic Engineering pg. 457}
diameter_cone=1.5 [in]                                    "Average diameter of
cone"
length_cone=4 [in]                                        "Length of cone:
Also length that HE II must travel"
L_Cone=length_cone*convert('in','m')
gap_cone=.005 [in]                                        "Distance between
cone and cone shape in G10 cover"
area_cone=(PI*((diameter_cone+gap_cone)/2)^2-
PI*(diameter_cone/2)^2)*convert('in2','m2')"Cross-sectional area of gap between cone and G10
cover"
Q_dot_cone=q_prime_cone*area_cone*convert('kW','W')
                                  "Heat Loss from mass transfer between HE I and HE II"

"!Heak leak from He II and He I at He I Heat Exchanger Flange to G10 mating surface"
q_prime_HE*L_HE^(1/3)=F_T                                 "Steady State Peak
Heat Flux Taken from the Handbook of Cryogenic Engineering pg. 457"
F_T=14.6835                                               "Integrated HE II
turbulent flow heat conductivity function taken from Handbook of Cryogenic Engineering pg. 457"
L_HE=length_HE*convert('in','m')                          "Length is the
distance of the gap that the HE II has to travel through"
gap_HE=.005                                               "Gap is the distance
between the stainless flange and the G10"
OD_HE=3.25                                                "Outside diameter of
flange"
ID_HE=2.504                                               "Inside diameter of
flange"
Length_HE=(OD_HE/2)-(ID_HE/2)
```

```
average_diameter_HE=(OD_HE+ID_HE)/2                                    "Average diameter of
flange"
area_HE=2*PI*(average_diameter_HE/2)*gap_HE*convert('in2','m2')        "Area is
circumference at average diameter*gap thickness"
Q_dot_Hxcher_G10=q_prime_HE*area_HE{*convert('kW','W')}                "Heat Loss from
mass transfer between HE I and HE II"

"!Heat leak from He II to He I through Hall Effect Access Cover Epoxy Bead"
L_epoxy_Hall_Effect=.5[mm]*convert('mm','m')                           "Thickness of epoxy
bead"
{k_epoxy=(4.29*10^(-4))*convert('W/cm-K','W/m-K')                      "Thermal
Conductivity of epoxy as given by Cryocomp program"}
OD_Hall_Effect=3.75                                                    "Outside Diameter of
epoxy bead"
ID_Hall_Effect=2.5                                                     "Inside Diameter of
epoxy bead"
r2_Hall_Effect=(OD_Hall_Effect/2)*convert('in','m')                    "Outside radius of
compressed epoxy bead"
r1_Hall_Effect=(ID_Hall_Effect/2)*convert('in','m')                    "Inside radius of
compressed epoxy bead"
avg_radius_H_effect=(r2_Hall_Effect+r1_Hall_Effect)/2                  "average radius"
{avg_exp_radius=3.496*10^(-2)                                          "average radius of
Pfotenhauer's epoxy seal test"}
scaling_H_effect=avg_radius_H_effect/(avg_exp_radius)                  "linear scaling of
calculated radius from experimental radius"
He_leak_H_effect=0.034 [W]                                             "Estimated helium
leak for a particular experimental radius"
Q_dot_epoxy_H_Effect_radial =2*Pi*L_epoxy_Hall_Effect*k_ep*(T_s2-
T_s1)/ln(r2_Hall_Effect/r1_Hall_Effect)"Calculate the conductive heat loss through the
compressed epoxy bead"
Q_dot_ep_H_effec_He_leak=He_leak_H_effect*scaling_H_effect
Q_dot_ep_H_effec_plus_He_leak=Q_dot_epoxy_H_effect_radial+(scaling_H_effect*He_leak_H_
effect)"Conductive heat loss through epoxy and from estimated helium leak"
```